UNIVERSITÄT BAYREUTH

Fakultät für Biologie, Chemie und Geowissenschaften

Bioanalytical and mechanistical analysis of isoform specific Sirtuin modulation

DISSERTATION

zur Erlangung des Grades Doktor der Naturwissenschaften der Fakultät für Biologie, Chemie und Geowissenschaften der Universität Bayreuth

vorgelegt von

M.Sc. Biochemiker

Benjamin Sünkel

Bayreuth, Mai 2016

Die vorliegende Arbeit wurde in der Zeit vom Oktober 2011 bis Mai 2016 in Bayreuth am Lehrstuhl für Biochemie unter Betreuung von Herrn Professor Dr. Clemens Steegborn angefertigt.

Vollständiger Abdruck der von der Fakultät für Biologie, Chemie und Geowissenschaften der Universität Bayreuth genehmigten Dissertation zur Erlangung des akademischen Grades eines Doktors der Naturwissenschaften (Dr. rer. nat.).

Dissertation eingereicht am:	25.05.2016
Zulassung durch die Promotionskommission:	15.06.2016
Wissenschaftliches Kolloquium:	15.11.2016

Amtierender Dekan: Prof. Dr. Stefan Schuster

Prüfungsausschuss:

Prof. Dr. Clemens Steegborn	(Erstgutachter)
Prof. Dr. Olaf Stemmann	(Zweitgutachter)
Prof. Dr. Birgitta Wöhrl	(Vorsitz)
Prof. Dr. Frank Hahn	

List of Publications

Results of this dissertation appeared in parts in the following publications:

Suenkel, B., Valente, S., Garg, N., Sinclair, D., Mai, A., Steegborn, C. Pharmacological activation of the mitochondrial Sirtuins Sirt3 and Sirt5. (in preparation).

Suenkel, B. and Steegborn, C. (2016). Recombinant preparation, biochemical analysis, and structure determination of Sirtuin family histone/protein deacylases. *Methods in Enzymology*. In press.

Suenkel, B., Fischer, F., Steegborn C. (2013). Inhibition of the human deacylase Sirtuin 5 by the indole GW5074. *BMC Letters*, 23, 143 – 146, doi: 10.1016/j.bmcl.2012.10.136.

Fischer, F.*, Gertz, M.*, **Suenkel, B.**, Lakshminarasimhan, M., Schutkowski, M., Steegborn C. (2012). Sirt5 deacylation activities show differential sensitivities to nicotinamide inhibition. *PLoS ONE* 7(9): e45098, doi: 10.1371/journal.pone.0045098.

Further publications

Gertz, M.*, Nguyen G. T., Fischer, F., **Suenkel, B.**, Schlicker, Ch., Fraenzel, B., Tomaschewski, J., Aladini, F., Becker, Ch., Wolters, D., Steegborn, C. (2012). A molecular mechanism for direct Sirtuin activation by resveratrol., *PLoS ONE* 7(11): e49761, doi: 10.1371/journal.pone.0049761.

Conferences & Courses:

2014	Poster presentation at the 5th Murnau Conference on Structural Biology in Murnau, Germany, titled 'Acyl-specific Physiological and Pharmacological Sirt5 Inhibition'
2012	Ion Trap Biotech Operations Course held by Thermo Scientific in Basel, Switzerland
2012	Oral presentation at the Rabensteiner Colloquium in Pottenstein, Germany, titled 'Modulation of Sirtuin Activity'

Table of Contents

List of Abbreviations

1,4-DHP:	1,4-Dihydropyridine
aa:	amino acid
ac:	acetyl
AB:	antibody
ACN:	acetonitrile
ACS2:	acetyl-CoA synthetase 2
ADPr:	ADP (adenosyldiphosphate) ribose
αTub:	α-Tubulin
ALS:	amyotrophic lateral sclerosis
Amp:	ampicillin
AMPK:	AMP (adenosine monophosphate) activated kinase
APS:	ammonium persulfate
adi:	adipoyl (5-carboxypentanoyl)
CB:	Cibacron Blue
Cmpd:	Compound
CPS1:	carbamoyl phosphate synthetase 1
CR:	Caloric Restriction
CV:	column volume
DMEM:	Dulbecco's modified eagle medium
DMSO:	dimethyl sulfoxide
DTT:	dithiothreitol
EDTA:	ethylenediaminetetraacetic acid
FA:	formic acid
FdL:	Fluor-de-Lys®
FBS:	fetal bovine serum
FITC:	fluorescein isothiocyanate
FOXO1:	forkhead box O1
GDH:	glutamate dehydrogenase
H3:	histone 3
HFBA:	heptafluorobutyric acid
Hif1α:	hypoxia-inducible factor 1 α
$His_{6:}$	hexahistidine
HMGCS2:	3-hydroxy-3-methylglutaryl-CoA synthase 2
IAA:	2-iodoacetamide
ICDH2:	isocitrate dehydrogenase 2
IP:	immunoprecipitation
λ_{ex}:	excitation wavelength
λ_{em}:	emission wavelength
LB:	Luria-Bertani
LCAD:	long chain-CoA decarboxylase
MCD:	malonyl-CoA decarboxylase
ML:	mitochondrial lysate
MS:	mass spectrometry, mass spectrometric
MST:	microscale thermophoresis
myr:	myristoyl (tetradecanoyl)
NAM:	nicotinamide
NCA:	nicotinamidase

n.d.:	not determined/not detected
OGG1:	oxoguanine glycosylase 1
ON:	overnight
OTC:	ornithintranscarbamoylase
PAGE:	polyacrylamide gel electrophoresis
PBS:	phosphate buffered saline
PCR:	polymerase chain reaction
PDAC:	protein deac(et)ylase
PDE:	phosphodiesterase
Pen/Strep:	100 units/ml penicillin and 0.1 mg/ml streptomycin
PGC1α:	peroxisome proliferator-activated receptor gamma coactivator 1 α
PMSF:	phenylmethylsulfonyl fluoride
PPARα:	peroxisome proliferator-activated receptor α
Prx1:	peroxiredoxin 1
PTM:	posttranslational modification
rel. activity:	relative activity normalized to a positive control (i.e. unmodulated sample)
rpm:	revolutions per minute
RelA:	NF-κB subunit p65
ROS:	reactive oxygen species
RT:	room temperature
SDS:	sodium dodecyl sulfate
succ:	succinyl (3-carboxybutanoyl)
SEC:	size exclusion chromatography
Sirt:	Sirtuin (silent mating-type information regulator 2 like protein)
Sirt1 – 7:	*H. sapiens* Sirt1 – 7
SOD:	superoxide dismutase
SUMO:	small Ubiquitin-related Modifier
STAC:	sirtuin activating compound
STDEV:	standard deviation
TAE:	Tris/Acetate/EDTA
TB:	terrific broth
TBS:	Tris buffered saline
TCA:	tricarboxylic acid cycle
TEMED:	N,N,N',N'-tetramethylethylendiamine
TEV:	tobacco etch virus
TFA:	trifluoro acetic acid
TNF:	tumor necrosis factor
ToF:	time of flight
UBCS:	abbreviation code for the lab internal compound library (University of Bayreuth Clemens Steegborn)
wt:	wild type
Z:	carboxybenzyl protecting group
zSirt5:	zebrafish (*D. rerio*) Sirt5

Summary

Sirtuins are protein deacylases involved in a variety of cellular pathways. Furthermore, they contribute to the effects of Caloric Restriction (CR), the reduction of calorie intake which results in health benefits and life-span extension in many organisms. In order to benefit from Sirtuin activity in therapeutic approaches, a detailed understanding of Sirtuin modulating strategies, e.g. by small molecule compounds, is necessary.

Although the enzymatic mechanism of Sirtuins is understood quite well, only limited data is available about physiological Sirtuin modulation. Furthermore, several pharmacological molecules are described for these enzymes. However, the majority of these modulators is only characterized against one or two out of the seven mammalian Sirtuins. In addition, for some Sirtuins no proper inhibiting compound is known and for the majority of Sirtuins no activator is described yet. Thus, it is important to identify novel pharmacological compounds targeting just a specific Sirtuin enzyme as it is known that Sirtuins can exhibit beneficial or negative effects in a context specific manner.

In this study physiological as well as pharmacological modulation mechanisms for specific Sirtuins were analyzed. Along with already identified but uncharacterized posttranslational modifications (PTMs) yet unknown Sirtuin PTMs were discovered using mass spectrometry. Mutational studies indicated that these PTMs affect both the stability and activity of these enzymes. In addition, the physiological Sirtuin inhibitor nicotinamide, which was the only physiological Sirtuin modulating ligand identified in mitochondrial lysate, was characterized towards its effects against the different activities of human Sirt5.

Specificity analyses revealed that already known Sirtuin modulators are not active against Sirt5 except for the Sirt2 inhibitor GW5074. Furthermore, structure based models as well as biochemical studies suggest acylated lysine derivatives as a promising starting point for the development of Sirt5 specific inhibitors. For Sirtuin activation, 1,4-dihydropyridines (1,4-DHPs) were confirmed as promising compounds. For the first time, specific activators for the human SIrt3 and Sirt5 were identified by derivatization of the 1,4-DHP scaffold.

This study contains detailed data about the specificity of Sirtuin modulators and identifies strategies for a specific regulation of distinct Sirtuins. These results provide important clues for the further optimization of pharmacological compounds.

Zusammenfassung

Sirtuine sind Proteindeacylasen, die an vielen zellulärer Prozesse beteiligt sind. Außerdem tragen sie zu den Effekten der Kalorienrestriktion (Caloric Restriction, CR) bei, d.h. der Reduktion der Kalorienaufnahme, die in vielen Organismen die Gesundheit fördert und die Lebensspanne verlängert. Um jedoch in therapeutischen Ansätzen von dieser Sirtuinaktivität profitieren zu können, ist ein genaues Verständnis über Regulationsmöglichkeiten dieser Enzyme nötig.

Obwohl der Reaktionsmechanismus der Sirtuine bereits gut verstanden ist, gibt es wenige Daten darüber, wie diese Enzyme physiologisch reguliert werden. Ferner wurden bereits einige pharmakologisch wirksame Moleküle gegenüber Sirtuinen identifiziert. Allerdings sind diese Modulatoren in den meisten Fällen nur gegen eines oder zwei der sieben unterschiedlichen Säuger-Sirtuine charakterisiert worden. Darüber hinaus sind nur für wenige Sirtuine gute Inhibitoren bekannt, Aktivatoren sind für die meisten Sirtuine nicht beschrieben. Daher ist es wichtig, neue pharmakologische Wirkstoffe zu identifizieren, die nur gegen ein spezifisches Sirtuin aktiv sind, da diese Enzyme kontextspezifisch positive oder negative Effekte aufweisen.

In dieser Studie wurden sowohl physiologische als auch pharmakologische Ansätze zur spezifischen Sirtuinmodulation untersucht. Neben bereits bekannten aber nicht charakterisierten posttranslationalen Modifikationen (PTMs) konnten bisher unbekannte PTMs an unterschiedlichen Sirtuinen identifiziert werden. Mutationsstudien deuten einen Einfluss auf die Stabilität und Aktivität dieser Enzyme an. Weiterhin wurde der Einfluss des physiologischen Sirtuininhibitors Nikotinamid, neben dem kein weiterer physiologischer Sirtuin modulierender Ligand in mitochondrialem Lysat identifiziert werden konnte, auf die unterschiedlichen Aktivitäten des humanen Sirt5 untersucht.

In Spezifitätsanalysen konnte erstmals gezeigt werden, dass bis auf den Sirt2 Inhibitor GW5074 bereits beschriebene pharmakologische Sirtuinmodulatoren gegen Sirt5 nicht aktiv sind. Anhand strukturbasierter Modelle und biochemischer Analysen konnten unterschiedlich acylierte Lysinderivate als Ausgangspunkt für die Entwicklung vielversprechender spezifischer Sirt5-Inhibitoren identifiziert werden. Weiterhin wurden 1,4-Dihydropyridine (1,4-DHPs) als vielversprechende Sirtuinaktivatoren bestätigt. Durch Derivatisierung des 1,4-DHP-Gerüstes konnten erstmals spezifische Aktivatoren für die humanen Sirtuine Sirt3 und Sirt5 identifiziert werden.

Diese Studie führt detaillierte Daten zur Spezifität von Sirtuinmodulatoren auf und identifiziert Strategien, die eine spezifische Regulation einzelner Sirtuine ermöglicht. Diese Ergebnisse sind wichtige Erkenntnisse für die weitere Optimierung pharmakologischer Substanzen.

1. Introduction

1.1. Posttranslational modification of proteins and nutrient availability

Once a eukaryotic protein is translated at the ribosome, it can be modified in many ways. These posttranslational modifications (PTMs) range from drastic alterations such as backbone cleavages (e.g. to release signal peptides or to form the final version of proteins like insulin) to the modification of amino acid (aa) side chains. One of the simplest ways of modifying proteins is the oxidation of Met or Cys by reactive oxygen species (ROS) or by oxidases and oxygenases. Protein phosphorylation of Ser or Thr side chains by kinases has often regulatory properties as it alters protein activity or interaction by introducing a negative charge, which can be removed by phosphatases. Apart from that, Lys residues are also important PTM targets, as their SUMOylation or ubiquitination regulates protein homeostasis. Moreover, accessibility of genomic loci is controlled by reversible methylation and acetylation of histone Lys (Figure 1).

With the development of high sensitive identification techniques, especially with the progress in high resolution MS/MS methods, more and more novel PTMs and PTM sites were discovered. In particular, the Lys ε-amino group was found to be modified with the well-established acetyl moiety but also with longer chain fatty acids. Among these so-called acyl moieties short aliphatic groups (e.g. propionyl Lys), charged moieties (e.g. succinyl Lys) and even long hydrophobic modifications (e.g. myristoyl Lys) were observed (Figure 1)[1–6].

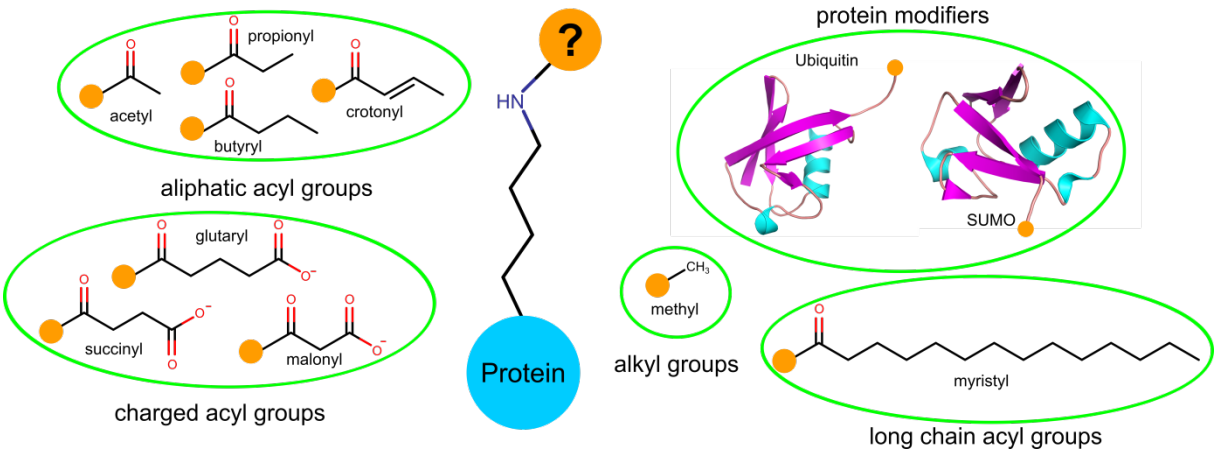

Figure 1: Known protein lysine modifications and their effect on major cellular metabolic pathways. Besides already known and well described modifications such as acetylation or methylation and the protein modifiers Ubiquitin & SUMO (cartoon representation colored by secondary structure elements of pdb entries 1UBQ & 4JWN, respectively)[7,8], novel aliphatic, charged and long chain acyl modifications were discovered (reviewed in Choudhary et al., 2014)[9].

Besides already known nuclear Lys PTMs, a plethora of extra-nuclear proteins were identified to be modified on the ε-amino group of their Lys moieties. Interestingly this acylation pattern can change depending on the nutrient availability[2,10]. Thus, distinct metabolic pathways as β-oxidation, the urea cycle and amino acid degradation (see below) can be switched on or off via reversible (de-)acylation to mobilize amino acids and fatty acids as energy source.

1.2. Sirtuins: Class III protein deacylases

1.2.1. Sirtuin classification

Protein lysine acylation is a reversible process. The attachment of acyl moieties can occur non-enzymatically or via acetyl-transferases[11–13]. For the removal of acyl groups from protein lysines four classes of protein deacetylases (PDAC) are described out of which the class III PDACs are also referred to as *Sirtuins*.

Sirtuins are highly conserved among archaea, prokaryotes and eukaryotes. While most organisms express one to three different Sirtuin proteins, mammalian organisms feature even seven Sirtuins. These enzymes are highly conserved as they share a common topology of a small Zn^{2+} binding domain and Rossmann-fold domain capable of NAD^{+} binding (Figure 2A). These domains form the highly conserved catalytic core of ~ 270 aa[14], which defines the Sirtuin family (Figure 2B & C, Table 1)[15,16]. Based on smaller sequence variation, subfamilies are defined: eukaryotic Sirtuins primarily belong to the Classes I and IV, Classes III and U are mainly composed of archaeal and prokaryotic Sirtuins and the mixed Class II contains both prokaryotic and eukaryotic Sirtuins. Different to all other mammalian Sirtuins, Sirt5 is most closely related to prokaryotic Sirtuins, which is reflected in its long cofactor binding loop, a typical feature of bacterial Sirtuins (Figure 2C)[17].

1.2.2. Sirtuin substrates

Mammalian organisms express seven Sirtuin enzymes. They differ in N- and C-terminal extensions next to the shared catalytic core, in their cellular localization and thus in their substrates (Figure 2B, Table 1)[18]. For example, the nuclear Sirt1 targets besides others histones and the transcription factors p53, PGC1-α thereby activating mitogenesis, gluconeogenesis as well as lipid metabolism[19,20]. The likewise nuclear Sirt6 is involved in transcriptional regulation and believed to play a key role in the switch between glycolytic and non-glycolytic metabolism, thereby opposing the Warburg effect[21]. The nucleolar Sirt7 deacetylates H3K18[22] and its deletion leads to down-regulation of the RNA polymerase I machinery and suppresses protein synthesis[23,24]. Sirt2 resides primarily in the cytosol targeting α-Tubulin and thereby affecting mitotic exit[25]. Sirt3 – 5 are located to the

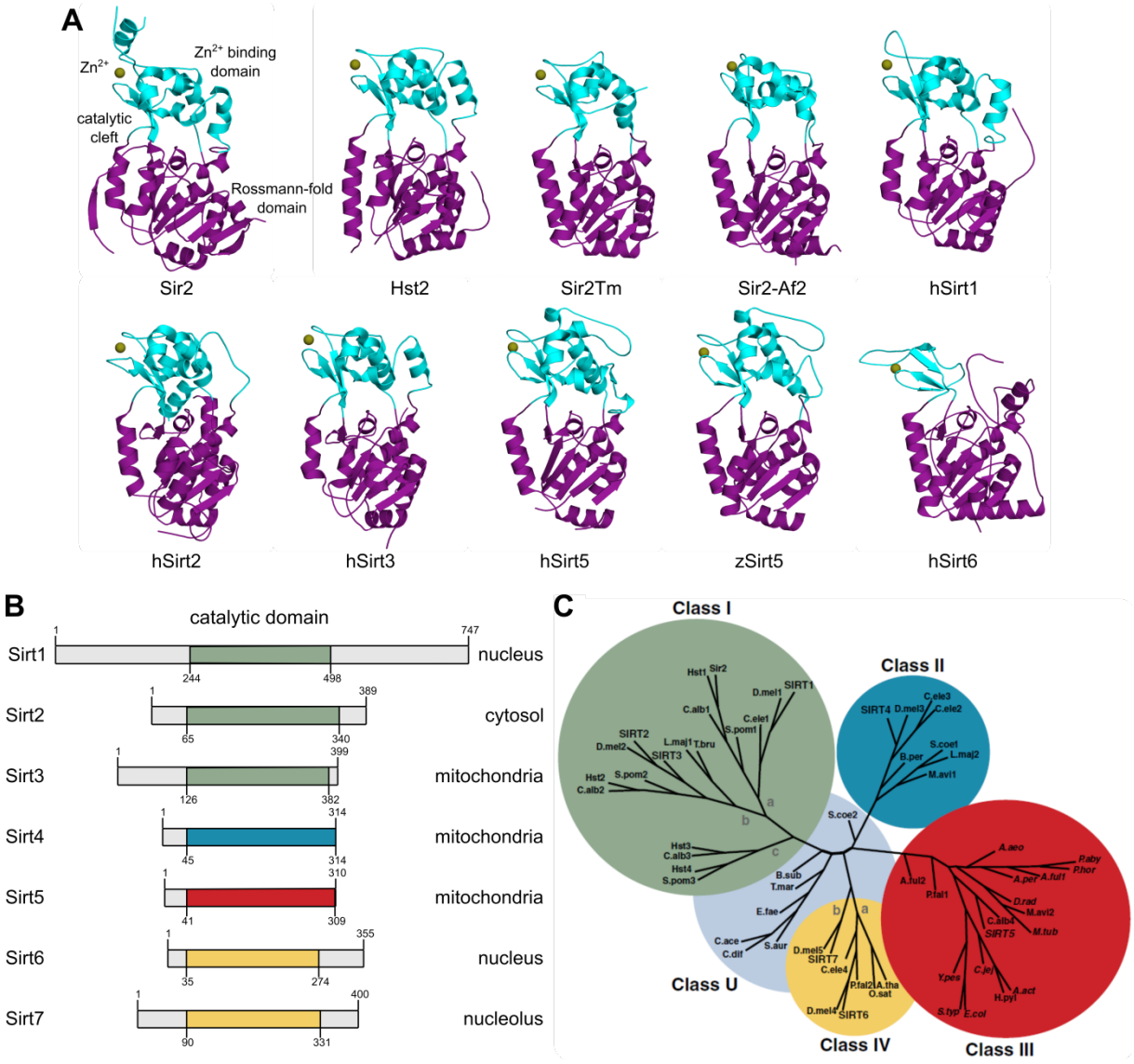

Figure 2: Sirtuins are a highly conserved class of enzymes. (A) Sirtuins share a conserved topology consisting of a Zn^{2+} binding domain (cyan) and a Rossmann-fold domain (magenta). This topology is conserved between *S. cerevisiae* Sir2 and Hst2 (pdb entry: 2HJH and 1Q17)[26], bacterial Sir2Tm (*Th. maritima*, pdb entry: 3JR3)[27], archaeal Sir2-Af2 (*A. fulgidus*, pdb entry: 1YC2)[28] and the Sirtuins from higher eukaryotes Sirt1, Sirt2, Sirt3, Sirt5 & Sirt6 from *H. sapiens* (pdb entries: 4ZZJ, 3ZGO, 3GLU, 3RIY & 3ZG6)[29–33] and zSirt5 from *D. rerio* (pdb entry: 4UTV)[34]. Cartoon representation of representative Sirtuins, Zn^{2+} as sphere (olive). (B) Besides the common topology, Sirtuins share a catalytic core with differing N- and C-terminal extensions and cellular localization (in case of mammalian Sirtuins, Color code resembles Sirtuin classification in C). (C) Based upon their core domain sequence similarity, Sirtuins are grouped into five different classes with Classes I (green) and IV (yellow) consisting of eukaryotic Sirtuins. Prokaryotic Sirtuins and the mammalian Sirt5 belong to Class III (red). Class II (dark blue) consists of pro- and eukaryotic Sirtuins, while Class U (light blue) contains only prokaryotic enzymes (adapted from Hirschey, 2011)[16].

mitochondria, where they activate key metabolic enzymes such as GDH, ACS2, ICDH2, LCAD, the respiratory chain and CPS1. This enhances β-oxidation, amino acid degradation, the tricarboxylic acid cycle (TCA) and cellular respiration and therefore the mobilization of fatty acids and amino acids as energy sources[6,35–37]. However, Sirt4 seems to counteract the activities of Sirt3 and Sirt5 as it inhibits GDH[38] (Figure 3). Sirt4 also represses MCD, thereby regulating the switch between lipid metabolism and catabolism[39]

Table 1: Mammalian Sirtuins, their classification, localization and exemplary substrates.

Sirtuin	Class	Localization	Substrates	Substrate acyls
Sirt1	I	Nucleus	AMPK, glycolytic enzymes, FOXO1, Hif1α, p53,PGC1α, PPARα, RelA, tau protein[19,20,40,41]	Acetyl, propionyl, butyryl[42]
Sirt2	I	Cytosol	α-Tubulin[25], FOXO1[43], H3K18[44], H4K16[45]	Acetyl, propionyl, butyryl[42]
Sirt3	I	Mitochondria	ACS2[35], complexes I – III of the respiratory chain, GDH, ICDH2, HMGCS2, LCAD, OGG1, OTC, SOD2[36,46–49]	Acetyl, propionyl, butyryl[42]
Sirt4	II	Mitochondria	GDH[38], MCD[39]	Acetyl[39]
Sirt5	III	Mitochondria	CPS1[37] , Cytochrome C[36], SOD1[50]	Acetyl, glutaryl, malonyl, succinyl[6,31,34,37,51]
Sirt6	IV	Nucleus	CtIP, GCN5, H3K9, H3K56, TNFα[32,52]	Acetyl, myristoyl[53]
Sirt7	IV	Nucleolus	H3K18, regulation of RNA polymerase I & III [22–24]	Acetyl[22]

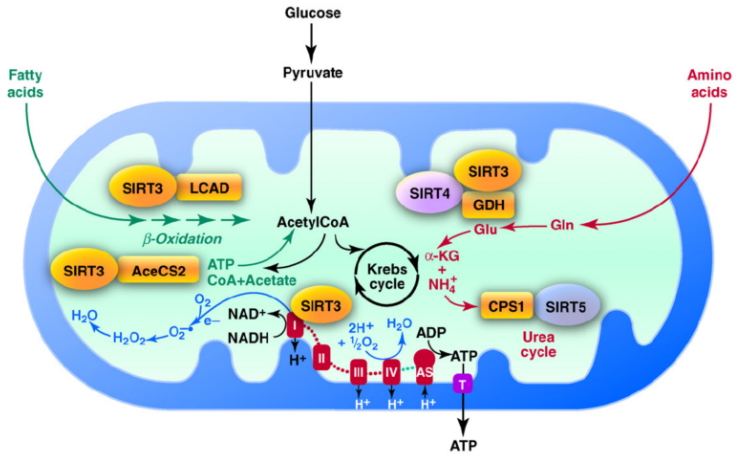

Figure 3: Three different Sirtuins regulate distinct metabolic pathways inside mitochondria. Sirt3 and Sirt5 promote mitochondrial metabolic pathways, while Sirt4 inhibits GDH (Figure taken from Verdin et al., 2009)[54].

1.2.3. The role of Sirtuins in health- and lifespan

1.2.3.1. Sirtuin effects on health and lifespan

More detailed investigations employing cell based assays and transgenic approaches revealed astounding results about Sirtuins contributing to beneficial health effects. Sirt1 is linked to improved wound healing and a reduced incidence of sarcomas and carcinomas resulting in increased lifespan[55]. Furthermore, it is implied that Sirt1 might protect against Alzheimer's Disease due to reduced levels of β-amyloid[40] and tau protein[55]. Sirt2 activity decreases the toxicity of the huntingtin protein[40]. Sirt6 acts as a tumor suppressor by inhibiting glycolytic metabolism under normoxic conditions[21]. This in turn opposes the so

called Warburg effect[56,57]. Loss of Sirt6 results in severe hypoglycemia and an early postnatal death in knockout mice[21,40].

Besides their role in metabolic regulation, mitochondrial Sirtuins exhibit beneficial effects, too. Interestingly, Sirt3 enhances both oxidative phosphorylation as well as protective measures against ROS[19,48], which might contribute to the Sirt3 mediated protection of age-related hearing loss[58,59]. On the contrary, Sirt3 loss results in increased lactate production, a switch to glycolytic metabolism[60], impaired mitochondrial function[55] and elevated ROS levels[60]. Sirt5 enhances cellular metabolism[6,37,61] and protects against oxidative stress[50,62]. Interestingly, loss of Sirt5 results in no dramatic phenotype apart from increased blood ammonia levels[61,63].

However, in some diseases and in some types of cancer, Sirtuin activity can be harmful as well: apoptosis of MCF-7 breast cancer cells is induced upon Sirt1 and Sirt2 inhibition[64]. Head and neck squamous cell carcinoma are associated with overexpression of Sirt3[65]. Elevated levels of Sirt5 are found in motor neurons of patients suffering from amyotrophic lateral sclerosis (ALS)[66] and high expression of Sirt5 predicts a poor survival of non-small cell lung cancer[67].

1.2.3.2. Caloric Restriction and its effect on health and lifespan

As Sirtuins aid in the mobilization of fatty acids and amino acids during calorie deprivation, it is no surprise that these enzymes are activated upon caloric restriction (CR)[68], i.e. the reduction of calorie intake by up to 60 %. Interestingly, already in the 1930s CR was observed to reduce tumor formation and to extend the lifespan of rats[69]. Since then further studies confirmed this effect in several other organisms (Figure 4A)[70,71] and revealed a dose dependent lifespan extension of max. 50 % if the calorie uptake was reduced by 60 % (Figure 4B)[72]. Despite this lifespan extension is not seen in all caloric restricted organisms, there is strong evidence that under CR conditions the health span of organisms is increased: the onset of metabolic disorders such as Diabetes mellitus type 2 is delayed under CR conditions[73]. Interestingly, beneficial effects of CR are not limited to metabolic disorders.

During CR, blood pressure and pulse wave velocities are reduced[74] and it was further shown, that neurodegenerative diseases, e.g. Alzheimer's, Huntington's and Parkinson's disease are observed less frequently or delayed in their onset upon CR [75,76].

Strikingly, several studies in *S. cerevisiae*[77–79] and further organisms (reviewed e.g. by Lee & Min)[68] revealed that the beneficial effects of CR are mediated by Sirtuins. Moreover, it was already shown that small molecule compounds can mimic a CR dependent Sirtuin activation even without reducing the calorie intake which still results in beneficial effects on health and lifespan[80,81]. Thus, a detailed understanding of the Sirtuin enzymatic mechanism and especially its modulation is highly desirable since this might reveal opportunities to benefit from CR effects for the treatment of cancer and metabolic & neurodegenerative diseases.

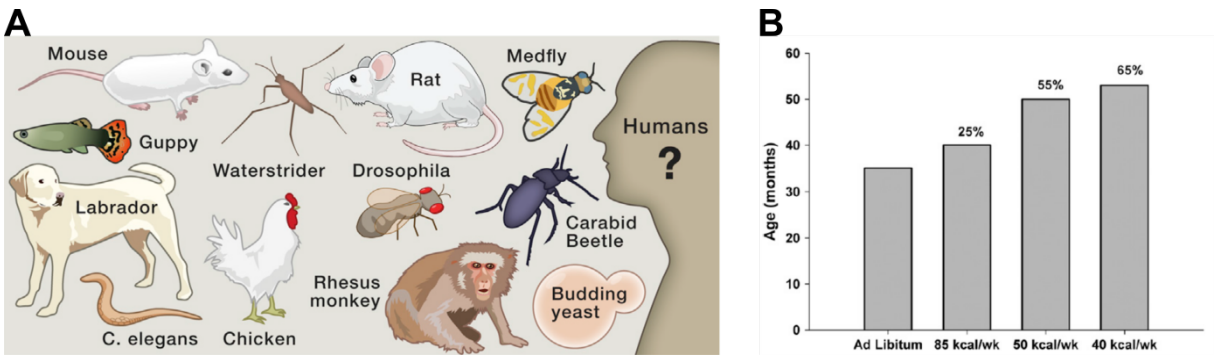

Figure 4: Caloric Restriction (CR) extends the health- and lifespan of various organisms. (A) Beneficial effects of CR on the health- and lifespan are observed in various lower and higher eukaryotes. (B) Dose dependent lifespan extension of mice upon CR started after weaning. (Figures taken from Fontana & Partridge, 2015 and McDonald & Ramsey, 2010)[70,71]

1.2.4. Sirtiuin activities and enzymatic mechanism

Sirtuins were first identified in *S. cerevisiae*, where the histone deacetylase Sir2 (silent information regulator 2) is part of a transcriptional silencing complex[77] and from which the name Sirtuin (Sir*Two*-in) is derived. Being a histone deacetylase, Sir2 catalyzes the removal of an acetyl moiety attached to an ε-amine of a Lys side chain. Different to other PDACs, Sirtuins do not rely on a catalytic Zn^{2+} ion in order to activate a water molecule during catalysis. Instead, Sirtuin activity depends on NAD^+ as a co-substrate, which deems these enzymes metabolic sensors[82]. During catalysis, NAD^+ is cleaved into NAM and ADP-ribose (ADPr), which finally accepts the acyl moiety from a substrate lysine. The Zn^{2+} bound to Sirtuins solely provides structural integrity and does not participate in the enzymatic reaction.

Many structural and biochemical studies helped elucidating the detailed enzymatic mechanism[14,83,84]. The substrate peptide/protein binds via β-sheet like interaction and the acylated lysine resides inside a hydrophobic tunnel. NAD^+ binds to Sirtuins via their Rossmann-fold domain. Once both substrates are bound to the enzyme, a conformational change is induced. This locates the acyl moiety in close proximity to the 1'-hydroxy moiety of the co-substrate NAD^+[85]. The NAM moiety of NAD^+ is localized into a hydrophobic pocket, the so called C-site[83]. With the substrates bound in this manner, an alkylimidate intermediate forms together with the simultaneous release of NAM from NAD^+. Aided by an invariant and conserved His residue, this intermediate is processed into a bicyclic form, from which then the now deacylated lysine is released. The subsequent hydrolysis of the bicyclic intermediate comprises the rate limiting step of catalysis[86] to form the third product, acylADPr. Thus, the net Sirtuin reaction consumes one molecule of acylated substrate and NAD^+ resulting in the products NAM, a deacylated peptide/protein and 2'-O-acyl ADPr (Figure 5).

Interestingly, for Sirt4 – 6 no profound or even no deacetylase activity is observed. With the smallest acyl being an acetyl group and a myristoyl group being the longest known substrate acyl (Figure 1), Sirtuins are rather deemed protein deacylases than protein deacetylases.

However, some Sirtuins are able to remove more than one specific acyl moiety from their substrate depending on the space within and the amino acid composition of the catalytic core. Besides their robust deacetylation activity Sirt1 – 3 are capable of removing propionyl and butyryl groups[42] (Figure 6A). On the contrary, for Sirt5 a weak deacetylase activity is observed while it exhibits robust and strong activity against longer chain and negatively charged acyls. This specificity is caused by an Arg residue within its catalytic core, which positions charged acyls for deacylation – a feature unique to Sirt5 as other Sirtuins contain aliphatic amino acids at this position[31,34] (Figure 6B). Sirt6 contains a long hydrophobic pocket accommodating long chain myristoyl residues (Figure 6C) thereby providing specificity for this acyl moiety[32,53].

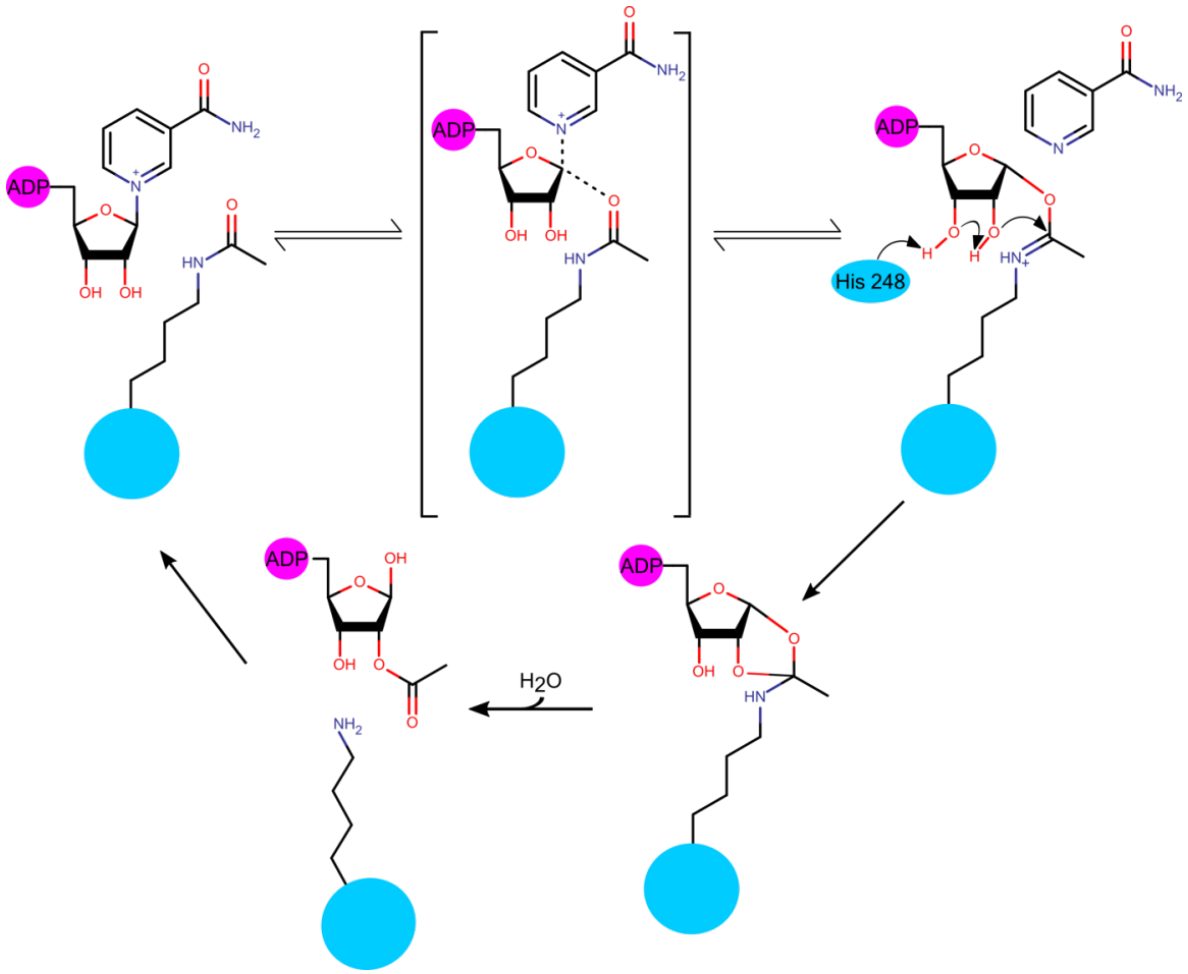

Figure 5: Detailed mechanism for the NAD$^+$ dependent Sirtuin deacylation reaction. The schematic deacetylation by human Sirt3 (blue) mediated by its catalytic His248 residue is shown.

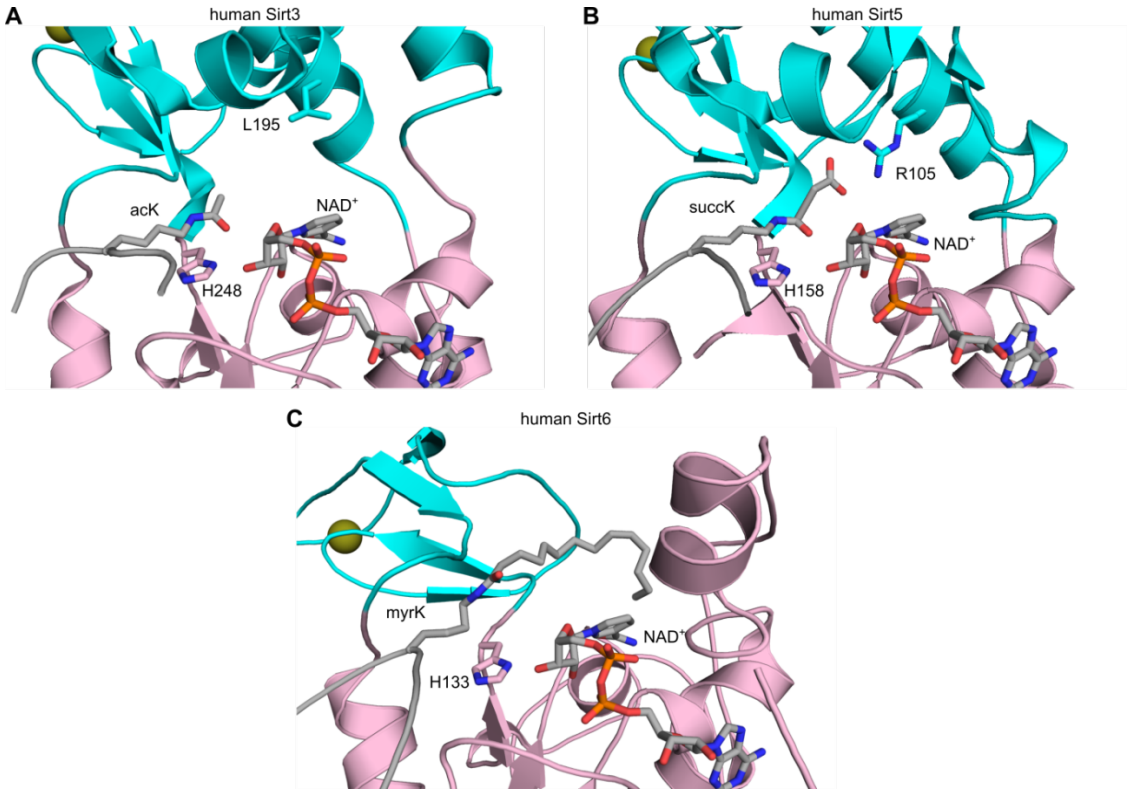

Figure 6: The catalytic core of Sirtuins is optimized for distinct acyl moieties. (A) Sirt3 can harbor substrate Lys that are acylated with aliphatic moieties, e.g. acetyl-Lys, propionyl-Lys and butyryl-Lys. (B) The active site R105 orients charged acylated Lys residues, e.g. malonyl-Lys, succinyl-Lys and glutaryl-Lys, inside the catalytic core of Sirt5. This feature renders Sirt5 a proper desuccinylase while it exhibits only weak deacetylase activity. (C) A hydrophobic pocket within the active site of Sirt6 accommodates long chain acyl moieties, e.g. myristoyl-Lys, resulting in a profound demyristoylation activity compared to a weaker deacetylation activity. Cartoon representation of pdb entries 3GLU, 3RIY & 3ZG6[31–33], with the Zn^{2+} binding domain colored in cyan and the Rossmann-fold domain colored in light pink. Zn^{2+} is displayed as sphere and colored in olive. The side chains of the respective catalytic His and the substrate Lys are depicted as grey sticks and colored by element (blue: nitrogen, red: oxygen). The NAD^+ molecule of 3RIY was modelled into the active sites of Sirt3 and Sirt6 by superimposition of all three Sirtuin structures.

1.3. Sirtuin activity modulation

1.3.1. Physiological Sirtuin modulation

Since organisms have to respond fast to nutrient deprivation and cellular stress, Sirtuins have to be regulated in a cellular context. Besides transcriptional regulation[19] Sirtuins might be affected by PTMs. Despite Sirtuins are well described PDACs, thus removing acyl groups from substrate proteins, only limited information is available about Sirtuins being post translationally modified. Although some studies reviewed by Flick and colleagues[87] already identified several PTMs, only a few of these were characterized. For instance, triple phosphorylation of Sirt1 (S27/47 & T530) upon stress activates its activity against histone 3, while the single phosphorylation of S47 inhibits Sirt1. For Sirt2 likewise inhibiting phosphorylations are reported. Turning to the remaining five mammalian Sirtuins,

phosphorylation sites for Sirt3, Sirt4 and Sirt6 are reported but not characterized. In addition, proteomic analysis of rat liver revealed an uncharacterized Sirt5 acetylation site[88].

Moreover, intracellular binding partners are known to affect Sirtuin activity. For example, Sirt1 can be activated by the nuclear AROS protein (active regulator of Sirt1)[89,90]. Furthermore, metabolites can modulate Sirtuins. Changing the cellular NAD^+ (Figure 7) level is a simple strategy to affect Sirtuin activity. Reduced levels of this molecule were shown to decrease physiological Sirtuin activity[91]. Interestingly, NAD^+ levels increase during CR which results in an enhanced Sirtuin activity[19].

High NAM concentrations result in inhibition of yeast transcriptional silencing and a reduced replicative lifespan[92]. As one of the Sirtuin reaction products, NAM acts as a negative feedback regulator for every Sirtuin: high cellular levels of NAM promote the back reaction resulting in Sirtuin inhibition (Figure 5). Furthermore, even higher NAM concentrations result in competitive binding of free NAM and the NAM part of NAD^+ in its extended and productive form within the C-site[93]. Interestingly, NAM inhibition can be resolved by iso-NAM (Figure 7)[94].

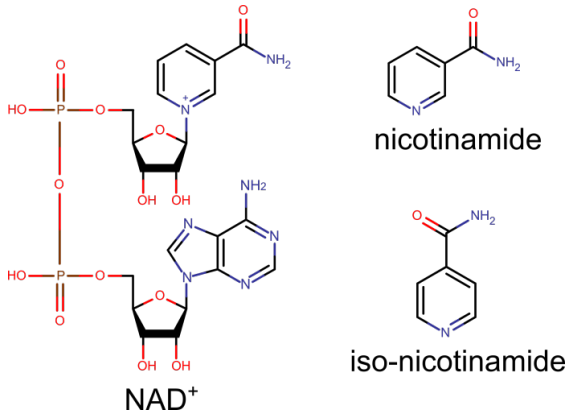

Figure 7: Physiological Sirtuin modulating compounds. Changing cellular NAD^+ concentrations are known to modulate Sirtuins[19]. Adversely, nicotinamide inhibits Sirtuins which can be resolved by iso-nicotinamide (iso-NAM)[93,94].

1.3.2. Small molecule compound regulation

1.3.2.1. Sirtuin inhibition by pharmacological compounds

Some Sirtuins are linked to diseases (see above). Thus, precise inhibition of individual Sirtuins might aid in cancer treatment and the therapy of metabolic or neurodegenerative diseases. With their unique complex enzymatic mechanism, Sirtuins can be targeted in multiple ways, e.g. by using substrate analogues. Peptides that contain an ε-thioacetylated lysine were soon discovered to inhibit Sirt1 – 3[86]. Such thioacyl peptides inhibit Sirtuins by forming a S-alkylimidate intermediate which is far more stable against hydrolysis compared to the standard Sirtuin substrate (cf. Figure 5)[86]. Using peptide sequences derived from their cellular substrates in combination with their preferred substrate acylation Sirt1, Sirt2, Sirt5 and Sirt6 specific inhibitors were already designed[95–97]. In addition, inhibitory peptides are

available, which contain bulky acyl moieties pointing into the C-site of e.g. Sirt5[34]. Inhibitory peptides with such properties then act competitively against both Sirtuin substrates. However, there are some disadvantages of peptide based Sirtuin inhibitors. Apart from their relative large size, peptide inhibitors exhibit a weak cell permeability and suffer from a low biostability[98,99], although they are active in cell based assays[97,100].

In many high throughput screenings, several Sirtuin inhibitor scaffolds were identified (reviewed in e.g. Cen 2010 and Chen 2011, Figure 8)[98,99]. Interestingly, among the first non-peptide Sirtuin inhibitors identified, was Suramin[80]. A complex structure of Suramin bound to Sirt5 revealed, that this symmetric inhibitor locates to both the substrate peptide binding site and the NAD^+ binding site of two Sirtuin enzymes[101]. This binding was also observed for Sirt2 in a computational model[102]. These models indicated that Suramin might act as a pan-Sirtuin inhibitor which was also observed during activity analyses. Other small molecule Sirtuin inhibitors were identified later on. For example, AGK2 was found to inhibit Sirt2 over Sirt1 and Sirt3[103]. Salermide and GW5074 are further yet moderate Sirt2 inhibitors[98,99].

Sirt1 is another prominent target for pharmaceutical modulation. Hence, several inhibitor scaffolds were identified for this Sirtuin as well (Figure 8)[98,99]. Splitomicin derivatives such as HR73 are described as effective Sirt1 inhibitors (IC_{50} < 5 µM). However, HR73 was not tested against further Sirtuins yet. Sirtinol, which is closely related to Salermide, acts as a weak Sirt1 inhibitor. The carboxamide EX527 was shown to inhibit Sirt1 moderately. However, it

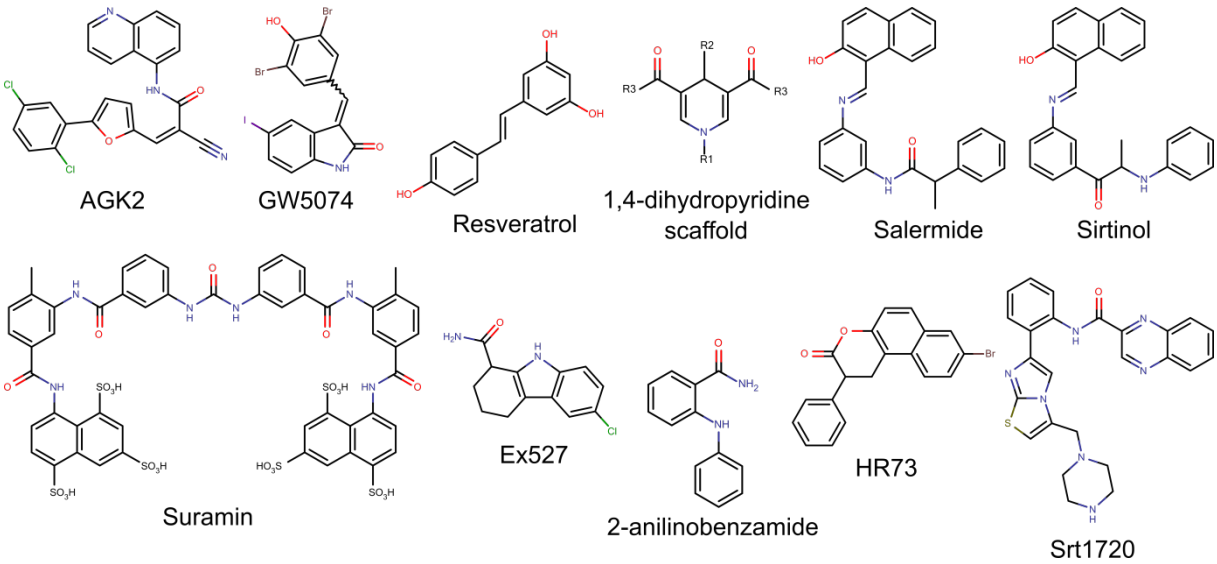

Figure 8: Pharmacological Sirtuin modulators. High throughput screens identified several Sirtuin modulating compounds. However, most of these molecules inhibit Sirtuins (Sirt1: 2-anilinobenzamide, Ex527, HR73, Salermide, Sirtinol; Sirt2: AGK2, GW5074, Salermide; Sirt3: Resveratrol, Srt1720, pan-Sirtuin: Suramin). Only a few Sirtuin activators are reported (Sirt1: Srt1720; Sirt1 & Sirt5: Resveratrol). Based on their structural similarity with NAM and iso-NAM the pharmacological inhibitor 2-anilinobenzamide and the 1,4-dihydropyridine scaffold were designed, with the latter turning out to activate Sirt1-3[98,99,104–106].

acts also against further Sirtuins by preventing product release[104]. Structural similarity towards the physiological inhibitor NAM lead to the development and identification of 2-anilinobenzamides as competitive Sirt1 inhibitors (Figure 7 & Figure 8)[105].

Despite some of these compounds seem to be promising candidates for further drug development, little is known about their specificity, as they were predominantly tested against Sirt1 – 3 using the commercially available fluorescence based Fluor-de-Lys assay (FdL, cf. section 2.4.14). Thus, little is known about their effects on e.g. the mitochondrial Sirt5. So far, only thiobarbiturates were reported as Sirt5 non-peptide inhibitors. However, these compounds also act against Sirt3[107].

1.3.2.2. Sirtuin activators

With the many positive effects Sirtuins contribute to, a specific activation of these enzymes using pharmacological compounds might be a strategy to benefit from Sirtuin activity even without facing CR.

Indeed, small molecule compounds can mimic the beneficial effects of CR without reducing the calorie uptake: Resveratrol – a stilbene found in e.g. grapes (Figure 8) – was observed to increase the lifespan of yeast[80] and metazoans[81] in a Sirtuin dependent manner. Further studies uncovered that Resveratrol activation is substrate sequence dependent[108] and that it locates to the catalytic core of Sirtuins[90]. In fact, the compound directly interacts with the substrate. This can result in both Sirtuin activation and inhibition, again dependent on the substrate sequence[109]. However, several off-targets of Resveratrol are known. (e.g. phosphodiesterases, PDEs)[110,111], which results in mimicking CR effects as well. This indicates the beneficial effects of Resveratrol to be caused by synergistic effects.

In search for more specific regulating compounds, the Sirtuin activating compound (STAC) Srt1720 (Figure 8) was discovered. Srt1720 and related compounds increase Sirt1 activity[112] and results in the health- and lifespan extension of mice[113–115]. Interestingly, Srt1720 and further compounds bind to Sirt1 via a distinct allosteric binding site, thereby increasing the activity of this Sirtuin[116]. Adversely, Srt1720 inhibits Sirt3[117] which is due to the compound binding partially to the enzyme's acLys site and is supported by the NAM part of NAD^{+}[118].

By rational design based on structural comparison of NAM and 2-benzanilinoamide, the 1,4-dihydropyridine (1,4-DHP) scaffold was designed (Figure 8). Surprisingly, this scaffold turned out to activate Sirt1 over Sirt2 and Sirt3 in the FdL-assay[106]. However, with no data available about their effect and specificity in label-free assays, the 1,4-DHP scaffold was not further optimized until recently (Valente et al., 2016 and Suenkel, in preparation)[119].

1.4. Aims of this Study

1.4.1. Identification and Characterization of Sirtuin Posttranslational Modifications

Despite the well-known effects of PTMs on proteins in general, very limited information on Sirtuin PTMs is available. Sirtuin PTMs were rather identified during large scale proteomic approaches[88,120–124] and remained uncharacterized. Targeted approaches that enrich Sirtuins first should facilitate the identification of yet unknown Sirtuin PTMs. Hence, Sirtuins will be purified from native tissue by a yet to establish purification protocol and/or transiently overexpressed from cultured human cells. Then, purified proteins will be analyzed by high resolution mass spectrometry in order to identify novel Sirtuin PTMs. Subsequently, identified Sirtuin PTMs will be characterized for their effect on enzyme activity and protein stability using PTM mimicking Sirtuin variants (e.g. by mutating Ser to Asp and Lys to Gln to mimic phosphorylation or acylation, respectively).

1.4.2. Identification of Physiological Small Molecule Sirtuin Regulators

Cells already contain Sirtuin modulating compounds: the “activator” NAD^+ and the “inhibitor” NAM. However, only until recently NAM could not be characterized thoroughly on its effect on Sirtuins *in vitro*. This was caused by the lack of proper Sirtuin substrates and label-free approaches. In addition, one robust Sirtuin activity assay relies on the consumption of NAM (cf. sections 2.4.14 – 2.4.16 & Figure 9). Therefore, a novel MS-based assay (Figure 9C)[125,126] will be employed to characterize the effects of NAM against the deacetylation and desuccinylation activity of mitochondrial Sirt5. In addition, further Sirtuin binding and thereby possibly regulating molecules might reside within cells. Thus, mitochondrial lysate depleted from its protein content will be tested on its effect on Sirtuin activity. In case of altered Sirtuin activity, the identification of any modulating metabolite (e.g. by mass spectroscopy or nuclear resonance spectroscopy) will be pursued.

1.4.3. Specificity Screening and Optimization of Pharmacological Sirtuin Modulators

Sirtuins are attractive pharmacological targets. However, Sirtuin activity can be either beneficial or even harmful in a condition and tissue specific manner. Thus, any modulating effect has to be specific towards an individual Sirtuin enzyme. Yet most already known compounds (Figure 8) are only tested against one or two different Sirtuin proteins. Besides these, a promising Sirtuin activator scaffold (1,4-DHPs, Figure 7)[106] will be tested in label-free approaches for its specificity against Sirt1 – 3 and Sirt5. If promising candidates can be identified, the modulating mechanism of these compounds will be elucidated. Furthermore, these compounds will be further optimized in collaboration with the laboratory of Prof. Dr. Mai (Sapienza University Rome) to develop potent and specific Sirtuin modulating compounds. These might serve as promising lead compounds for pharmacological research which might even result in future therapeutic applications.

2. Materials & Methods

2.1. Materials

2.1.1. Chemicals, Enzymes, Standards

If not stated differently chemicals were purchased from *Sigma-Aldrich, Applichem, Serva* and *Roth*. Buffers were prepared with ddH_2O (X-CAD, *TKA*), growth media was prepared using desalted water. DNA and protein standards as well as enzymes used for PCR were purchased from *Fermentas, Promega* and *New England Biolabs*. Peptides used were either synthesized by *GL Biochem* or were provided by the Schutkowski group (University of Halle-Wittenberg, Germany; see Table A 1 for peptides used). Sirtuins used for assays were purified using affinity and gel filtration chromatography. If not stated differently, all Sirtuins used contained a N-terminal hexahistidine-tag (His_6) as well as a tobacco etch protease (TEV-protease) cleavage site[18]. Human Sirt4 (aa 25 – 314) was provided by M. Pannek from our lab. Small molecule compounds were either purchased from *Sigma-Aldrich*, provided by Prof. Dr. Wolfgang Bracher (LMU Munich, UBCS 164 – 169) or synthesized by the lab of Prof. Dr. Antonello Mai (Sapienza University Rome, all other UBCS compounds used). The compounds from Munich and Rome were numbered upon reception according to the laboratory's internal compound library (UBCS XXX).

2.1.2. Bacterial Strains

E. coli BL21 (DE3) pLys, *E. coli* BL21 CodonPlus (DE3)-RIL (*Stratagene*) (T7 expression system) or *E. coli* M15 (pREP4) (T5 expression system) were used for heterologous expression of proteins. Vectors were amplified either in *E. coli* TOP10 (*Invitrogen*), *E. coli* GC5 or *E. coli* DH5α. All cells were chemically competent.

Genotype of E. coli strains used:

BL21 (DE3) pLys	*F^- ompT hsdSB (r_B^- m_B^-) gal dcm (DE3) pLysS (Cam^R)*
BL21 CodonPlus (DE3)-RIL	*F^- ompT hsdS (r_B^- m_B^-) dcm^+ Tet^r gal λ(DE3) endA Hte, [argU ileY leuW Cam^r]*
DH5α	*F^- Φ80lacZΔM15 Δ(lacZYA-argF) U169 recA1 endA1 hsdR17 (rK–, mK+) phoA supE44 λ– thi-1 gyrA96 relA1*
GC5	*F^- F80lacZDM15 D(lacZYA-argF) U169 endA1 recA1 relA1 gyrA96 hsdR17 (rk-, mk+) phoA supE44 thi-1 l–T1R*
M15 pREP4	*NaIs Strs Rifs Thi- Lac- Ara+ Gal+ Mtl- F- RecA-Uvr+ Lon+*
	TOP10 *F^-mcrA Δ(mrr-hsdRMS-mcrBC) Φ80lacZΔM15 ΔlacX74 recA1 araD139 Δ(araleu) 7697 galU galK rpsL (StrR) endA1 nupG*

2.1.3. Plasmids

Hst2 (aa 1-294) was expressed from a pRSET vector (*Invitrogen*). The vector containing the Hst2 gene was kindly provided by the Marmorstein group (Wistar Institute/Department of Chemistry, University of Pennsylvania, Philadelphia). Sirt6 full length protein for mutational studies was encoded on a pQE80L vector (*Qiagen*), kindly provided by the Denu group (Madison School of Medicine and Public Health/Department of Biomolecular Chemistry, University of Wisconsin, Madison). All other Sirtuins (Sirt3 aa 114 – 380 or 118 – 399; Sirt5 aa 34 – 302; zSirt5 aa 30 – 298) used for assays and crystallization were expressed from a pET151/D-TOPO vector (*Invitrogen*). All vectors contained an ampicillin (Amp) resistance and a N-terminal His_6-tag. With the exception of the T5 promoter containing pQE80L vector, all vectors contained a T7 RNA polymerase promoter. Sirtuins expressed from human tissue culture were encoded on a pcDNA3.1+ vector which contained a CMV promoter and codes for neomycin and Amp resistance[127].

2.1.4. Oligonucleotide Primers

Oligonucleotide primers for PCR were purchased from *Sigma-Aldrich* (HPLC purified). All primers used are listed in Table A 2 and Table A 3.

2.1.5. Additional Materials

Expendable materials were purchased from *Biorad, Eppendorf, Greiner Bio-One, Hampton Research, Millipore, Molecular Dimensions, Promega*, *Qiagen, TPP* and *SARSTEDT* if not stated differently.

2.2. Microbiology

2.2.1. Sterilization

Instruments, buffers and media were sterilized at 121 °C for 20 min with a DX-150 autoclave (*Systec*).

2.2.2. Transformation of Competent Cells

Chemically competent cells were transformed by adding 100 – 200 ng circular DNA to 50 µl cells followed by 15 min incubation on ice. Cells were afterwards heat shocked for 45 sec at 42 °C. Then 800 µl of Luria-Bertani (LB) medium were added, followed by 1 h incubation at 37 °C. Cells were subsequently plated on LB agar (LB medium with 1.5 % (w/v) agarose) supplemented with 100 µg/ml Amp or directly added to 50 – 100 ml LB medium supplemented with 100 µg/ml Amp as overnight (ON) culture for heterologous protein expression and incubated ON at 37 °C.

LB medium: 1 % (w/v) tryptone, 0.5 % (w/v) yeast extract, 1 % (w/v) NaCl

2.2.3. *E. coli* Cultivation & Heterologous Overexpression of Recombinant Proteins

For overexpression of Hst2 in *E. coli* BL21 (DE3) pLys LB medium supplemented with 100 µg/ml Amp was inoculated 1:250 with cells from ON culture and incubated under shaking at 37 °C. At an OD_{600} of 0.6 – 0.8, cells were cold shocked (20 min on ice) before expression was induced by addition of 0.5 mM IPTG. Afterwards cells were incubated ON at 20 °C. Sirt3 and Sirt5 were overexpressed in *E. coli* BL21 CodonPlus (DE3)-RIL cultured in LB medium supplemented with 100 µg/ml Amp and 34 µg/ml chloramphenicol. For overexpression of Sirt6 (*E. coli* M15 pREP4) terrific broth (TB) medium supplemented with 100 µg/ml Amp was used.

TB medium: 12 % (w/v) tryptone, 24 % (w/v) yeast extract, 0.1 % (v/v) glycerol, 0.07 M KH_2PO_4, 0.072 M K_2HPO_4 (10x stock solution of KH_2PO_4 and K_2HPO_4 was sterilized separately and added before inoculation of the expression culture)

2.2.4. Cell Harvesting and Disruption

Cells were harvested by 15 min centrifugation (*Beckman* JLA 8.1000, 7000x g). If not subsequently disrupted, cell pellets were snap frozen and stored at -80 °C. For disruption, cell pellets were resuspended in a ratio of 1:7 in lysis buffer supplemented with 5 mM PMSF and protease inhibitor cocktail (Sirt6 and Sirt7 expression, *cOmplete EDTA-free*, *Roche*). Lysozyme (0.25 mg per 1 g cell pellet), DNase I (5 µg per 1 g cell pellet) and Sodium Desoxycholate (5 mg per 1 g cell pellet) were added during homogenization (30 min, 4 °C). Afterwards cell suspension was filtered through soft tissue paper. Cells were then disrupted using an Emulsiflex C3 (*Avestin*). Cell debris was cleared by centrifugation (1 h, 4 °C, 50000x g, *Beckman* JA-30.50).

Lysis buffer: 50 mM Tris/HCl pH 7.8, 200 mM NaCl, 0.1 % (v/v) Triton X-100

2.3. Cell Biology

2.3.1. Preparation of Mitochondrial Lysate from Bovine Liver

Bovine liver was cut and washed with ice cold isolation buffer. Using a mezzaluna the liver was further pulpified and homogenized with a chilled tissue homogenizer (type Potter-Elvehjem, *VWR*). The homogenate was then cleared from cell debris by centrifugation (3 min, 4 °C, 500x g). Afterwards the pellet was resuspended in isolation buffer and cleared from cell debris two additional times. All supernatants were further cleared by centrifugation at 20000x g (10 min, 4 °C). The supernatant from this centrifugation was discarded and the pellet was washed at least twice with ice cold isolation buffer. After each washing step, reddish particles were removed and discarded. The remaining mitochondria were then

resuspended in ice cold 20 mM Tris/HCl pH 7.8, 150 mM NaCl and homogenized (tissue homogenizer type Potter-Elvehjem, *VWR*)
Mitochondrial lysate (ML) was prepared by sonication (*Branson* Sonifier 250; four times of 30 – 45 strokes, duty cycle 60 %, and output control 4) from 10 ml of mitochondria suspension (15 mg/ml). Afterwards lysate was distributed into 2 ml reaction tubes and cleared by centrifugation (16000x g, 4 °C, 45 min). The cleared ML was stored in 1 ml aliquots at -80 °C. For isolation of small molecule modulators from mitochondrial lysate, 30 ml of mitochondria suspension were lysed and filtered (10 kDa cutoff) and incubated with 0.05 mg/ml nicotinamidase, 3.3 mM α-ketoglutarate and 2 U GDH (2 h, 37 °C) in order to remove Sirtuin assay interfering nicotinamide (NAM) and NADPH. Afterwards the lysate was boiled (10 min, 95 °C) for protein inactivation.

Isolation buffer: 2 mM HEPES/NaOH pH 7.4, 220 mM mannitol, 70 mM sucrose

2.3.2. Mammalian Cell Culture

For all experiments with cultured human cells either HEK 293T cell line (human embryonic kidney cell line transformed with SV40 large T antigen) or HeLa K were used. These cells were kindly provided by Prof. M. Haigis (HEK 293T, Department of Cell Biology/Harvard Medical School, Boston) and by Prof. Dr. Olaf Stemmann (HeLa K, Department of Genetics, University of Bayreuth).

2.3.3. Cultivation of Mammalian Cells

Cells were cultivated in Dulbecco's Modified Eagle Medium (DMEM, *PAN Biotech*) supplemented with 10 % (v/v) fetal bovine serum (FBS, *PAA*), 100 units/ml penicillin and 0.1 mg/ml streptomycin (Pen/Strep, *PAN Biotech*). Cells were grown in cell culture flasks (*Greiner bio-one*) at 37 °C and 5 % CO_2 in a Binder C150 Incubator (*Binder*). Cells were split twice a week 1:5 to 1:10: after removal of the medium cells were washed once with 1x PBS and incubated with 16 µg/cm^2 Trypsin/EDTA solution (*PAN Biotech*) at room temperature (RT) or 37 °C for 5 min or 1 min, respectively. Trypsination was stopped by adding fresh medium. In order to detach cells from the surface and from each other, fresh medium was pipetted repeatedly. Then the cell suspension was diluted with fresh medium and distributed on new cell culture flasks. Cells were counted using a Neubauer hemocytometer (*Marienfeld*).

1x PBS: 137 mM NaCl, 2.7 mM KCl,10 mM Na_2HPO_4, 2 mM KH_2PO_4, pH 7.4

2.3.4. Storage of Mammalian Cells

Cells were grown to 80 % confluency and harvested by trypsination (300x g, 4 °C, 5 min). Afterwards cells were resuspended to a density of 1.8 million cells/ml. 1 ml aliquots were distributed in cryo vials (*SARSTEDT*) in freezing medium and cooled to -80 °C in an insulated container (*Thermo Scientifc*) at a rate of ca. 1 °C/min. Afterwards cells were stored in liquid nitrogen.

For thawing, one cell aliquot was removed from the liquid nitrogen and placed into a 37 °C water bath. Then the aliquot was used to inoculate 5 ml DMEM supplemented with FBS and antibiotics (see above) and incubated at 37 °C and 5 % CO_2 until the cells attached to the surface (after ca. 4 h). Then the medium was changed to remove remaining dimethyl sulfonate (DMSO).

Freezing medium: DMEM supplemented with 10 % (v/v) FBS and 10 % (v/v) DMSO

2.3.5. Transfection of Mammalian Cells

HEK 293T cells were transfected using the X-tremeGENE HP DNA transfection reagent (Roche) and its corresponding manual. Cells were harvested 48 h post-transfection. For transient Sirtuin expression under serum starvation, medium was exchanged with serum free DMEM supplemented with Pen/Strep 8 h after transfection.

2.4. Bioanalytical & Biochemical Methods

2.4.1. Photometric Determination of Concentrations

The concentration of protein and nucleic acid solutions were measured with a NanoDrop2000 spectrophotometer (*Thermo Scientific*) or a Cary® 50 UV-Vis spectrophotometer (*Varian*) in combination with the appropriate extinction coefficient and the Lambert-Beer equation (Equation 1). Concentration of purified mitochondria was determined via the Bradford method[128].

$$A = \varepsilon \cdot c \cdot d \qquad \text{Equation 1}$$

A:	absorbance	c:	concentration [M]
ε:	absorbance coefficient [$M^{-1}cm^{-1}$]	d:	cuvette thickness (1 cm)

2.4.2. Polymerase Chain Reaction (PCR)

2.4.2.1. Single-Step Mutagenesis

PTM mimics were generated by site-directed mutagenesis using PCR according to Table 2 in a *FlexCycler* PCR machine (*analytikjena)*. Reaction samples of a total volume of 50 µl consisted of 100 ng plasmid DNA coding for the wild type (wt) Sirtuin, 1.5 µM of forward and

Table 2: PCR protocol for site directed mutagenesis (single step).

Step	Temperature	Duration
Start	95 °C	2 min
Cycles	10*	
Denaturation	95 °C	60 sec
Annealing	5 °C below average primer T_m	60 sec
Elongation	68 °C (*Pfu Turbo*) or 72 °C (*Phusion High Fidelity*)	5 min
End	68 °C (*Pfu Turbo*) or 72 °C (*Phusion High Fidelity*)	15 min
	4 °C	∞

*After 10 cycles mutagenesis PCR an additional1 µl polymerase was added and PCR proceeded for 12 further cycles.

reversed primer, 200 µM dNTPs and 1 µl of polymerase and its appropriate polymerase buffer. As polymerases, *Pfu Turbo* (2.5 U/µl, *stratagene*) or *Phusion High Fidelity* (2 U/µl, *NEB*) were used. After mutagenesis PCR template DNA was digested with DpnI (20 U, 1 h/37 °C) before 2.5 µl of the digestion mixture were transformed into *E. coli* Top10, DH5α or GC5. Correct mutations were verified by DNA sequencing (*Eurofins MWG Operon*).

2.4.2.2. Two-Step Mutagenesis

If necessary, a two-step mutagenesis protocol was applied. A vector specific primer (i.e. 'outside primer' that also codes for a restriction enzyme consensus sequence) was used in combination with a mutagenesis primer and plasmid DNA of the respective wt Sirtuin as template DNA. This yielded in amplicons ranging from the 5' end of the Sirtuin coding sequence to the mutation site and from the mutation site to the 3' end of the Sirtuin coding sequence, respectively. Both amplicons were united in equimolar amounts and used as template for a subsequent PCR, in which only the outside primers were used. Afterwards the PCR product was digested with the respective endonucleases and ligated into the target vector. After every PCR, products were analyzed for their correct size by agarose gel electrophoresis and gel purified (Gel extraction kit, *Favorgen Biotech Corp.*, used according to the manufacturer). Outside primers, their corresponding restriction site and sequence are listed in Table A 2. PCR was conducted according to Table 3 and using 2 U *Vent* polymerase (*NEB*). Concentrations of template DNA, primers and polymerase were identical to the single-step mutagenesis protocol.

Table 3: PCR protocol for site directed mutagenesis (two-step).

Step	Temperature	Duration
Start	95 °C	2 min
Cycles	30*	
Denaturation	95 °C	60 sec
Annealing	65 °C	60 sec
Elongation	74 °C	2 min
End	74 °C	15 min
	4 °C	∞

2.4.2.3. Colony PCR

After ligation and prior to sequencing, correct insertion of mutated Sirtuin constructs into the target vector was verified by colony PCR. A single colony from the transformation of the ligated vector was used to inoculate the PCR sample composed of 1.5 µM forward and reverse primer (sequence corresponding to the restriction site motif used for insertion) 200 µM dNTPs and 1 µl of *Phusion High Fidelity* and its corresponding buffer in a total volume of 50 µl.

2.4.3. DNA Digestion

In order to generate single stranded DNA ends ('sticky ends') prior to ligation, 10 U of each endonuclease (*NEB*, cf. Table A 2 for endonucleases used) was incubated with 100 – 500 ng of DNA in its appropriate endonuclease buffer and a total volume of 50 µl for 1 h at 37 °C. Digested DNA was purified by agarose gel electrophoresis and subsequent gel extraction (see above).

2.4.4. DNA Ligation

Ligation of 50 ng linear vector and 37.5 ng insert (molar ratio of 1:3) was performed using 10 U T4 DNA ligase (*NEB*) in a total volume of 20 µl. Ligation mixture was incubated at RT for 10 min or at 16 °C ON. Afterwards 5 µl of ligation sample was transformed into *E. coli* Top10, DH5α or GC5.

2.4.5. Preparation of Plasmid DNA

Plasmid DNA was either purified using the FavorPrep™ Plasmid Extraction Mini Kit or Endotoxin free Maxi Kit, if plasmids were used for mammalian cell transfection (*Favorgen Biotech Corp.)* according to the manufacturer's manuals.

2.4.6. Agarose Electrophoresis

DNA was separated and analyzed using agarose gel electrophoresis. Gels were composed of 0.7 – 2 % (w/v) agarose in 1x TAE buffer supplemented with 1 µg/ml ethidiumbromide. Electrophoresis was performed within a *Sub-Cell GT Agarose Gel Electrophoresis System* (*Biorad*).

1x TAE buffer: 40 mM Tris/Acetate pH 8.0, 0.2 mM. EDTA

DNA sample buffer: 2 mM Tris/HCl pH 8.0, 0.2 mM EDTA, 10 % (v/v) glycerol, 0.01 % (w/v) bromophenol blue

2.4.7. SDS-Polyacrylamide Gelelectrophoresis (SDS-PAGE)

Proteins were separated according to their molecular weight by discontinuous denaturing SDS-PAGE[129]. Gels consisted of 2 cm stacking gel (5 % polyacrylamide, 37.5:1 acrylamide:bisacrylamide) and 5 cm resolving gel (15 % polyacrylamide, 37.5:1 acrylamide:bisacrylamide). SDS-sample buffer (50 mM Tris/HCl pH 6.8, 2 % (w/v) SDS, 100 mM β-Mercaptoethanol, 0.02 % (w/v) bromophenol blue) was added to the samples which were subsequently boiled (5 min at 95 °C). For electrophoresis a *Mini Protean 3 Cell* (*Biorad*) was used with a constant current of 130 – 180 V.

Gels were visualized by staining for 30 sec with hot Coomassie staining solution (0.025 % (w/v) Coomassie Brilliant Blue R-250 (*Applichem*), 50 % (v/v) methanol, 10 % (v/v) acetic acid). Background color was destained by hot water (2x 10 min). The *broad range* (*Biorad*) molecular weight marker was used for molecular weight estimation.

Stacking gel: 125 mM Tris/HCl pH 6.8, 0.1 % (w/v) SDS, 0.1 % (v/v) TEMED (N,N,N',N'-tetramethylethylendiamine), 0.65 % (w/v) ammonium-persulfate (APS), 5 % (v/v) polyacrylamide (37.5:1 acrylamide: bisacrylamide) (*Roth*)

Resolving gel: 375 mM Tris/HCl pH 6.8, 0.1 % (w/v) SDS, 0.1 % (v/v) TEMED, 0.6 % (w/v) APS, 15 % (v/v) polyacrylamide (37.5:1 acrylamide: bisacrylamide) (*Roth*)

SDS running buffer: 25 mM Tris/HCl, 192 mM Glycin, 0.1 % (w/v) SDS

2.4.8. Western Blotting

Prior to Western blotting, samples were separated by SDS-PAGE in combination with a prestained molecular weight standard (Color Plus broad range, *NEB*). Then the gel was placed on a polyvinylidene fluoride (PVDF) membrane of an appropriate size, which was activated in 100 % methanol and washed twice with blotting buffer. Membrane and gel were

packed tightly between both electrodes using Whatman filters soaked in blotting buffer. Proteins were transferred using a Trans-Blot SD Semi-Dry Transfer Cell (*Biorad*) and a current of 2 mA/cm² for 80 min. After protein transfer the membrane was blocked in milk buffer (30 min, RT) followed by an ON incubation with primary antibody at 4 °C. Secondary antibody incubation was performed at RT for 1 h. After each antibody incubation step the membrane was washed thrice with 1x TBST (15 min, RT). Membranes were analyzed by fluorescence scan using an Odyssey SA infrared imaging system (*Licor*).

Blotting buffer:	25 mM Tris/HCl pH 8.5, 190 mM glycine, 0.05 % (w/v) SDS, 20 % methanol
Milk buffer:	5 % (w/v) milk powder in 1x TBST
1x TBST:	50 mM Tris/HCl pH 7.4, 150 mM NaCl, 0.1 % (w/v) Tween20
Primary antibodies:	rabbit anti-Sirt5 (*Sigma*) or mouse anti-Flag (*Sigma*); antibodies were diluted 1:2000 in milk buffer supplemented with 0.02 % (w/v) NaN_3
Secondary antibodies:	goat anti-rabbit or goat anti-mouse (IR-Dye LT689, *LICOR*) were diluted 1:15000 in 1x TBST supplemented with 0.01 % (w/v) SDS

2.4.9. Purification of Recombinant Proteins after Heterologous Expression in *E. coli*

Wild type and PTM-mimicking Sirtuins were purified as already described[18]. In brief, recombinant proteins were purified from cell lysate by immobilized metal ion affinity chromatography (IMAC) using TALON® Cobalt Beads (*Clontech*) or Ni^{2+} beads (*Roche*). Afterwards size exclusion chromatography (SEC) was performed using either a Superose 12 3/100 column, a Sephadex 200 3/100 column or a Superose 75 16/30 column (*GE Healthcare*) in combination with an ÄKTApurifier (*GE Healthcare*).

Affinity material (2 ml beads per 1 l expression culture) was equilibrated with 20 column volumes (CV) lysis buffer and incubated with the cleared cell lysate for 1 h at 4 °C on a magnetic stirrer or on a rotator. Then beads were separated from the supernatant and washed with 10 CV of each washing buffer. Protein was eluted with elution buffer in 4 ml fractions. If needed for crystallization trials, protein was digested with TEV-protease in a ratio of 1 mg TEV-protease per 20 mg protein to remove the N-terminal His_6-tag. Proteolytic cleavage was performed ON at 4 °C in a 10 kDa cutoff dialysis membrane in order to exchange the IMAC elution buffer against SEC buffer (without reducing agent). Subsequently the digestion mixture underwent a second affinity chromatography in order to remove uncleaved protein, cleaved His_6-histidine peptides as well as the His_6-histidine tagged protease. SEC columns were equilibrated with 1.5 CV SEC buffer before protein was loaded and eluted with 1.5 CV SEC buffer in 300 µl fractions.

Buffers for human Sirtuin and zebrafish purification:

Washing buffer 1: 50 mM Tris/HCl pH 7.8 or 8.5[(a)], 500 mM NaCl

Washing buffer 2: 50 mM Tris/HCl pH 7.8 or 8.5, 200 mM NaCl, 5 mM imidazole

Elution buffer: 50 mM Tris/HCl pH 7.8 or 8.5, 200 mM NaCl, 250 mM imidazole

SEC buffer: 20 mM Tris/HCl pH 7.8 or 8.5, 150 mM NaCl, 2.5 mM DTT or 1x PBS (for subsequent chemical modification)

a) buffer pH varied for the respective Sirtuin: pH 7.8 for Sirt5 &Sirt6, pH 8.5 for Sirt3 and zSirt5

Hst2 purification buffers:

Washing Buffer: 20 mM Tris/HCl pH 8.5, 150 mM NaCl, 10 mM imidazole

Elution Buffer: 20 mM Tris/HCl pH 8.5, 150 mM NaCl, 150 mM imidazole

SEC buffer: 20 mM Tris/HCl pH 8.5, 100 mM NaCl, 10 mM DTT

2.4.10.Sirtuin Purification from Native Tissue

2.4.10.1. Blue Sepharose Purification

Sirtuins from bovine ML were purified using Blue Sepharose CL-6B. 500 µl ML were set to pH 6 and supplemented with 0.1 mM Cibacron Blue (CB) to prevent unspecific binding and incubated ON with 50 µl blue sepharose CL-6B beads. Afterwards beads were washed with 10 CV of each washing buffer and eluted in 100 µl fractions.

Washing buffer 1: 20 mM Bis-Tris pH 6, 25 µM $ZnCl_2$, 1 mM DTT, 0.25 mM CB, 1 M NaCl

Washing buffer 2: 20 mM Bis-Tris pH 6, 25 µM $ZnCl_2$, 1 mM DTT, 0.25 mM CB, 150 mM NaCl

Elution buffer: 20 mM CHES pH 10, 150 mM NaCl, 1 mM CB

2.4.10.2. Immunopurification

Pulldown experiments with Sirt5 specific antibodies (AV40125, *Sigma-Aldrich,* also used for Western blotting) were performed using the Protein G Immunoprecipitation Kit (*Sigma-Aldrich*) and its corresponding manual. In brief, 400 µl ML were pre-cleared from unspecific binding proteins with 20 µl Protein G Sepharose (1.5 h, 4 °C, overhead shaker). Then ML was transferred into a spin column, supplemented with 5 µg Sirt5 antibodies (*Sigma*), adjusted to a final volume of 600 µl and incubated ON (4 °C, overhead shaker). Then 30 µl of Protein G sepharose was added and incubated 2 h at 4 °C. Afterwards beads were recovered (12000x g, 4 °C, 30 sec) and washed twice with 1x IP buffer supplemented with 0.5 mM NaCl and 0.1 % (w/v) SDS, three times with 1x IP buffer and once with 0.1x IP buffer. The beads were boiled in 50 µl 1x SDS sample buffer (10 min, 95 °C)

2.4.11.Anti-FLAG® Sirtuin Purification from Cultured Human Cells

Sirtuins overexpressed from mammalian cells were purified using the ANTI-FLAG® M2 Affinity Gel (*Sigma-Aldrich*) and its corresponding manual. Cells were lysed in 1x PBS, pH 7.4 supplemented with phosphatase inhibitor (PhosSTOP, Roche), protease inhibitor (cOmplete EDTA-free, *Roche*) and 2 % (v/v) Triton X-100. Protein was eluted with either SDS-Sample buffer or 0.1 M glycine HCl, pH 3.5 (20 min, 37 °C, neutralized with 10 % (v/v) 10x PBS).

2.4.12.Interaction Analysis using Microscale Thermophoresis (MST)

The interaction between Sirtuins and ligands was analyzed by MST using a Monolith NT.labelfree (*Nanotemper Technologies*, LED power 20 %, laser power 25 %)[130,131]. This technique analyzes the mobility of protein/ligand complexes in a temperature gradient of 1 – 5 K via the protein's Trp fluorescence. Increasing ligand concentrations alter this mobility, which can be used for K_D determination.

If a substance interfered with labelfree MST analysis (e.g. when a substance exhibits the similar fluorescence excitation and emission as Trp thereby overshadowing complex MST) a Monolith NT.115 (*Nanotemper Technologies*, LED power 20 %, laser power 20 %) in combination with fluoresceinthioisocyanate (FITC) labeled protein was used.

For protein labelling Lys residues a 1 mg/ml protein solution in 1x PBS, pH 7.4 was incubated with FITC in a molar ratio of 1:2 (dissolved in 1x PBS, pH 7.4) for 1 h at RT in the dark. Afterwards free FITC was removed by gel filtration over a NAP10 column (*GE Healthcare*) against 1x PBS, pH 7.4.

10 nM of labeled protein or 1 µM of unlabeled protein was used in combination with varying concentrations of the respective titrant in absence or presence of saturating concentrations of additional ligands (e.g. small molecule compound or Sirtuin substrates). Raw MST data was background corrected and normalized to the upper baseline (= 100 % bound) then fitted using Equation 4.

Monolith NT.115:	λ_{ex}:	470 nm	λ_{em}:	520 nm
Monolith NT.labelfree:	λ_{ex}:	270 nm	λ_{em}:	370 nm

2.4.13.Thermal Shift Denaturation Assay

The thermal shift denaturation assay was performed as described[132]. 2 µM of protein were supplemented with 1x Sypro Orange (*Invitrogen*) in a total volume of 50 µl 20 mM Tris/HCl pH 7.8, 150 mM NaCl in absence or presence of either 2.5 mM NAD^+, 100 µM substrate peptide or 100 µM substrates peptide in combination with 2.5 mM ADPr. Samples were sealed with 15 µl mineral oil and thermal denaturation was analyzed with a FluoDia T70 (*Photal*, λ_{ex} = 465 nm, λ_{em} = 580 nm).

2.4.14.Fluorometric Activity Assay

Initial activity screens were conducted using a commercial fluorescence based activity assay kit (*Fluor-de-Lys*® (FdL), *ENZO,* Figure 9A). 1.5 µM Sirtuin was incubated with 50 – 100 µM acetylated or succinylated FdL-peptide and 100 – 500 µM NAD^+ at 37 °C. Reaction was stopped by adding FdL developer (10 mg/ml trypsin, 1 mM NAM in 50 mM Tris/HCl pH 7.5). During a further incubation at RT for 1 h the fluorophore was released specifically from deacylated peptides by a tryptic digest. Afterwards the fluorescence signal was measured with a FluoDia T70 (*Photal*, λ_{ex} = 360 nm, λ_{em} = 460 nm.)

2.4.15.Coupled Enzymatic Deacylation Assay

Sirtuin kinetics as well as dose-response experiments were performed using a continuous deacylation assay (Figure 9B)[133] that couples three different enzymatic reactions. Briefly, 1 – 10 µM Sirtuin was incubated with 0.1 – 1 mM NAD^+ and varying substrate peptide concentrations or with 200 µM substrate peptide and varying NAD^+ concentrations, respectively. Deacylation reaction was monitored utilizing several enzymatic reactions: NAM formed by the Sirtuin reaction was converted into ammonia and nicotinic acid by 2 µM nicotinamidase from *S. enterica* present in the reaction mixture. Formed ammonia was transferred onto α-keto glutarate (3.3 mM) by 2 U GDH which stochiometrically oxidizes NADPH (0.2 mM) to $NADP^+$ per ammonia molecule and thus per peptide deacylated. The decrease of NADPH absorbance at a wavelength of 340 nm was measured with a LAMBDA-Scan spectrophotometer (*MWG Biotech*).

Kinetic data derived from the continuous peptide deacylation assay was processed using Equation 2 to convert the NADPH consumption by GDH to the production of deacylated peptide per Sirtuin mass and per minute.

$$v[\mathrm{nmol}/(\mathrm{mg}\cdot\mathrm{min})] = \frac{\Delta A_{340}\cdot V}{m(\mathrm{Sirtuin})\cdot \varepsilon_{340}\cdot d} \qquad \text{Equation 2}$$

v: formed product per Sirtuin mass and per minute

ΔA_{340}: change in NADPH absorption at 340 nm per minute

d: path length (0.3 cm)

ε_{340}: extinction coefficient NADPH at 340 nm ($6220\cdot10^{-6}$ $\mu M^{-1}cm^{-1}$)

V: sample volume (80 µl)

2.4.16.Mass Spectrometric Deacylation Assay

If the continuous deacylation assay was not applicable (e.g. if compounds interfered with the coupled enzymatic reactions) a mass spectrometric (MS) deacylation assay was used as described (Figure 9C)[125,126]. Reaction samples contained 1 – 10 µM Sirtuin, 0.1 – 2.5 mM NAD^+ and varying peptide concentrations in 20 mM Tris/HCl pH 7.8. Deacylation reaction was started by adding peptide and stopped after 2.5 – 20 min incubation at 37 °C with a final concentration of 0.25 % (v/v) trifluoroacetic acid (TFA). Samples were diluted with 0.1 % formic acid (FA) to reach a peptide concentration of 1 µM before they were filtered (10 kDa cutoff, *Amicon*) to remove the enzyme. Samples were stored at – 20 °C if not analyzed directly.

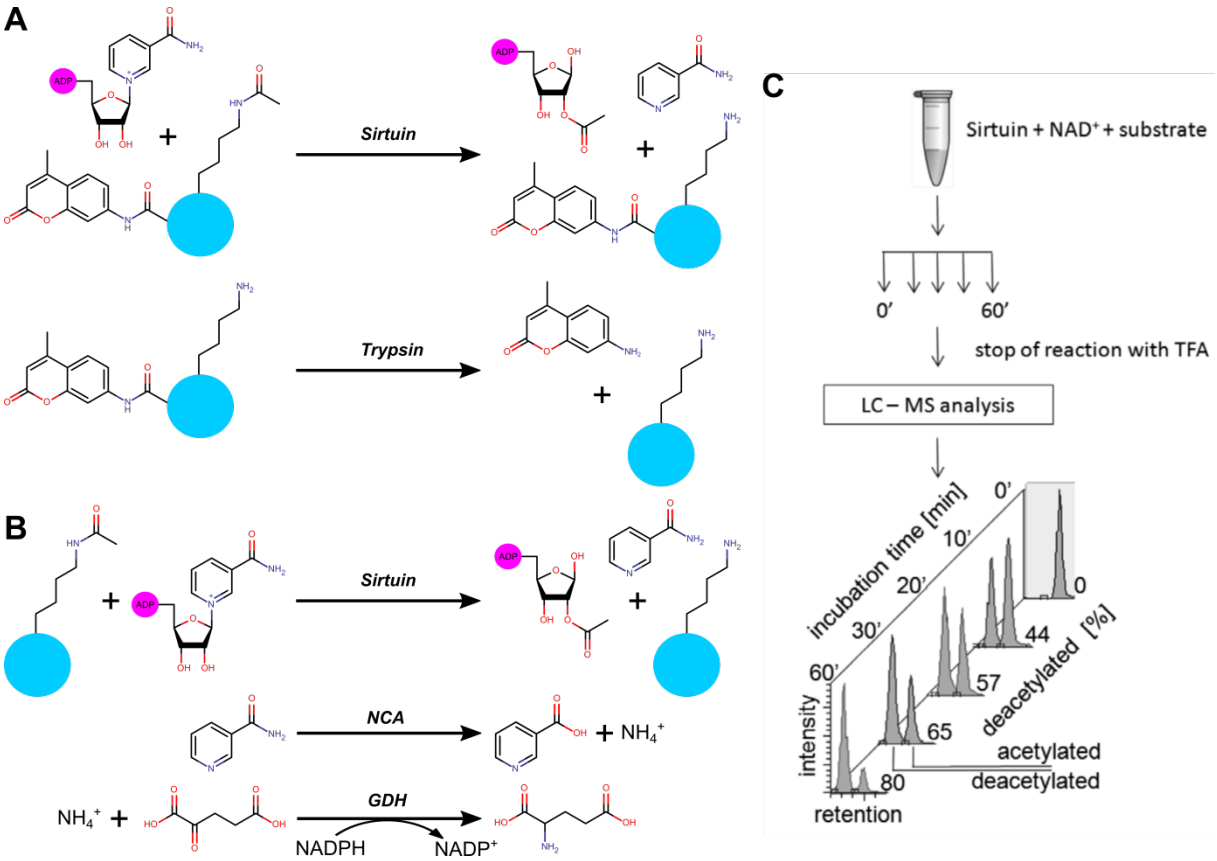

Figure 9: Available Sirtuin activity assays. (A) The commercially available Fluor-de-Lys (*Enzo Lifesciences*) employs substrate peptides labelled with a coumarin derivative via a peptide bond. The Sirtuin reaction removes the acetyl moiety from the substrate lysine thereby turning the peptide into a substrate for the trypsin protease. Upon proteolytic cleavage the fluorophore is released which results in an increased fluorescence signal. (B) The coupled continuous assay[133] can be used in combination with label-free substrate peptides or proteins. NAM produced from the Sirtuin reaction is consumed by nicotinamidase (NCA) and the released ammonia is transferred onto α-ketoglutarate to form glutamate. This reaction depends on the oxidation of NADPH which can be monitored by an absorption decrease at a wavelength of 340 nm. (C) The MS-based Sirtuin activity assay is a semi-quantitative approach to directly analyze the amount of substrate and product peptide after a given period of time[125,126]. Thus, this assay circumvents artifacts sometimes observed for small molecule compounds, e.g. label/ligand interaction, interfering optical properties or off-target modulation of coupled enzymes (Figure adapted from Fischer et al., 2012)[126].

2.4.17. Assay Data Processing

Data derived from enzymatic assays, MST experiments and thermal denaturation shift assays were fitted using *GraFit7* (*Erithacus Software Ltd.*). IC_{50} values were determined using the "IC50 1-100" equation (Equation 3). The K_d was determined with the "1-site with background" equation (Equation 4). Kinetic constants were derived according to Michaelis & Menten[134] and a steady state assumption[135] ("enzyme kinetics" equation, Equation 5). Melting temperatures were determined using Equation 6. Graphs were exported from *GraFit7* and arranged using the open source software *Inkscape 0.91* (www.inkscape.org).

$$y = \frac{100\%}{1 + \left(\frac{x}{IC_{50}}\right)^{s}} \qquad \text{Equation 3}$$

y: rel. activity [%] x: inhibitor concentration [µM]
s: slope factor IC_{50}: half maximal inhibitory concentration [µM]

$$[\text{Bound}] = \frac{\text{Capacity} \cdot [\text{Free}]}{K_d + [\text{Free}]} + \text{Background} \qquad \text{Equation 4}$$

[Bound]: concentration of bound ligand [Free]: concentration of free ligand
Capacity: amplitude of binding curve K_D: dissociation constant
Background: background signal

$$v = \frac{v_{max} \cdot [S]}{K_m + [S]} \qquad \text{Equation 5}$$

v: reaction rate K_m: Michaelis-Menten constant
v_{max}: maximum rate [S]: substrate concentration

$$y_T = \frac{f + n \cdot z(d + u \cdot z)e^{-\frac{H}{R} \cdot \left(\frac{1}{z} - \frac{1}{T_m}\right) - \frac{C}{R} \cdot \left(1 - \frac{T_m}{z} + h\frac{T_m}{z}\right)}}{1 + e^{-\frac{H}{R} \cdot \left(\frac{1}{z} - \frac{1}{T_m}\right) - \frac{C}{R}\left(1 - \frac{T_m}{z} + h\frac{T_m}{z}\right)}} \qquad \text{Equation 6}$$

f: native protein H: reaction enthalpy
z: temperature [°C] + 273.15 T_m: melting temperature
n: baseline slope native protein R: gas constant
d: denatured protein C: constant (6000)
u: baseline slope denatured protein

2.5. Mass Spectrometry

2.5.1. In Gel Tryptic Digest

After SDS-PAGE protein bands were sliced out from the destained acrylamide gel, milled using a scalpel and transferred into a 1.5 ml reaction tube. Then 100 µl of 50 % (v/v) methanol were poured on the gel pieces. After a few seconds the methanol was discarded and the gel slices were destained with 100 µl of 50 mM NH_4HCO_3, 50 % (v/v) acetonitrile (ACN) at 37 °C (1000 rpm, Thermomixer compact, *Eppendorf*) until they were completely clear. Destaining solution was changed every 15 min. Afterwards gel pieces were completely dried in a vacuum concentrator (max. rpm, 55 °C, BA-VC-300H, *H. Saur Laborbedarf*), subsequently re-hydrated with 50 µl of 25 mM DTT in 25 mM NH_4HCO_3 pH 8.5 and 20 min reduced at RT. Afterwards the supernatant was removed and samples were alkylated in 50 µl 55 mM iodoacetamide (IAA, in 25 mM NH_4HCO_3 pH 8.5) for 20 min at RT in the dark. After removing the supernatant, gel pieces were washed with 20 volumes of ddH_2O for 30 sec and dehydrated with 200 µl 25 mM NH_4HCO_3 pH 8.5, 50 % (v/v) ACN (15 min) and with 100 µl 100 % ACN (5 min) and dried in a vacuum concentrator again. Afterwards, gel slices were re-hydrated with 10 µl of 12.5 ng/µl porcine trypsin (dissolved in 25 mM NH_4HCO_3 pH 8.5, *Promega*) for 10 min at RT. Then the gel slices were covered with 25 mM NH_4HCO_3 pH 8.5. After ON incubation at 37 °C the supernatant was recovered and stored separately. Gel pieces were resuspended in 50 % (v/v) ACN, 0.5 % (v/v) TFA until they were completely covered with buffer and sonified for 20 min at RT (ultrasonic cleaner USC 300TH, *VWR*). The supernatant was pooled with the supernatant from ON digestion and evaporated in a vacuum concentrator. Afterwards peptides were dissolved in 20 µl 0.1 % (v/v) FA prior to MS analysis.

2.5.2. In Solution Tryptic Digest

For in solution tryptic digest 2.5 µg protein were dissolved in a final volume of 50 µl with NH_4HCO_3 pH 8.5. If wanted, cystines were reduced using 10 mM DTT and incubated 30 min at RT. Then free sulfhydryl moieties were alkylated with 20 mM IAA (30 min, RT, dark) followed by addition of 1.25 µg porcine trypsin and 4 h or ON digestion at 37 °C. Afterwards the sample was acidified with 25 µl of 10 % (v/v) TFA and filtered (10 kDa cutoff, *Amicon*) prior to MS analysis.

2.5.3. Mass Spectrometric Analysis

2 pmol of filtered sample were analyzed using either a LTQ/XL mass spectrometer (*Thermo Scientific*) connected to a dual pump EASY-nLC II (*Thermo* Scientific) or Triple ToF 5600+ mass spectrometer (*AB SCIEX*) connected to a dual pump Prominence UPLC (*Shimadzu*) and the corresponding software. Peptides were separated with a linear gradient from 0 % to

45 % (v/v) buffer B within 30 min (buffer A: 0.1 % (v/v) TFA; buffer B: 70 % (v/v) ACN, 0.1 % (v/v) TFA) and a fritless 100 µm ID capillary reversed phase column (Dr. Maisch, Repsosil C18, AQ, 3 µm) with a flow rate of 250 nl/min. For the Prominence UPLC/Triple ToF setup the following gradient was used: 0 – 35 min 5 – 55 % (v/v) buffer B, 35 – 37 min 55 – 100 % (v/v) buffer B, 37 – 45 min 100 % (v/v) buffer B, 45 – 60 min 5 % (v/v) buffer B.

With the LTQ/XL a full MS was scanned between 375 and 1600 m/z followed by a full MS/MS scan of the three peaks of the highest intensity. Desolvation capillary was set on 180 °C, the relative collision energy was set to 35 %, dynamic exclusion was enabled with a repeat count of 1 and a one minute exclusion duration window. The Triple ToF recorded a full MS scan between 375 – 1800 m/z followed by a MS/MS scan between 100 – 1500 m/z. Accumulation time for ToF was set to 0.25 sec, for MS/MS to 0.1 sec. The ion spray voltage was set to 2900 V, for the curtain gas to 35 V and for the ion source gas to 4 V. The curtain plate was heated to 150 °C.

For the MS based Sirtuin activity assay peptides were relatively quantified using either *Qual Browser* (*Thermo Xcalibur 2.1* software) or *Skyline* software[136]. For each (de)acylated peptide species of the substrate peptide used extracted ion chromatograms with a mass window of ± 2 m/z were generated, peak areas were calculated by the software and transferred to *Excel 2010* and *Grafit7* for analysis. All MS based assays were analyzed by calculating the relative amount of deacylated peptide (= Deacylation [%]) according to Equation 7. For dose response experiments the relative amount of deacylated peptide of the control sample without compound was set to 100 % to calculate the relative activity in presence of compound.

In case of protein identification, MS raw data was processed using either *Proteome Discoverer 1.3* (*Thermo Scientific*) or *Protein Pilot (AbSciex)*. For data analysis using Protein Pilot 2+ – 5+ charged ions were used in combination with an exclusion isotope window of 4. Exclusion window was set to 30 sec after the first occurrence. Top 20 precursor ions were used for protein identification.

$$\text{Deacylation}[\%] = \frac{\text{area}(\text{deacylatedPeptide})}{\text{area}(\text{deacylatedPeptide}) + \text{area}(\text{acylatedPeptide})} \cdot 100\% \quad \text{Equation 7}$$

2.6. Crystallographic Methods

2.6.1. Crystallization Experiments

Proteins were crystallized using the vapor diffusion method at 20 °C. Commercial crystallization screens from *Qiagen* (*JCSG Core I – IV, JCSG+*) and *Molecular Dimensions* (*PACT Premier Screen*) in combination with MRC2 or MRC3 96-96-good plates and *Crystal Clear* cover (*Hampton Research*) were used for identifying protein crystallization conditions. Crystallization screens were composed of 50 µl reservoir solution and 0.4 µl drops (ratio

protein to reservoir solution = 1:1) were set up with a *Phoenix* pipetting robot (*Art Robbins Instruments*).

Crystallization conditions were optimized in 24 well *Cryschem* plates (sitting drop, *Hampton Research*) or pre-greased *VDX* plates (hanging drop, *Hampton Research*) sealed with *Crystal Clear* tape or glass cover slips (*Hampton Research*), respectively. Conditions were optimized by varying precipitant and/or salt concentration in one dimension and pH in the second dimension. Optimization experiments contained 1 ml reservoir solution and 1 µl drops (ratio protein to reservoir solution = 2:1 – 1:2). Microseeding was performed by transferring crystal debris with a cat's hair into freshly set up crystallization drops.

2.6.2. Data Collection

Crystals were fished with a *Cryo-Loop* (*Hampton research*) and snap frozen with liquid nitrogen in cryo-protecting solution (reservoir solution supplemented with 25 % (v/v) glycerol). Diffraction was tested with a *marµX* micro beam system (*MAR Research*). Data sets were collected at BESSY II beam line 14.1 (Helmholtz Zentrum Berlin-Adlershof, Berlin, Germany) using 100 K liquid nitrogen cooling.

2.6.3. Analysis of Diffraction Data and Model Building

XDS[137] *or XDSapp*[138] were used for space group determination, diffraction data indexing, integration and scaling. Missing phase information was gained by molecular replacement using the *Molrep* software[139] and the following model structures: Hst2 in complex with ADPR (pdb entry: 2QQF)[140], Sirt3 in complex with ADPr (pdb code 4BN4)[118], Sirt3 with a PEG molecule or an acPeptide bound to its active site (pdb entries: 3GLS & 3GLR)[33] or Sirt5 from *D. rerio* in complex with ADPr (unpublished model from in house-data). Before molecular replacement only the Zn^{2+} was kept in the model structures and water and any ligand molecule were removed. Maximum likelihood restraint refinement was performed using *Refmac5*[141] (isotropic B-factor refinement). *Molrep* and *Refmac5* were used within the interface of the software package CCP4[142], which also included the temperature factor analysis software *baverage*[143] to determine B-factors. Models were built using *coot*[144], graphical representations were generated using *PYMOL* (www.pymol.org).

Sirt5 models with lysine derivatives bound were created by fitting lysine derivatives into the electron density of Sirt5 substrate peptides or inhibitory peptides from zSirt5/peptide complex structures[34] and subsequent superposition of zSirt5 and Sirt5 in complex with a succinylated peptide and NAD^+ (pdb entry: 3RIY)[31].

All compounds were drawn using *marvinsketch* (*ChemAxon*). Topology information was generated from the .mol-file generated by *marvinsketch* via the ProDRG server (http://davapc1.bioch.dundee.ac.uk/cgi-bin/prodrg)[145].

3. Results

3.1. Identification of Sirtuin Posttranslational Modifications

3.1.1. Purification of endogenous Sirtuins from Bovine Liver Mitochondria

3.1.1.1. Sirtuin Purification using Blue Sepharose CL-6B

After they are translated, eukaryotic proteins can undergo many different kinds of modifications, which are known to affect protein/ligand interaction, enzymatic activity and cellular localization. However, little is known about posttranslational modifications of Sirtuins and their effect on these enzymes. Although some phosphorylation sites on Sirt3-6 were already identified, nothing is known about their influence on these enzymes. Only for the two isoforms Sirt1 and Sirt2 some data are available (cf. section 1.3.1). Thus, in a first approach to identify and subsequently characterize PTMs on mitochondrial Sirtuin, purification of Sirt3 and Sirt5 from a native tissue was aimed.

While recombinant proteins usually contain tags to facilitate purification, endogenous proteins are missing such a feature. Hence, a purification protocol for the purification of endogenous Sirtuins had to be developed.

Blue Sepharose CL-6B can be used as an affinity material for many NAD(P)$^+$/NAD(P)H binding proteins (e.g. for NADOX from *Th. thermophilus*[146] or archaeal Sir2-Af2 from *Archeoglobus fulgidus*[147]). The cibacron dye coupled to the resin remotely resembles these dinucleotides (Figure 10A). Therefore, the capability of this material for isolating Sirtuins from crude extracts obtained from bovine liver mitochondria was tested.

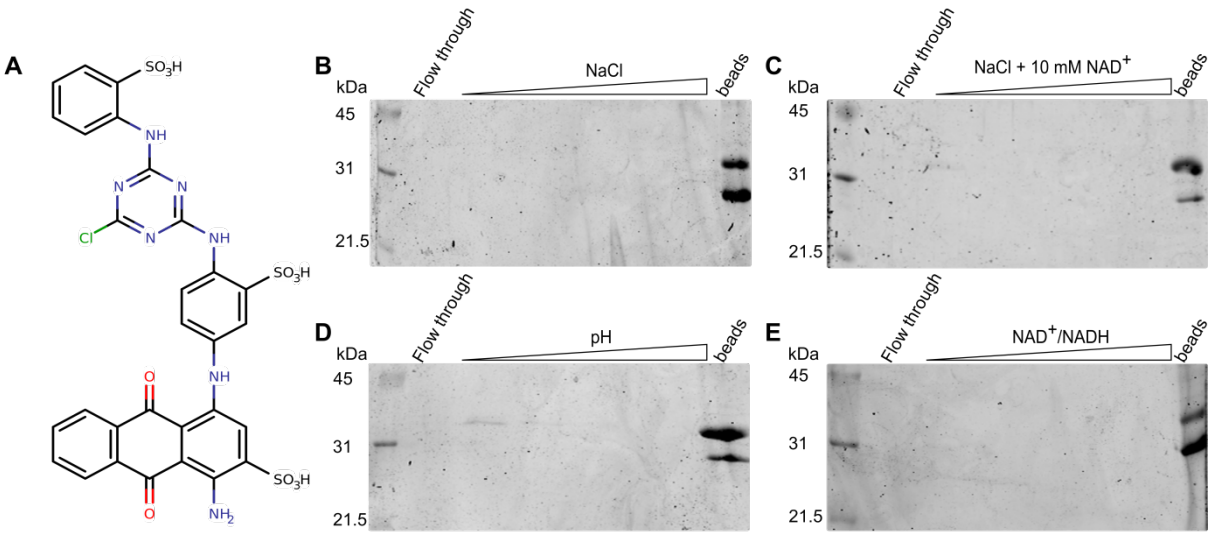

Figure 10: Purification strategy for endogenous Sirtuins using Blue Sepharose. (A) Blue Sepharose CL-6B consists of Cibacron Blue 3GA attached to sepharose beads at its triazine ring. (B – E) Initial purification strategies for recombinant and already purified Sirt5 were unsuccessful: neither a salt gradient in absence or presence of the Sirtuin co-substrate NAD$^+$, pH shift nor increasing NAD$^+$/NADH concentrations eluted any protein.

At first, the binding and elution behavior of recombinant Sirt5 expressed from *E. coli* was tested. 25 µg recombinant protein were incubated with 50 µl Blue Sepharose CL-6B beads in 20 mM Bis-Tris pH 6.0, 150 mM NaCl, 1 mM DTT and 25 µM $ZnCl_2$ (loading buffer; buffers were adapted from Smith, et al.[147] with the buffer pH adjusted according to the pI of the different Sirtuins). Since the cibacron moiety can act as affinity material and due to its three sulfonate groups as a cation exchange material as well, different elution strategies were pursued after two washing steps (high salt and low salt wash): 1) elution using a NaCl gradient in presence and absence of NAD^+, 2) applying a pH gradient as it is used for Sir2-Af2[147] and 3) using a NAD^+/NADH gradient. As seen in Figure 10B – E, neither competing ions in absence or presence of the co-substrate NAD^+, nor pH shift nor high concentrations of NAD^+ and NADH were able to elute recombinant human Sirtuins from the column material.
In order to verify Blue Sepharose as a proper pan-Sirtuin purification material, recombinant Sir2-Af2 was purified as already reported[147]. Then the binding behavior of this purified Sir2-Af2 to the resin was analyzed by SDS-PAGE. Indeed, Sir2-Af2 was both during and after purification able to bind to the column material after equilibration in loading buffer. The protein eluted after a high salt and a low salt wash using a pH shift from pH 6 to pH 8.5. For Sirt3 and Sirt5 buffers were adapted: while Sir2-Af2 washing buffers were set to pH 6 (thus ranging near the pI of 5.95 for this protein), human Sirtuin washing buffers were adjusted to pH 8.5 (pI_{Sirt3} = 8.98, pI_{Sirt5} = 8.52) and the elution buffer set to pH 10. However, both Sirt3 and Sirt5 could not be released from the Blue Sepharose (Figure 11).
The already reported purification approach for Sir2-Af2 via Blue Sepharose CL-6B could not be adapted to Sirt3 and Sirt5. Although both human Sirtuins bound to the column material, neither treating the resin as dinucleotide affinity material, nor treating it as cation exchange material resulted in Sirtuin elution. Since competing NAD^+, competing ions and pH shift were not able to release the protein from the column, the free Cibacron Blue 3GA dye (Figure 10A) was tested as competing agent and thus for its ability to elute human Sirtuins from Blue Sepharose. After incubation of Sirt5 with the resin, two washing steps were performed: 1) loading buffer with 1 M NaCl and supplemented with 0.1 mM Cibacron Blue (high salt wash) and 2) loading buffer supplemented with 0.25 mM Cibacron Blue (low salt wash). Afterwards protein was successfully eluted using 20 mM CHES pH 10, 150 mM NaCl, 1 mM DTT, 25 µM $ZnCl_2$ and 1 mM Cibacron Blue (Figure 12).
The interaction between human Sirtuins and Blue Sepharose CL6-B turned out to be surprisingly strong. Since it was assumed that the dye – either in its resin bound form or as free molecule – would bind to the NAD^+ binding site of Sirtuins, the free dye was tested for modulation properties on Sirt5 desuccinylation activity. However, dose response experiment revealed only a weak inhibitory effect with an IC_{50} value of 94.4 µM (Figure 13) despite the strong interaction between Blue Sepharose and mitochondrial Sirtuins.

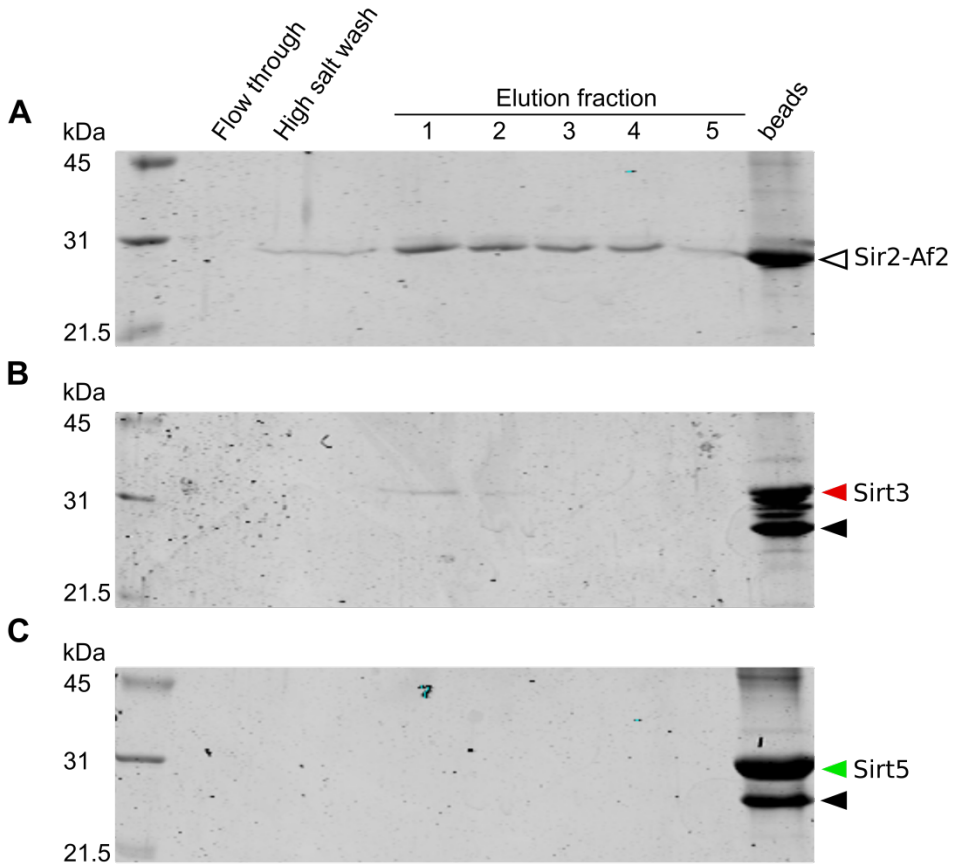

Figure 11: The Sir2-Af2 Blue Speharose purification protocol is not suitable for mammalian Sirtuins. Sir2-Af2 from *A. fulgidus* can be purified easily by pH shift from pH 6 to 8.5 (A). However, adapted elution buffers for Sirt3 (B) and Sirt5 (C) cannot release these proteins from the resin. Empty triangle: Sir2-Af2, red triangle: Sirt3, green triangle: Sirt5, black triangle: contaminant on Blue Sepharose.

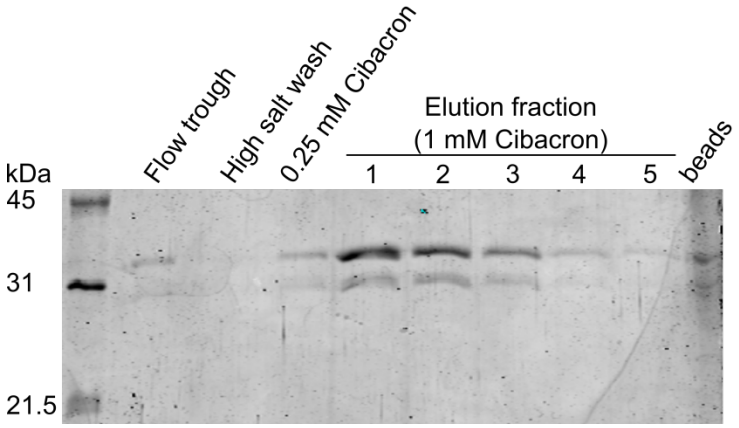

Figure 12: Mammalian Sirtuin elution from Blue Sepharose using free Cibacron as eluent. Sirt5 can easily elute from Blue Sepharose CL-6B if the elution buffer contains 1 mM of the free Cibacron Blue dye.

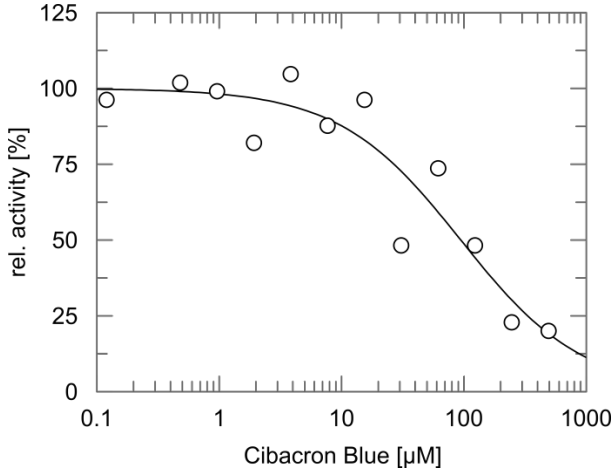

Figure 13: Cibacron Blue is only a weak Sirt5 desuccinylation inhibitor. Despite the strong binding interaction of Blue Sepharose and mitochondrial Sirtuins the free Cibacron Blue dye inhibits Sirt5 desuccinylation activity with an IC_{50} value of 94.4 µM. Dose response experiment consisting of 1.5 µM Sirt5, 100 µM succCPS1 and 500 µM NAD^+.

With a proper Blue Sepharose purification protocol in hand, the isolation of endogenous Sirtuins from bovine liver mitochondria was pursued. Purified mitochondria (as a 15 mg/ml solution determined by Bradford analysis)[128] were lysed by sonication and cleared from membrane debris. Afterwards 500 µl of the cleared lysate was set to pH 6 and supplemented with 25 µM $ZnCl_2$ and 1 mM DTT, which already resulted in precipitation of some mitochondrial proteins. The supernatant was incubated with 50 µl Blue Sepharose and treated afterwards according to the above established protocol. As seen in Figure 14A, the purification scheme removed contaminant mitochondrial proteins, yielding in an enrichment of proteins of ~ 30 kDa – the molecular weight range of mitochondrial Sirtuins as confirmed by Western blotting (Figure 14B). However, the yield and purity after Blue Sepharose purification was not satisfactory. Hence, this Sirtuin enrichment strategy was not further pursued on favor of other strategies, which were expected to exhibit both higher purity and yields.

3.1.1.2. Immunopurification of bovine Sirt5

The purification of endogenous Sirtuins from native source via Blue Sepharose turned out to yield too low amounts of protein of too low purity. Hence, another purification strategy for enriching Sirtuins from crude lysate was tested: by employing specific antibodies, Sirt5 purification from bovine ML was aimed.

In order to immunopurify Sirt5 from bovine ML, a Protein G immunoprecipitation kit was used. This commercial kit employs protein G coupled agarose beads, which are recognized by almost any antibody (AB) and thus allows immunoprecipitation of antigen/AB complexes. At first, ML was incubated with protein G beads in order to clear the lysate from proteins unspecifically binding to the beads (Figure 15). Afterwards, beads were exchanged by fresh

beads and Sirt5 AB were added to the pre-cleared lysate. Then beads were recovered and after extensive washing a faint band of the expected molecular weight was identified by SDS-PAGE (Figure 15A & B). Comparison of the migration behavior of the final product from immunopurification and heterologous expressed Sirt5 supported this faint band to be bovine Sirt5 (Figure 15C). This migration pattern resembles the pattern of bovine Sirt5 purified from ML, which was already compared with Sirt5 and confirmed by Western blot analysis (Figure 14B). But still, immunopurification as well as Blue Sepharose purification resulted in protein yields insufficient for PTM identification.

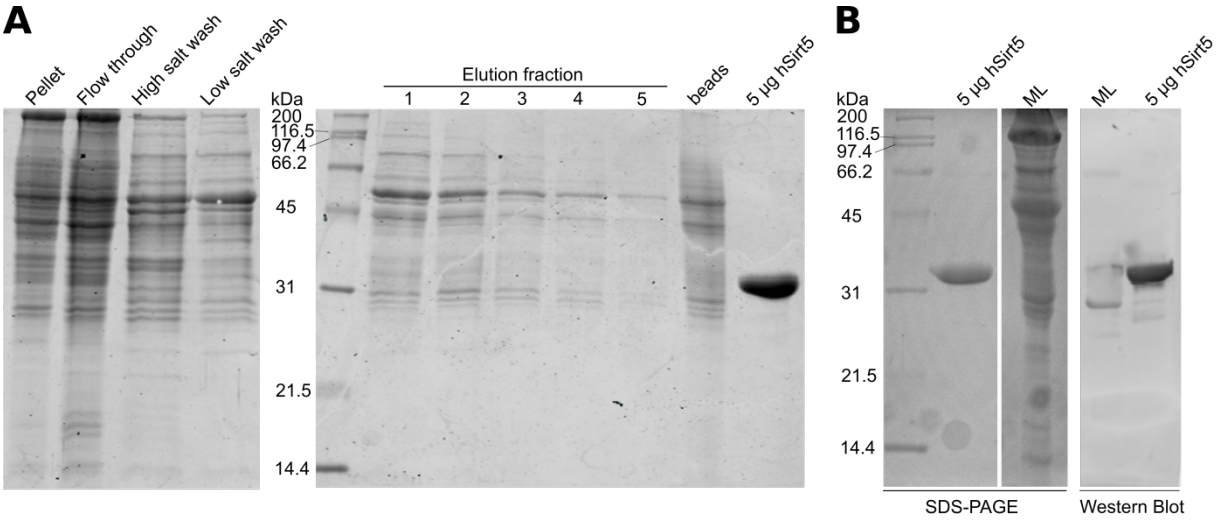

Figure 14: Endogenous Sirtuin purification from bovine mitochondria. (A) Proteins of ~ 30 kDa, possibly bovine Sirtuins, can be enriched using the established Blue Sepharose purification scheme as seen via SDS-PAGE. However, the elution fractions were still contaminated with further mitochondrial proteins. (B) Western Blot analysis confirms bovine Sirt5 present in mitochondrial lysate and running at ~ 30 kDa. ML: mitochondrial lysate.

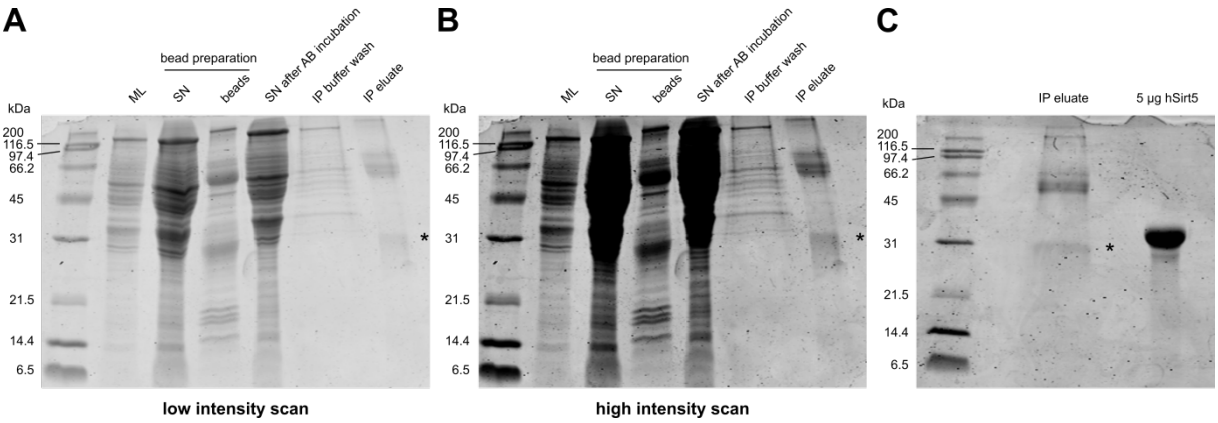

Figure 15: Immunopurification of Sirt5 from bovine ML. (A) After clearing bovine ML from proteins binding unspecifically to protein G agarose, SDS-PAGE analysis of Sirt5 immunopurification reveals a faint band of ~ 30 kDa (asterisk) which corresponds to the expected molecular weight of bovine Sirt5. (B)High intensity scan of this gel highlights this band and its molecular weight. (C) The migration behavior comparison of the final product with Sirt5 from heterologous expression supports the notion of this band being bovine Sirt5. It resembles the migration pattern of bovine compared to human Sirt5 in Western blot analysis (Figure 14). Asterisk: bovine Sirt5.

3.1.2. Transient Expression of Sirtuins from HEK 293T

Purification of human Sirtuins from native tissue turned out to be too low yielding for PTM identification. Thus, human cultured cells were used as host for the transient expression of human Sirtuins and for subsequent PTM identification. HEK 293T cells were transiently transfected and Flag-tagged Sirt3 – 7 were affinity purified 48 h post-transfection. Since Sirtuins expressed from HEK 293T cells were not used in activity assays but were only used for PTM analysis via LC-MS/MS, proteins were eluted from anti-Flag affinity resin by boiling in SDS-sample buffer. SDS-PAGE and Western blotting confirmed the presence of Sirtuin amounts suitable for PTM identification (Figure 16). Hence, bands of the proper molecular weight were sliced from the gels and, following tryptic digest, analyzed for the presence of PTMs.

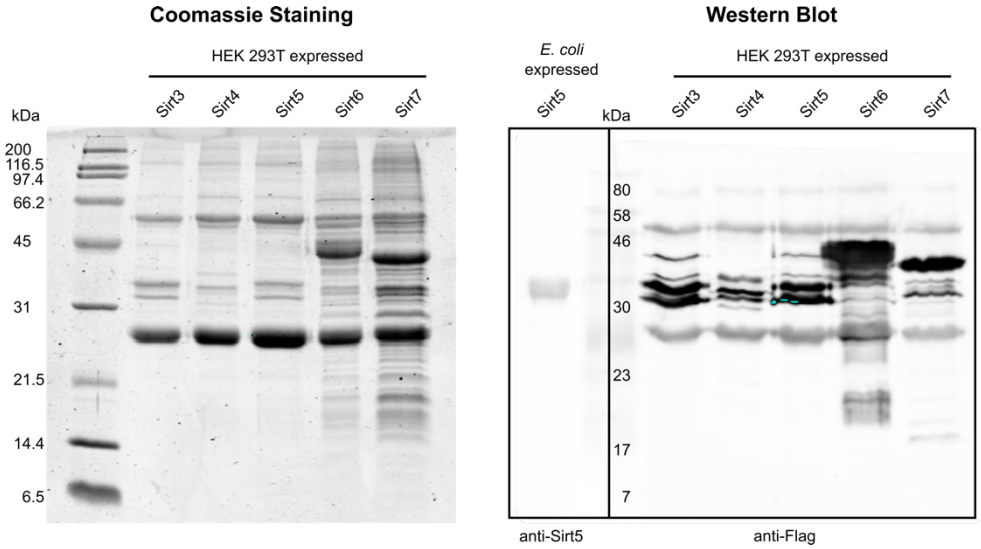

Figure 16: Transient expression of Sirtuins from HEK 293T. Overexpression of Sirt3 – 7 in HEK 293T and Flag affinity purification yields in protein amounts visible after SDS-PAGE and Coomassie staining (left). Successful transfection and purification was confirmed by Western blot analysis (right).

Transient transfection of Sirt3 – 7 was performed several times and resulted in the repeated identification of PTMs (Table 4). While no PTM could be identified on Sirt4, two acLys were found on Sirt3. Furthermore, several acylation sites and one phosphorylation site were observed on Sirt5. In addition, several phosphorylation sites were detected for the nuclear Sirtuins Sirt6 and Sirt7.

None or just two PTMs were detected on Sirt4, Sirt3 and Sirt7, respectively. In order to identify further PTMs, HeLa K cells were employed for transient overexpression. This was supposed to exclude expression and/or (de)modification artifacts caused by HEK 293T cells. However, overexpressed human Sirtuins purified from HeLa K did not bear any further modifications apart from those already detected from HEK 293T expression. Both cell lines

differed only in their protein yield, which was higher in HEK 293T (Figure 17). Thus, identified PTMs seem to occur cell line independent.

Given their role in the metabolic adaption adapting to limited nutrient availability (cf. section 1.2.2), transient expression of Sirt3 – 7 was repeated with HEK 293T cells under nutrient limiting conditions. 12 h post transfection, cells were exposed to DMEM medium lacking FBS and harvested 48 h post transfection. Indeed, after Flag affinity purification and LC-MS/MS analysis, two further Sirt6 phosphorylation sites as well as one further on Sirt7 were identified (Table 4).

Table 4: PTMs identified from Sirt3 – 7 transiently expressed in human cultured cells.

Sirt3	Sirt4	Sirt5	Sirt6	Sirt7
acK122	n.d.	ac/succ/malK45 [a]	pS10	pS9[b]
acK219		ac/succ/malK49 [a]	pT72[b]	pS166
		ac/succ/malK51 [a]	pS191	pT263
		succK79	pT294	
		acK85	pS303	
		acK112	pS330[b]	
		pS185	pT337	
		acK203	pS338	
		acK219		

a) A single acetylation, succinylation and malonylation were detected from the same peptide which included K45, K49 and K51. Thus, the precise position of each modification cannot be determined. Nevertheless, K45/49/51 have to bear one of these acylations

b) PTM only detected during serum starved expression conditions

n.d.: none detected

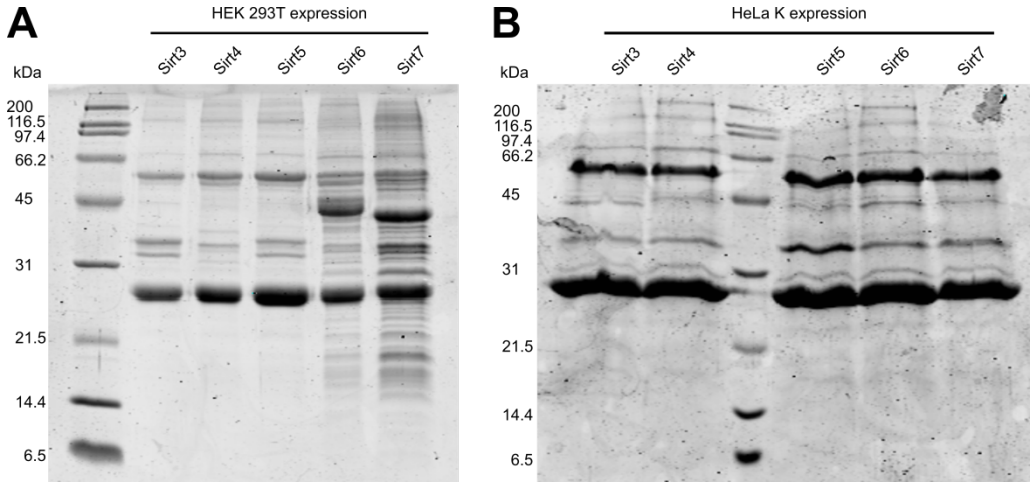

Figure 17: Higher yields of Sirtuin overexpression are achieved in HEK 293T compare to HeLa K. Using the anti-Flag AB chains as reference reveals HEK 293T (A) to yield higher amounts of transiently expressed Sirtuins compared to HeLa K as expression host (B). Especially the nuclear Sirtuins Sirt6 and Sirt7 are higher expressed in HEK 293T. The HEK 293T SDS-PAGE image from Figure 16 was used for comparison reasons.

3.1.3. A Possible Conserved Sirtuin PTM Site

Several PTMs were discovered by LC-MS/MS analysis of Sirt3 – 7 transiently expressed from HEK 293T cells. Sirtuins share both a highly similar topology[83] and a highly conserved catalytic core[14]. Interestingly, sequence alignment of Sirt4 – 7 performed by *Clustal Omega* (www.ebi.ac.uk/Tools/msa/clustalo/) highlighted Sirt7 T263 (Figure 18), which was detected as phosphorylation site. It aligns with Sirt4 S255, with a CXXC motif in Sirt5 (CDLC 242 – 245) and with Sirt6 S210. All of these sites can be modified in principle by phosphorylation or by disulfide bridging or oxidation, respectively. However, phosphorylation of Sirt6 S210 is neither reported nor was it identified during transient expression of Sirt6 in HEK 293T. Sirt5 CDLC 242 – 245 might face reversible modification as well, since CXXC motifs are known to be redox regulated by redox enzymes[148]. Besides these putative regulatory sites, Sirt4 S255 is already reported to be phosphorylated[149].

```
Sirt1      LPEQFHRAMKYDKDE---VDLLIVIGSSLKVR---PVALIPSSIPHEVPQ 461
Sirt2      LPARFFSCMQSDFLK---VDLLLVMGTSLQVQ---PFASLISKAPLSTPR 282
Sirt3      LPQRFL-LHVVDFPM---ADLLLILGTSLEVE---PFASLTEAVRSSVPR 340
Sirt4      VNPD---KVDFVHKRVKEADSLLVVGSSLQVYSG--YRFILTAWEKKLPI 282
Sirt5      LDPAILEEVDRELAH---CDLCLVVGTSSVVYP--AAMFAPQVAARGVPV 271
Sirt6      LPD---RDLALADEASRNADLSITLGTSLQIR---PSGNLPLATKRRGGR 235
Sirt7      GTLGQPLNWEAATEAASRADTILCLGSSLKVLKKYPRLWCMTKPPSRRPK 292
                                 *  : :*:*  :
```

Figure 18: Sequence alignment indicates a putative conserved PTM site in Sirtuins. Sequence alignment of all human Sirtuins reveal Sirt7 T263, which was identified as phosphorylation site, to align with an already reported phosphorylation site in Sirt4 (S255)[149] but also with a CXXC motif in Sirt5 (CDLC 242 – 245) and with Sirt6 S210 Sequence alignment was performed with Clustal Omega (www.ebi.ac.uk/Tools/msa/clustalo).

3.2. Physiological Sirtuin Modulation

3.2.1. Sirtuin Modulation by Posttranslational Modifications

3.2.1.1. Characterization of Sirt5 PTMs

With several PTMs being detected via MS/MS for Sirt3 – 7 transiently expressed in HEK 293T cells (Table 4), the effect of some of these modifications was investigated. For this purpose, Sirtuin PTM mimicking variants were created: The coding sequence of wt Sirtuins on bacterial expression vectors coding for a N-terminal His_6-tag was altered by site-directed mutagenesis. This resulted in either the exchange of Ser to Asp or of Lys to Gln in order to mimic a specific phosphorylation or acetylation site.

E. coli is able to modify proteins as well[150,151], thus heterologous expression of the Sirtuin variants might result in PTMs as well. However, global modification of overexpressed proteins by *E. coli* was neglected, since it should occur only to a very little extent. Bacterial kinases and acetyltransferases should not be able to cope with the unnatural high amount of Sirtuin protein caused by the IPTG induced overexpression. Nevertheless, every site specific PTM mimic was accompanied by an unmodified control which was generated by the exchange of Ser or Lys by Ala.

All PTM mimicking variants were then expressed in *E. coli* and purified by IMAC and SEC. Interestingly, during purification all variants behaved identical to the wt Sirtuins (Figure 19). This indicates that the aa exchanges did not induce protein oligomerization or aggregation.

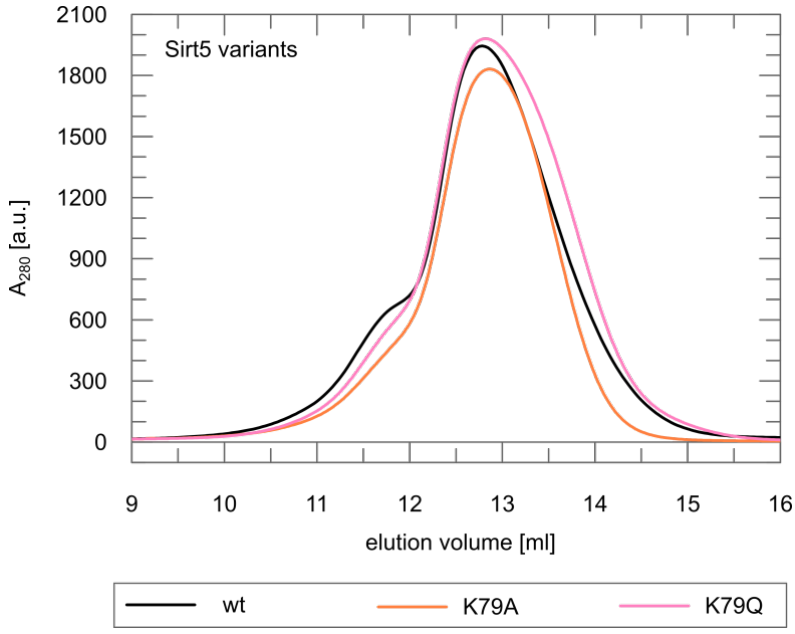

Figure 19: Sirtuin PTM mimics behave as the wt variant. Exemplary SEC elution profile of different Sirt5 variants. For comparison equal amounts of protein were loaded to a Superose 12 column.

After all Sirt5 variants were expressed from *E. coli*, the thermal stability of all variant pairs (K to A/Q or S to A/D) was determined. In addition an unmodified Sirt5 variant (i.e. Sirt5 expressed from the wt coding sequence which could be globally modified by *E. coli*; nevertheless it will be termed as wt in the following) was compared in absence or presence of substrate (analogues) (Figure 20A, Table 5), revealing little differences between all Sirt5 variants. Only the K112Q variant exhibited a decreased thermal stability with a lowered T_m value by ca. 4 °C. Since substrate binding stabilizes Sirtuins (Figure 20B), the effect of substrate presence on the Sirt5 variants was analyzed as well. As for the wt Sirt5 all other Sirt5 variants' thermal stability increased slightly. However, Sirt5 K112Q remained the least stable Sirt5 variant, which strongly suggests acylation at this specific Lys to destabilize Sirt5 (Figure 20A).

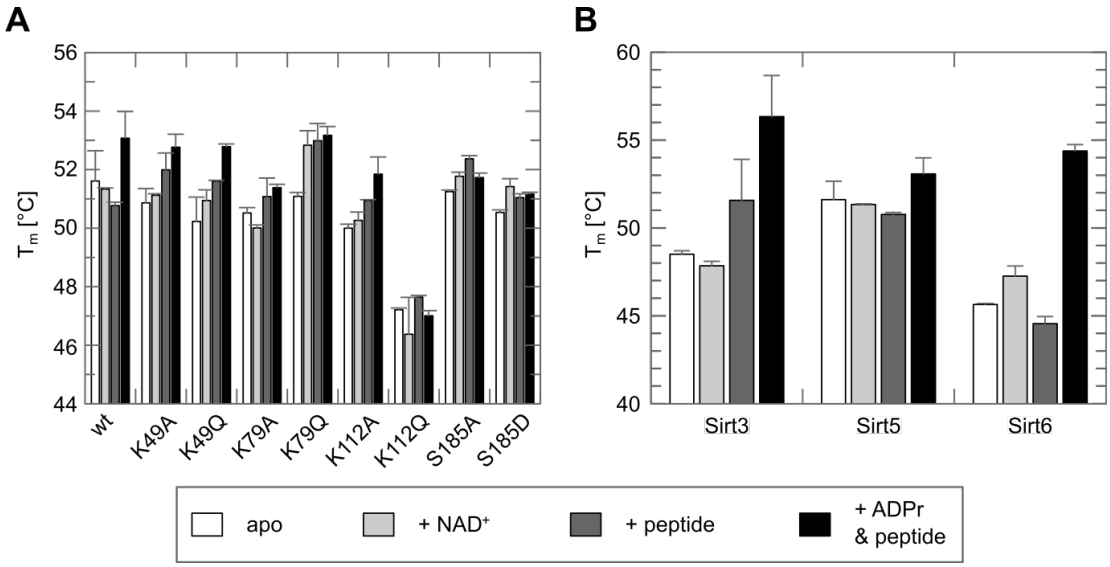

Figure 20: Acetylation at K112 destabilizes Sirt5. Only Sirt5 K112Q exhibits a decreased thermal stability by 4 °C (A), while thermal stability of all other PMT mimics was comparable with wt Sirt5. Different to other Sirtuins, substrate binding has only little effect on Sirt5 thermal stability and does not rescue Sirt5 K112Q stability to wt Sirt5 levels (B): (Error) bars represent the average and STDEV of at least two independent experiments. If added, saturating substrate were used (5 mM NAD^+ or ADPr, 0.5 mM succCPS1). Values are summarized in Table 5.

Table 5: Characterization of PTM mimicking Sirt5 variants

Sirt5	T_m [°C]				succCPS1 titration	
	Apo	+ NAD^+	+ succCPS1	+ ADPr +succCPS1	K_m [µM]	v_{max} [nmol/(mg·min)]
wt	51.6 ± 1.0	51.3 ± 0.0	50.8 ± 0.1	53.1 ± 0.9	34.3 ± 12.4	2.27 ± 0.17
K49A	50.9 ± 0.5	51.1 ± 0.0	52.0 ± 0.6	52.8 ± 0.4	33.7 ± 1.2	0.94 ± 0.11
K49Q	50.2 ± 0.4	50.9 ± 0.4	51.6 ± 0.0	52.8 ± 0.1	12.0 ± 3.8	0.58 ± 0.07
K79A	50.5 ± 0.2	50.0 ± 0.1	51.1 ± 0.6	51.4 ± 0.1	3.9 ± 1.5	0.93 ± 0.08
K79Q	51.1 ± 0.1	52.8 ± 0.5	53.0 ± 06	53.2 ± 0.3	23.9 ± 7.8	0.82 ± 0.08
K112A	50.0 ± 0.1	50.3 ± 0.3	50.9 ± 0.0	51.8 ± 0.6	13.1 ± 0.1	0.54 ± 0.03
K112Q	47.2 ± 0.1	46.4 ± 1.3	47.6 ± 0.1	47.0 ± 0.2	42.4 ± 3.9	1.80 ± 0.16
S185A	51.2 ± 0.1	51.8 ± 0.1	52.4 ± 0.1	51.7 ± 0.2	14.7 ± 3.4	1.05 ± 0.07
S185D	50.5 ± 0.1	51.4 ± 0.3	51.0 ± 0.1	51.2 ± 0.1	12.5 ± 2.6	0.98 ± 0.05

With some differences in their T_m, possible effects of the mimicked PTMs on Sirt5 kinetic constants were analyzed. Since the presence of NAD^+ left the thermal stability of most variants unaffected, only the kinetic constants during a peptide titration were determined in a coupled enzymatic assay. Comparing all pairs of variants with wt Sirt5 revealed only slight differences in K_m for the K49A, K79A/Q and K112Q variants (Figure 21, Table 5). Comparing the individual pairs of variants revealed a threefold decreased peptide K_m for K49Q compared to its Ala counterpart and the wt variant (Figure 21A, Table 5). Likewise, Sirt5 K79A and K112A K_m were three- to fivefold decreased compared to their Gln counterpart and wt Sirt5 (Figure 21B & C). However, K_m values for Sirt5 S185A and S185D were comparable but twofold decreased compared to wt Sirt5 (Figure 21D).

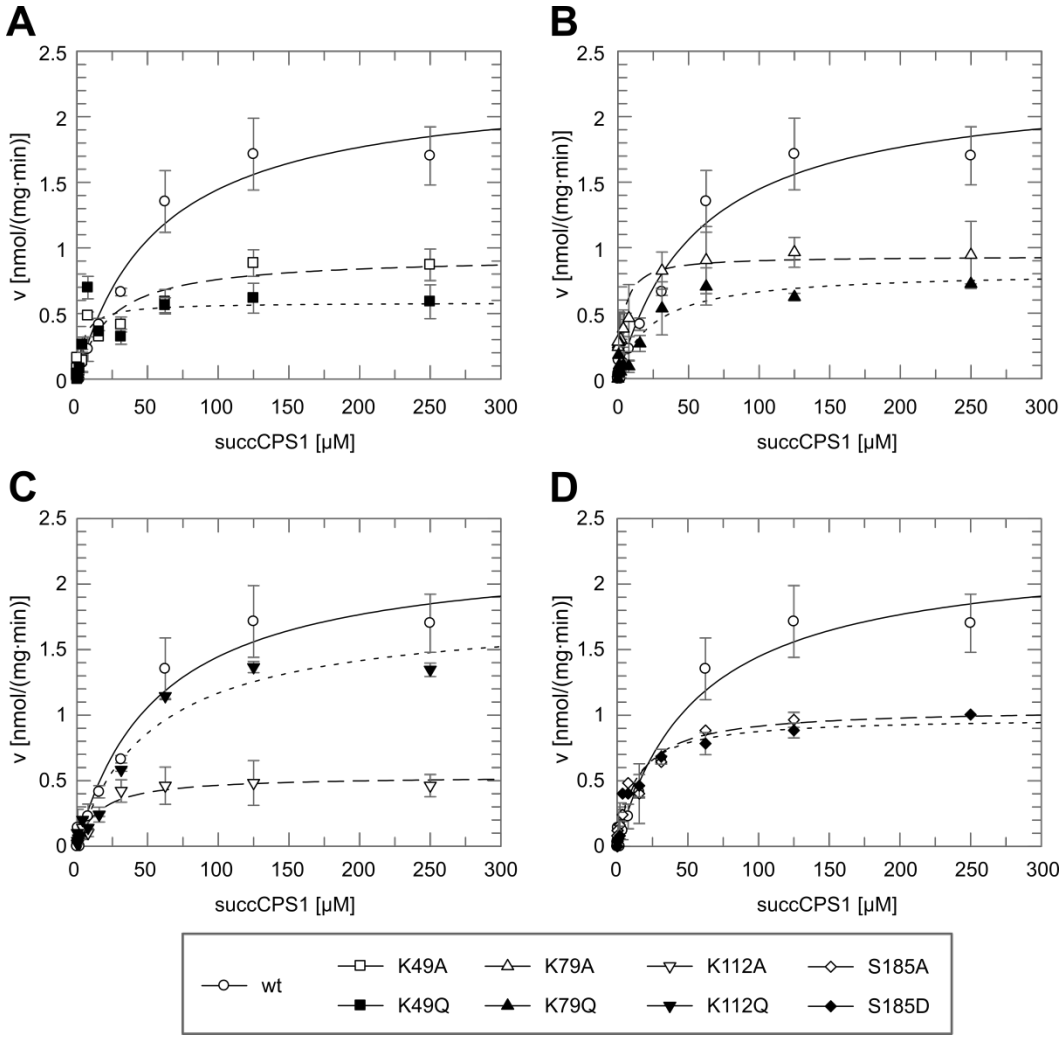

Figure 21: Sirt5 modifications affect substrate peptide K_m. Coupled enzymatic assays of wt Sirt5 compared to the individual PTM mimics revealed a decreased v_{max}. However, K_m values of Sirt5 K49A (A), Sirt5 K79A/Q (B) and Sirt5 K112Q (C) are decreased compared to wt Sirt5 and their Gln and Ala counterpart, respectively. K_m values Sirt5 S185A/D are threefold lower compared to wt Sirt5 (D). v_{max} of variants tested differed significantly due to different amounts of enzymatically active Sirt5 variant per purification rather than due to the amino acid exchange. Coupled enzymatic assay of 1.5 µM wt Sirt5 (A – D), Sirt5 K49A/Q (A), Sirt5 K79 A/Q (B), Sirt5 K112A/Q (C) or Sirt5 S185 A/D (D), 2.5 mM NAD^+. Data points represent the average including the STDEV of at least two independent experiments. Values are listed in Table 5.

On the contrary, v_{max} of all PTM mimicking variants decreased compared to wt Sirt5. Comparing each variant pair, Sirt5 K49A as well as Sirt5 K112Q exhibit higher v_{max} values as their Q or A counterpart, respectively (Figure 21A & C). However, with the exception of Sirt5 S185A/D, which were purified in parallel, all other Sirt5 variants were purified on separate days. This probably resulted in different amounts of enzymatically active Sirt5 variants per final purification product. This would account for decreased v_{max} but similar K_m values between all Sirt5 variants tested. Nevertheless, peptide titration experiments suggest a modulating effect of Sirt5 modification on K49 and K112.

3.2.1.2. Characterization of Sirt6 PTMs

With several PTMs identified on Sirt6, their effect on this enzyme was characterized as well. As for Sirt5, several PTM mimicking variants were constructed. Since no significant difference between the wt Sirt5 and the K/S to A variants was observed, only the Sirt6 phospho mimics (i.e. exchange of S to D) but not their respective unmodified counterpart (i.e. exchange from S to A) were generated and expressed. In addition to all Sirt6 variants mimicking phospho-Ser identified by MS/MS, the additional S210D variant was generated. This variant mimics a putative modification site which might be conserved between Sirt4 – 7, which was identified only on Sirt7 transiently expressed in HEK 293T cells. No significant difference during protein purification was visible among all Sirt6 variants either during IMAC or gel filtration (Superdex 200: elution peak at ca. 15.5 ml).

Only one Sirt5 PTM mimic differed in its thermal stability compared to the wt variant and its Ala counterpart, whereas no differences in their *in vitro* activity could be observed: Thus, at first the thermal stability of the purified Sirt6 variants was analyzed (Figure 22, Table 6). Comparing the thermal stability of all Sirt6 variants revealed a dramatically decreased T_m value for Sirt6 S210D (decrease by ca. 10 °C, Figure 22A). While Sirt6 itself is less stable than other Sirtuins during thermal denaturation (Figure 22B), all Sirt6 variants apart from Sirt6 S210D are comparably stable and are stabilized if both substrates are bound. Interestingly, Sirt6 S338D was already stabilized if only peptide was bound. However, substrate binding to Sirt6 S210D restored its thermal stability to wt Sirt6 apo level, which renders this variant still the least stable – even if substrates were bound (Figure 22A).

Having identified the Sirt6 S210D variant to be significantly destabilized compared to all other Sirt6 variants, the effect of this amino acid exchange on the enzyme's activity was analyzed. Sirt6 was initially described as a Histone 3 K9 deacetylase[152]. However, this activity was barely reproducible with standard *in vitro* Sirtuin activity assays. Furthermore, recent publications indicated Sirt6 to be rather a demyristoylase than a deacetylase[32,53]. Due to these controversial findings, a proper Sirt6 substrate had to be determined first. Hence, Sirt6 deacetylation of H3K9 peptide was compared to the consumption of longer and charged

acyls (succinylated and adipoylated CPS1 and myristoylated TNFα) in a coupled enzymatic assay. As seen in Figure 23, Sirt6 is indeed a proper demyristoylase, consuming myrTNFα more than twice as fast as acH3K9 or adiCPS1 and almost seven times faster than succCPS1 (Table 7). However, compared to Sirt3 deacetylation activity and Sirt5 desuccinylation activity, Sirt6 demyristoylation is slightly slower. Furthermore, Sirt3 and Sirt5 major activity was twice as fast as Sirt3 or Sirt5 demyristoylation activity. Thus, demyristoylation might not be the major Sirt6 activity, although it is the best activity in the setup used.

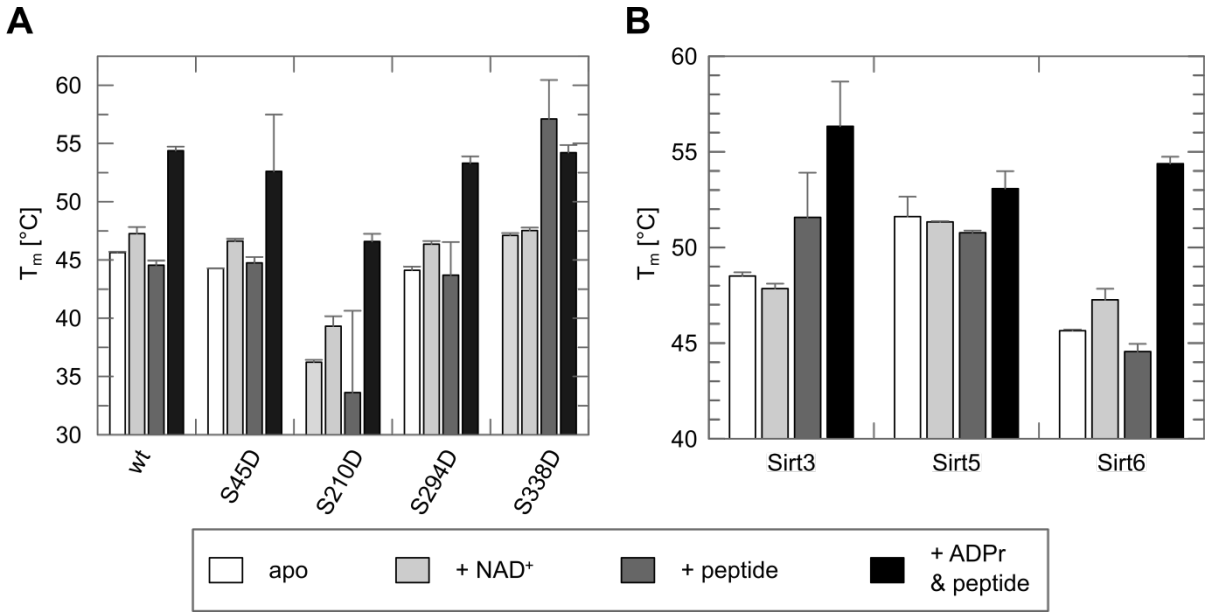

Figure 22: Sirt6 S210D is highly destabilized. Phospho mimicking Sirt6 variants exhibit similar thermal stability as the wt Sirt6 (A), which is in general lower compared to other Sirtuins (B). However, Sirt6 S210D T_m is decreased drastically by ca. 10 °C, and can be improved to wt Sirt6 apo levels if both substrates are present – an effect observed for all other variants except for Sirt6 S338D, which is already stabilized by peptide only (A). (Error) bars represent the average and STDEV of at least two independent experiments. If added, saturating substrate were used (5 mM NAD^+ or ADPr, 0.5 mM myrTNFα). Values are summarized in Table 6.

Table 6: Thermal stability of Sirt6 PTM mimics

Sirt6	T_m [°C]			
	Apo	+ NAD^+	+ myrTNFα	+ ADPr & myrTNFα
wt	45.6 ± 0.1	47.3 ± 0.6	44.6 ± 0.4	54.4 ± 0.4
S45D	44.5 ± 0.0	46.6 ± 0.2	44.7 ± 0.5	52.6 ± 4.9
S210D	36.2 ± 0.2	39.3 ± 0.8	33.6 ± 7.0	46.6 ± 0.6
S294D	44.1 ± 0.3	46.4 ± 0.3	43.7 ± 2.8	53.3 ± 0.6
S338D	47.1 ± 0.2	47.5 ± 0.3	57.1 ± 3.3	54.2 ± 0.7

For stability analyses, Sirt6 stability in absence and presence of saturating substrate (analogue) concentrations was determined (5 mM NAD^+ or ADPr, 0.5 mM myrTNFα). Stability values denote the average and STDEV from at least two independent experiments.

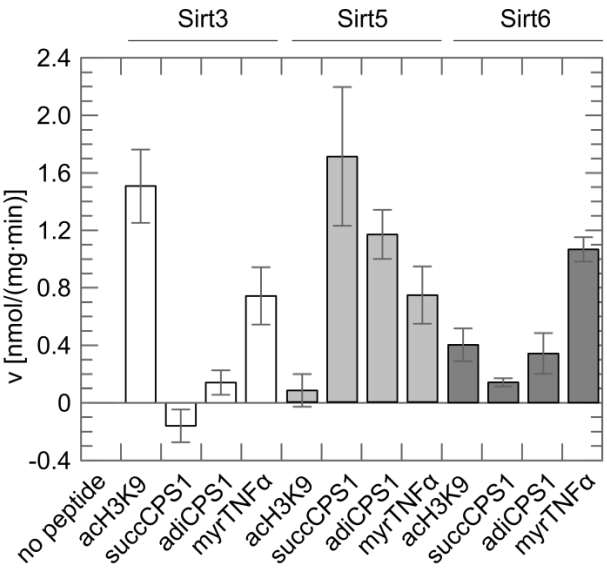

Figure 23: Sirt6 is a proper demyristoylase. Sirt6 prefers myrTNFα over acH3K9, succCPS1 and adiCPS1 *in vitro*. However, this activity is weaker compared to Sirt3 and Sirt5 main deacylation activities but still slightly higher than Sirt3 and Sirt5 myrTNFα consumption. Coupled enzymatic assay using 1.5 µM enzyme, 0.1 mM peptide, 1 mM NAD^+ and 5 % DMSO. (Error) bars represent the average and STDEV of two independent experiments, values are listed in Table 7.

Table 7: Comparison of Sirt3, Sirt5 and Sirt6 consumption of differently acylated peptides.

	v [nmol/(mg·min)]		
Peptide	Sirt3	Sirt5	Sirt6
acH3K9	1.51 ± 0.26	0.08 ± 0.11	0.40 ± 0.11
succCPS1	-0.16 ± 0.11	1.71 ± 0.48	0.14 ± 0.03
adiCPS1	0.14 ± 0.09	1.17 ± 0.17	0.34 ± 0.14
myrTNFα	0.74 ± 0.20	0.74 ± 0.2	1.07 ± 0.09

Coupled enzymatic assay of 3 µM enzyme, 0.1 mM peptide, 1 mM NAD^+ and 5 % DMSO. Values denote the average and STDEV of two independent experiments.

With a proper substrate peptide in hand, the activity of wt Sirt6 and its S210D variant could be analyzed. Protein phosphorylation is not observed in *E. coli* and considering the similar behavior of Sirt5 S185A and Sirt5 S185D in all experiments, no Ala variants were generated for Sirt6. Different to Sirt5, only the presence of peptide together with the NAD^+ mimicking ADPr improved Sirt6 thermal stability. Thus, kinetic constants for myrTNFα and NAD^+ were determined at first for Sirt6 wt and the S210D variant. Only Sirt6 S210D was used in NAD^+ kinetic experiments as this amino acid exchange was expected to affect the binding of the co-substrate (cf. section 4.1.1). Kinetic experiments with increasing NAD^+ concentrations confirmed the previous observation of Sirt6 being less active than Sirt3 and Sirt5 (Figure 24A, Table 8). Although in comparison to other Sirtuins for wt Sirt6 the lowest $K_m(NAD^+)$ of 15.2 ± 7.7 µM was determined, it was not significantly different than that of Sirt6 S210D (Figure 24B). Sirt6 and its S210D variant were not purified in parallel. Hence, comparing v_{max} was not sensible as already seen with Sirt5 and its PTM mimicking variants (see above).

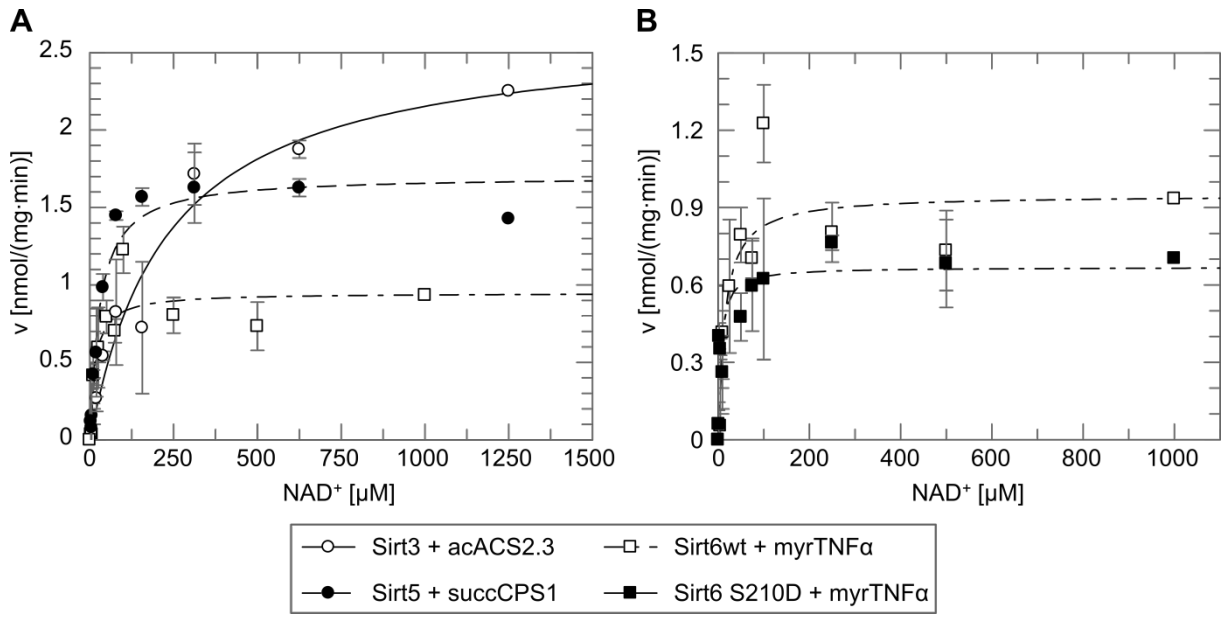

Figure 24: $K_m(NAD^+)$ for Sirt6 and its S210D variant is comparable to Sirt5. (A) NAD^+ titration of Sirt3, Sirt5 and Sirt6 reveals comparable K_m values for Sirt5 and Sirt6, while Sirt3 exhibits an increased K_m towards NAD^+ (A). (B) Sirt6 S210D exhibits the same $K_m(NAD^+)$ as wt Sirt6. Coupled enzymatic assay using 1.5 µM enzyme, 0.1 mM peptide and a final DMSO concentration of 5 %. Values and error bars denote the standard deviation of at least three independent experiments. Values are listed in Table 8.

Table 8: Kinetic constants of Sirt3, Sirt5 and Sirt6 towards NAD^+.

Sirtuin/substrate pair	K_m [µM]	v_{max} [nmol/(mg·min)]
Sirt3 / acACS2.3	103.3 ± 30.7	2.65 ± 6.2
Sirt5 / succCPS1	28.8 ± 5.6	1.70 ± 0.09
wt Sirt6 / myrTNFα	15.2 ± 7.7	0.95 ± 0.10
Sirt6 S210D / myrTNFα	4.8 ± 3.3	0.67 ± 0.05

Coupled enzymatic assay of 3 µM enzyme, 0.5 mM peptide and 5 % DMSO. Values denote the average and STDEV of at least two independent experiments.

In order to see, if Sirt6 phosphorylation had any influence on peptide kinetic constants, myrTNFα titration experiments were performed for wt Sirt6, Sirt6 S210D and one N- and C-terminally modified Sirt6 (S45D and S338D, respectively) as well. As for the previous kinetic experiments, Sirt6 variants exhibited deviating v_{max} values (Figure 25, Table 9), possibly due to the differing amounts of active enzyme per purification batch. However, comparing the individual K_m(myrTNFα) values revealed no difference between wt Sirt6 and Sirt6 S45D (Figure 25A). Surprisingly, both phospho mimics Sirt6 S210D and S338D exhibited an increased K_m towards the substrate peptide (Figure 25B & C). This suggests that Sirt6 phosphorylation might interfere with peptide binding.

In summary, only few of the PTM mimics tested turned out to affect either activity or thermal stability of Sirtuins. Thermal stability of Sirt6 was dramatically decreased if S210 phosphorylation was mimicked. In addition, this modification increased Sirt6 K_m in a similar

manner as S338 phosphorylation did. In case of Sirt5, the acyl-Lysine mimic on K49 decreased K_m(succCPS1), suggesting a modulating effect on Sirt5 activity. Interestingly, exchanging K79 and K112 by Ala also resulted in a decreased K_m when compared to their Gln counterpart and the wt Sirt5. This indicates that either a long chained amino acid is crucial for peptide affinity or that for proper substrate binding an acylated lysine might be necessary. However, considering the high amount of overexpressed Sirt5 within *E. coli* the chances of a majority of overexpressed protein being acetylated at K79 or K112 seem very low. Thus, the lysine at position 79 and 112 seem to be necessary for proper Sirt5 activity regardless of being modified or not. Nevertheless, these two residues seem to be important for Sirt5 stability, since mimicking K112 acetylation resulted in enzyme destabilization and mimicking of acK79 resulted in Sirt5 stabilization already upon NAD^+ binding, whereas all other Sirt5 variants were not stabilized upon NAD^+ binding.

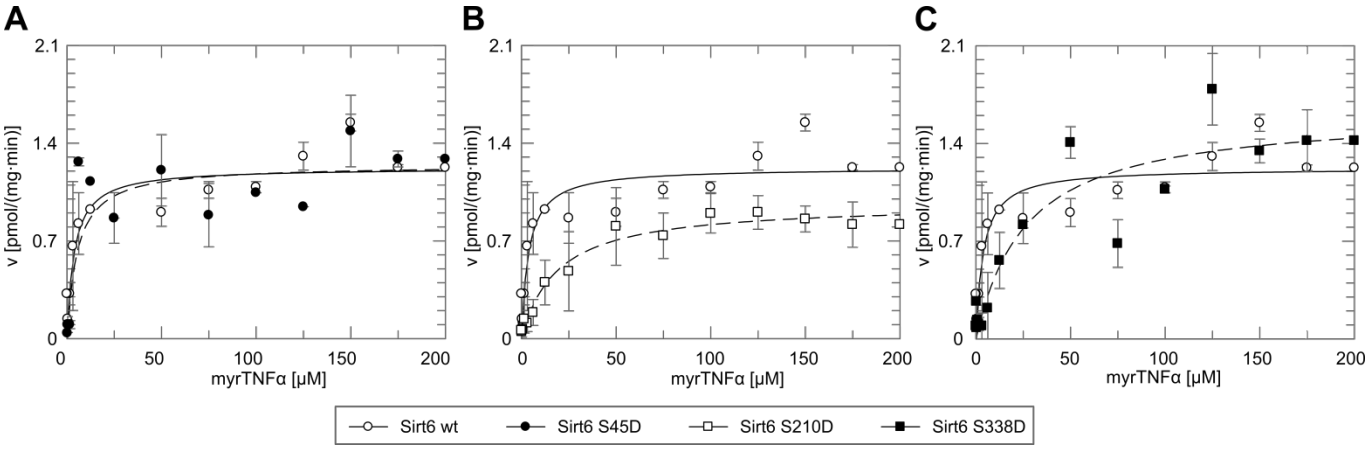

Figure 25: Sirt6 phosphorylation at S210 and S338 interfere with peptide binding. While wt Sirt6 and Sirt6 S45D do not differ in their K_m(myrTNFα) (A), Sirt6 S210D (B) and S338D (C) exhibit an increased K_m value compared to the wt variant. Coupled enzymatic assay using 1.5 μM enzyme, 1 mM NAD^+ and a final DMSO concentration of 5 %. Values and error bars denote the standard deviation of at least three independent experiments. Values are listed in Table 9.

Table 9: Kinetic constants of Sirt6 variants towards myrTNFα.

Sirt6 variant	K_m [μM]	v_{max} [nmol/(mg·min)]]
wt	7.5 ± 2.8	1.22 ± 0.07
S45D	11.4 ± 7.1	1.24 ± 0.12
S210D	45.8 ± 10.3	0.97 ± 0.04
S338D	67.8 ± 34.1	1.63 ± 0.19

Coupled enzymatic assay of 3 μM enzyme, 1 mM NAD^+ and 5 % DMSO. Values denote the average and STDEV of at least two independent experiments.

3.2.2. Sirtuin Regulation by Metabolites

3.2.2.1. Acyl specific NAM inhibition of Sirt5

Sirtuin reaction can be influenced by cellular ligands (e.g. activation of Sirt1 by AROS)[89]. But cellular metabolites affect Sirtuin activity as well: on the one hand they depend on NAD^+ as co-substrate, on the other hand one of their products, NAM, is known to inhibit Sirtuins by promoting the reversed enzymatic reaction *in vitro* with micro molar K_i and IC_{50} values[94]. For long time, knowledge about NAM inhibition was restricted due to the lack of proper assays (the coupled enzymatic assay is not applicable since it depends on NAM consumption) and proper substrates in fluorescence based assays. Using MS based assays in combination with novel label-free substrates the influence of NAM on Sirtuins could be analyzed more thoroughly. This resulted in the interesting observation of Sirt5 deacetylation being insensitive against NAM inhibition with a millimolar IC_{50} value *in vitro* (1.6 ± 0.3 mM) while almost all other Sirtuins were inhibited with IC_{50} values in the micromolar range[125,126].

Since Sirt5 was identified to act predominantly as a desuccinylase[31], NAM inhibition was analyzed against this activity as well. Surprisingly, increasing NAM concentrations during a MS based activity assay revealed Sirt5 desuccinylase activity being well inhibited with an IC_{50} value of 20.6 ± 4.1 µM. Hence, Sirt5 desuccinylase activity is inhibited by NAM comparably to other Sirtuin/substrate pairs (Figure 26A)[125,126]. Since the substrate peptide binds via β-sheet like interaction, the acyl specificity of Sirt5 NAM inhibition might be caused by the enzymes unique active site amino acid composition. Unlike most other Sirtuins, Sirt5 contains an Arg residue that ensures proper positioning of the succLys via salt bridge formation for proper substrate turnover and thus renders this enzyme a desuccinylase (Figure 26B, R105-1)[31]. However, if a shorter and uncharged acLys binds to Sirt5, R105 could adopt a different conformation (Figure 26B, R105-2), thus pointing towards the C-site thereby preventing or even repelling the likewise positively charged NAM.

In order to validate if R105 might indeed mediate the differing NAM sensitivities of the two Sirt5 activities, a Sirt5 R105L variant was generated. By exchanging R105 with an aliphatic residue, the NAM sensitivity of Sirt5 deacetylation should increase due to the lack of a NAM repelling sidechain. Indeed, Sirt5 R105L exhibits a higher sensitivity against deacetylation inhibition by NAM than the wt variant (Figure 26A). This supports the critical role of R105 in establishing the acyl specificity of Sirt5 inhibition by NAM.

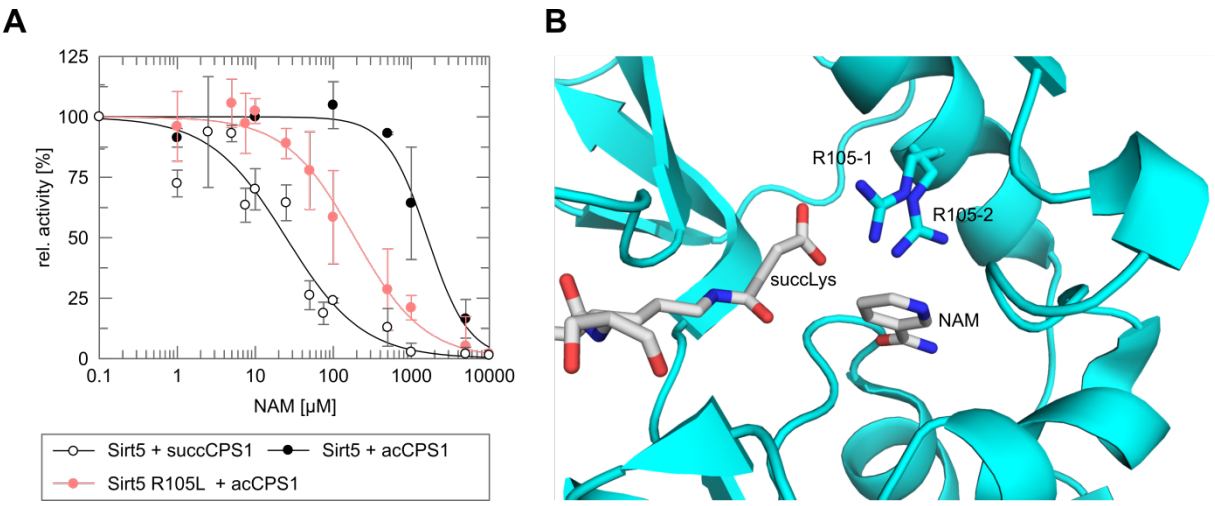

Figure 26: Acyl-dependent NAM inhibition of Sirt5. (A) While Sirt5 deacetylation is NAM insensitive, Sirt5 desuccinylation activity is well inhibited by this metabolite. (B) Modelling NAM inside Sirt5 active site suggests Sirt5 R105 to mediate NAM sensitivity, since it can either interact with the substrate succLys by salt bridge formation (B, R105-1) or repel the likewise positive charged NAM in presence of an acetylated substrate (B, R105-2). Mutational analysis supports this inhibition mechanism, as Sirt5 R105L deacylation is more sensitive towards NAM inhibition (A). MS based assay of 15 µM (desuccinylation) or 30 µM enzyme (deacetylation), 0.5 mM peptide, 2.5 mM NAD^+ and 20 min incubation at 37 °C (Sirt5 + succCPS1: 30 min). Data points and error bars represent the average and STDEV of two (Sirt5 + succCPS1) or three independent experiments (all other assays). Active site model of Sirt5 (pdb code: 3RIY, cartoon representation, cyan)[31] in complex with succPeptide (sticks, colored by element; C: grey, N: blue, O: red). NAM (sticks, colored by element) was modelled inside Sirt5 active site by superposition with Sir2-Tm/NAM complex structure (pdb entry: 1YC5)[140].

3.2.2.2. The search for novel Sirtuin metabolite modulators

For binding the co-substrate NAD^+, Sirtuins contain a Rossmannn fold domain. This domain is able to bind further dinucleotides, e.g. ADPr, NAD(P)H and $NADP^+$. Hence, these molecules could act as competitive Sirtuin inhibitors. Considering the high number of metabolites inside cells – especially within mitochondria – other small molecules capable of Sirtuin interaction might exist and thereby affect these enzymes.

In order to identify novel physiologically relevant Sirtuin-interacting small molecules and possible physiological small compound modulators, bovine ML was boiled and filtered to remove denatured proteins. Afterwards, the effect of this filtered ML on Sirt3 activity was determined using the MS-based assay. As seen in Figure 27A this resulted in proper inhibition of deacetylation of ACS2.3 by Sirt3. Interestingly, Sirt5 deacetylation activity was not affected in presence of filtered ML (Figure 27B), whereas its desuccinylase activity was well inhibited (Figure 27C).

The differential effects of filtered ML on the different Sirt5 activities were highly similar to the effects observed for NAM inhibition by Sirt5 (see above). Thus, the filtered ML was further treated with NCA and GDH to validate whether its inhibitory effect is due to the presence of NAM. Indeed, proper Sirt3 deacetylase and Sirt5 desuccinylase activity was observed as

soon as the filtered ML was pre-cleared from NAM (Figure 27A & C). This indicates that the ML contained NAM concentrations sufficient for Sirtuin inhibition. Moreover, the reactions in presence of NAM-cleared mitochondrial lysate revealed an identical behavior compared to the control reactions in absence of ML (Figure 27A & C), which suggest that no further physiological Sirtuin modulator is present in the mitochondrial lysate used.

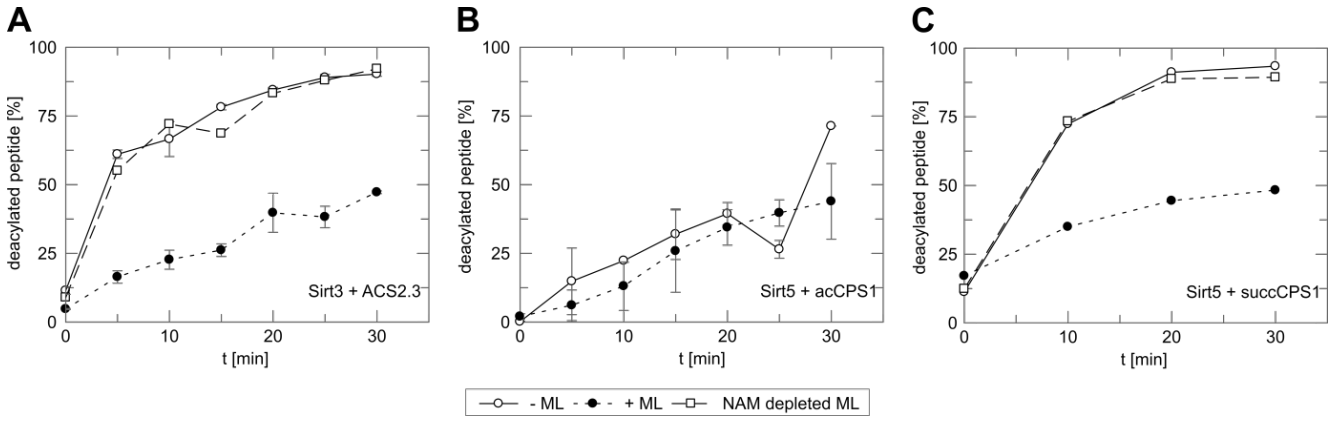

Figure 27: Mitochondrial lysate contains nicotinamide (NAM) concentrations sufficient for Sirtuin inhibition. (A) Sirt3 deacetylation of ACS2.3 is well inhibited in presence of mitochondrial lysate (ML), Treating ML with nicotinamidase (NCA) rescues Sirt3 activity, indicating the lysate's inhibitory effect being caused by NAM. (B) Sirt5 deacetylation is not affected by ML while Sirt5 desuccinylation activity is only observed in NCA treated ML (C). This finding is in good agreement with the *in vitro* studies on the NAM effects towards Sirt5 (Figure 26) and confirms the inhibiting effect of ML being caused by NAM.

3.3. Pharmacological Modulation of Sirtuins

Apart from the possibility to modulate Sirtuins activity physiologically – either by metabolites or by PTMs – Sirtuin activity can be modulated by pharmacological small molecule compounds. Considering their participation in nutrient state adaption and beneficial effects regarding aging and age-associated diseases, Sirtuins are in fact very attractive targets for pharmacological modulation. However, so far only limited knowledge about pharmacological modulation of all human Sirtuin isoforms is available, since research initially neglected mitochondrial Sirtuins due to the lack of proper substrates and assays. In addition, little is known about the specificity of already available (mainly) Sirt1 and Sirt2 modulators. Thus, the identification of Sirt3 and Sirt5 specific compounds was aimed.

3.3.1. Specificity Screening of known Sirtuin Modulators Reveals Acyl SpecificSirt5 Inhibition by GW5074

Proper pan-Sirtuin activity assays were not known until recently[133]. Completely unbiased methods are only available since even more recently[125,126] together with the identification of proper substrates for more and more Sirtuins[31,36,53,153]. Thus, already available Sirt1 and Sirt2 modulators were never tested for their Sirtuin specificity. In order to overcome this lack of knowledge and in order to identify modulator scaffolds for mitochondrial Sirtuins, selected small molecule compounds (Figure 8, Table 10) were tested on both Sirt5 deacetylation as well as its more pronounced desuccinylation activity.

Table 10: Compounds selected for testing their modulating effect on Sirt5[98,99].

Compound	Target Sirtuin[(a)]	Effect	Other Sirtuins affected
AGK2	Sirt2	Inhibitor	Sirt1, Sirt3
EX527	Sirt1	Inhibitor	Sir2-Tm
GW5074	Sirt2	Inhibitor	
HR73	Sirt1	Inhibitor	
Salermide	Sirt2	Inhibitor	
Sirtinol	Sirt1	Inhibitor	
SRT1720	Sirt1	Activator	Sirt3 (inhibitor)
Suramin	Pan-Sirtuin[(b)]	Inhibitor	

a) i.e. the Sirtuin the compound was designed for

b) Suramin is believed to act on all Sirtuins due to its mode of action[101]. By now, it is only reported to inhibit Sirt1 stronger than Sirt2 and Sirt5 deacetylation activity.

In a first screen, all selected compounds were tested against the pronounced Sirt5 desuccinylation activity in a coupled enzymatic activity assay[133] using a succinylated substrate peptide derived from peroxiredoxin 1 (Prx1, Table A 1). Due to its inhibitory effect on GDH in the nanomolar range[154,155] GW5074 modulation on Sirt5 was analyzed with a MS-based activity assay[125,126]. These assays in absence or presence of 10 or 100 µM compound

revealed no significant effect on Sirt5's desuccinylation activity except for GW5074 (Figure 28A). While 100 µM of most compounds tested had either no effect on Sirt5 (e.g. HR73) or reduced Sirt5 activity only by ~ 20 – 30 % (e.g. Salermide or Suramin), 100 µM GW5074 were able to reduce Sirt5 desuccinylation activity to ~ 15 %. Thus, a GW5074 titration experiment was performed revealing an IC_{50} value of 19.5 ± 7.3 µM (Figure 28C).
In order to identify possible acylation specific modulation effects, a phenomenon already observed for Sirt5 inhibition by the metabolite NAM (cf. section 3.2.2)[126], the same panel of compounds was tested again at 10 and 100 µM for their inhibitory effects on Sirt5 deacetylation. Since acPrx1 is a very weak Sirt5 substrate both in the coupled enzymatic and the MS-based assay, an acetylated peptide derived from CPS1 was used. Surprisingly, Sirt5 deacetylation was reduced to ~ 30 % activity in presence of 100 µM GW5074 (Figure 28B). A dose-response experiment yielded only in an IC_{50} value of 97.8 ± 18.6 µM (Figure 28D), 4-fold higher than compared to the inhibition of Sirt5's desuccinylation activity. On the other hand, Suramin exhibited a significant inhibition of Sirt5's deacetylation activity, in contrast to the previous result in the desuccinylation assay. All other compounds tested yielded in no Sirt5 deacetylation inhibition at 100 µM concentration, similar to the negligible effects in the desuccinylation assay. Further analysis of Sirt5 deacetylation inhibition by Suramin titration experiments revealed an IC_{50} value of 14.2 ± 5.7 µM against acCPS1 (Figure 28D & E), ranging in the same order of magnitude as already reported[101]. However, this effect seemed to be peptide substrate sequence dependent, since Sirt5 deacetylation of acPrx1 was inhibited weaker with an estimated IC_{50} value of 200 – 400 µM (Figure 28D & F).

3.3.2. GW5074 Inhibitory Mechanism

3.3.2.1. Structural analysis of GW5074 inhibition

Suramin is assumed to be a competitive inhibitor against both Sirtuin substrates. Thus, its differing effects on the Sirt5 activity were surprising. Likewise the differential effects of GW5074 on Sirt5 were unexpected, although they render GW5074 an acyl specific Sirt5 inhibitor. This interesting finding deems this compound a possible scaffold for the design of not only acyl but also isoform specific inhibitors. For this, a detailed characterization of GW5074 inhibitory mechanism is crucial.
With GW5074 bearing two electron-rich bromine atoms, this compound is well suited for structural analysis via x-ray crystallography: these substituents exhibit strong anomalous diffraction signal at a wavelength of 0.918 Å, thus the compound would be easily detected e.g. from data collected at a synchrotron facility. Hence, structural determination of GW5074 inhibitory mechanism was aimed.
In a first step factorial screens were employed to identify co-crystallization conditions of Sirt5 and GW5074. Since human Sirt5 hardly crystallizes and diffracts poorly, the better

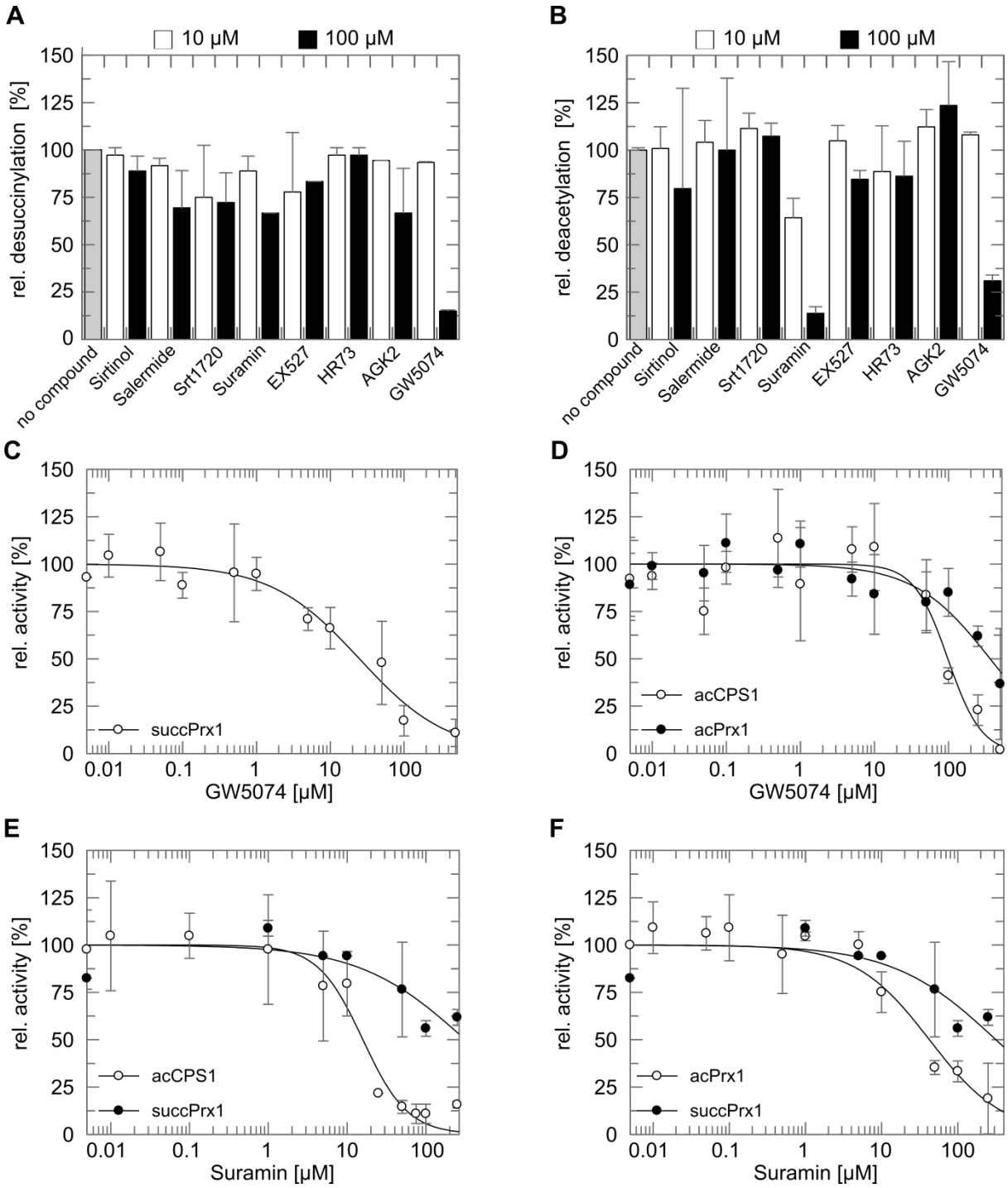

Figure 28: Screening known Sirtuin modulators reveals acyl specific Sirt5 inhibition. Sirt5 desuccinylation is not affected by any known Sirtuin modulator except for GW5074 (A), whereas the less pronounced deacetylation activity is strongly inhibited by Suramin and to a lesser extent by GW5074 (B). Dose response experiments confirm GW5074 to be a potent Sirt5 desuccinylase inhibitor (C) while its deacetylase activity seems to be almost unaffected (D). On the contrary, Suramin is a potent Sirt5 deacetylase inhibitor and a very weak Sirt5 desuccinylase inhibitor. This effect seems to be peptide substrate sequence dependent, since Sirt5 deacetylation activity against acCPS1 was well inhibited with an IC_{50} value of 14.2 ± 5.7 µM while deacetylation of acPrx1 was inhibited with an estimated IC_{50} value of 200 – 400 µM (D – F). (For comparison reasons data from C and D are repeated in E and F).

crystallizing and diffracting Sirt5 from the zebrafish *D. rerio* (zSirt5), which is similarly inhibited by GW5074 (Figure A 1) was used in crystallization trials[109]. Indeed, several crystallization conditions were identified (Figure 29). Even increasing DMSO concentrations for improved compound solubility yielded in crystals that diffracted poorly and did not contain the GW5074 (crystallization experiments are summarized in Table 11). With the indication of NAD^+ improving GW5074 slightly (see below), crystallization experiments were also performed in presence of varying NAD^+ concentrations, again yielding zSirt5 crystals without any ligand bound.

Since optimization strategies (micro- & macroseeding, GW5074 soaking, crystallization at 4 °C instead of 20 °C, supplementing Triton X-100 for even better compound solubility) did neither improve crystallization nor diffraction and still resulted in protein structures without bound compound, two Sirtuins known for their good crystallization behavior, human Sirt3 and yeast Hst2 were also co-crystallized accordingly to zSirt5 (GW5074 inhibition of these enzymes cf. Figure 31 & Figure A 2). Again, several crystallization conditions were identified (Table 11, Figure 29). However, with the exception of one Sirt3 crystallization condition (cf. Table 11 & Figure A 3), which resulted in a complex in which GW5074 bound as a crystallization artifact inside the axis between the asymmetric units, these crystals were composed of Sirtuin without GW5074 bound.

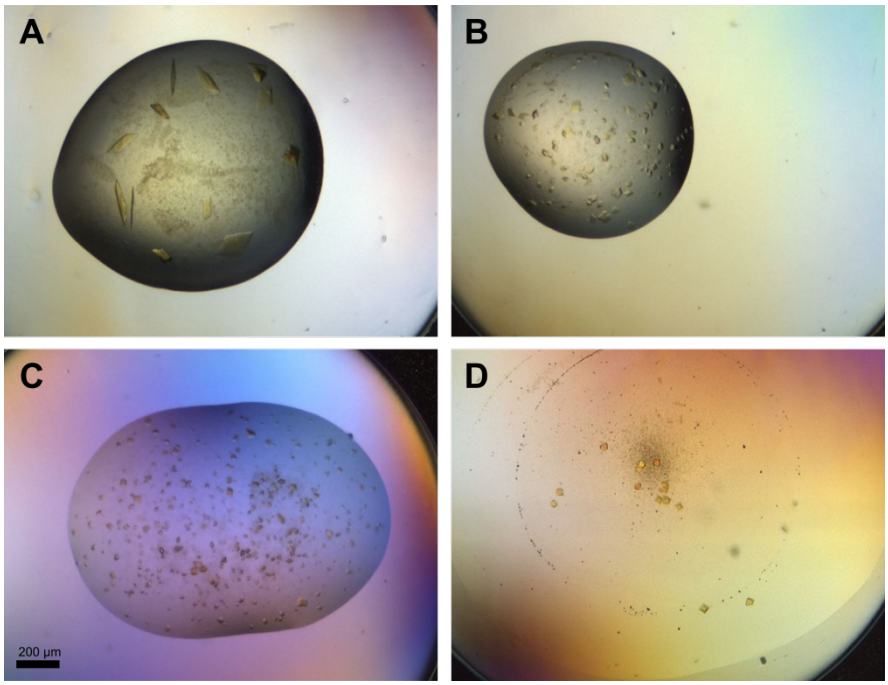

Figure 29: Sirtuin crystallization in presence of GW5074. Exemplary crystals from co-crystallization trials of zSirt5 (A – C) or Sirt3 (D) and GW5074. All crystals grown were either rod-shaped (A) or bi-pyramidal (B – D). A: co-crystallization of GW5074 and zSirt5 in 0.2 M Magnesium chloride, 0.1 M Tris pH 8.5, 30% PEG 4000; B & C: co-crystallization of zSirt5, NAD^+ and GW5074 in 1.26 M tri-Sodium citrate, 0.09 M HEPES pH 7.5, 10% Glycerol and 1.4 M tri-Sodium citrate, 0.1 M HEPES pH 7.5, respectively; D: co-crystallization of Sirt3, NAD^+ and GW5074 in 1.0 M Sodium citrate, 0.2 M Sodium chloride, 0.1 M Tris pH 7.0.

Table 11: Overview of crystallization hit to determine GW5074 inhibitory mechanism.

	Crystallization condition	Reproducible/ Optimizable	Diffracting	Structure
zSirt5	0.2 M Calcium acetate, 0.1 M Tris pH 7.0, 20% PEG 3000	-	-	-
	0.1 M acetate pH 4.6, 30% PEG 2000, 0.2 M Ammonium sulfate	-	-	-
	0.02 M Calcium chloride, 0.1 M Na-acetate pH 4.6, 30% MPD	-	-	-
	0.2 M Zinc acetate, 0.1 M Imidazole pH 8.0, 25% 1,2-propanediol, 10% glycerol	-	-	-
	0.2 M Zinc acetate, 0.1 M Imidazole pH 8.0, 40% PEG-600	-	-	-
	0.2 M Lithium sulfate, 0.1 M acetate pH 4.5, 30% PEG 8000	-	-	-
	1.4 M tri-Sodium citrate, 0.1 M HEPES pH 7.5	yes	yes	apo structure, no compound present
	0.1 M HEPES pH 7.0, 2.4 M Ammonium Sulfate	-	-	-
	0.2 M Magnesium chloride, 0.1 M Tris pH 8.5, 30% PEG 4000	yes	yes	apo structure, no compound present
	1.26 M tri-Sodium citrate, 0.09 M HEPES pH 7.5, 10% Glycerol	yes	-	-
	0.2 M Zinc acetate, 0.1M Imidazole pH 8.0, 40% (v/v) PEG-300	-	-	-
Sirt3	0.1 M imidazole pH 8.0, 1.0 M Sodium citrate	yes	yes	-
	1.4 M tri-Sodium citrate, 0.1 M HEPES pH 7.5	yes	yes	ADPr in NAD^+ binding pocket, GW5074 density in axis between asymmetric units (Figure A 3)
	1.0 M Sodium citrate, 0.2 M Sodium chloride, 0.1 M Tris pH 7.0	yes	yes	apo structure, no compound present
Hst2	0.2 M Na sulfate, 0.1 M Bis Tris propane pH 8.5, 20% PEG 3350	yes	yes	apo structure, no compound present

Crystallization experiments consisted of 8 – 10 mg/ml Sirtuin and 2.5 mM GW5074 ± 5 - 15 mM NAD^+, 15 – 30 % DMSO ± 0.1 % Triton X-100; crystals diffracted at BESSY beamline 14.1 to 3 – 3.5 Å

3.3.2.2. GW5074 inhibitory properties and specificity

With its IC_{50} value in the micromolar range and its off-target inhibition of kinases and GDH[154,155] GW5074 would need two major improvements in order to become a proper pharmaceutical Sirt5 modulator: 1) the compound has to become more specific and 2) it has to become more potent. Thus, several GW5074 derivatives, in which the halides are substituted with other moieties (Figure 30A, kindly provided by Prof. Dr. Franz Bracher, LMU Munich, Germany), were analyzed for their ability to inhibit Sirt5 desuccinylation activity. Of all compounds tested, UBCS 164 appeared to inhibit Sirt5 in a similar manner as GW5074 (Figure 30B, Table 12): Sirt5 activity decreased to 75.5 ± 16.5 % in presence of 10 µM compound (10 µM GW5074: 94.1 ± 0.4 %), whereas 100 µM of UBCS 164 lowered Sirt5

desuccinylase activity to 35.8 ± 2.1 % (100 µM GW5074: 39.6 ± 4.7 %). UBCS 165 inhibited Sirt5 weaker than GW5074 with 82.3 ± 9.6 % and 52.5 ± 18.9 % residual activity when using 10 or 100 µM compound, respectively. A similar behavior was seen with UBCS167 with residual Sirt5 activities of 93.4 ± 37.2 % and 58.4 ± 5.4 % in presence of 10 or 100 µM compound, respectively.

Although none of the substances were more potent than GW5074, important clues about the compound's inhibitory properties could be deduced: small unbranched and electron-rich phenolic substituents in meta and para position were crucial for the compounds' inhibitory capacity, while changing substituents at the indole part did not alter the inhibitory effect.

For a more thorough understanding of this compound, the three best inhibiting GW5074 derivatives, UBCS 164, 165 & 167, were tested for their ability to inhibit other Sirtuin isoforms in combination with substrate peptides derived from their natural substrate proteins: Sirt1 with a peptide derived from p53, Sirt2 with an α-Tubulin peptide and Sirt3 with an ACS2 peptide (cf. Table A 1 for peptide sequences). As seen in Figure 31 and Table 12, GW5074 and its derivatives showed the same effect on the other Sirtuin/substrate pairs as on Sirt5. However, inhibition of the nuclear Sirt1 and the cytoplasmic Sirt2 by GW5074 and UBCS 164 was significantly stronger compared to the mitochondrial Sirt3 and Sirt5.

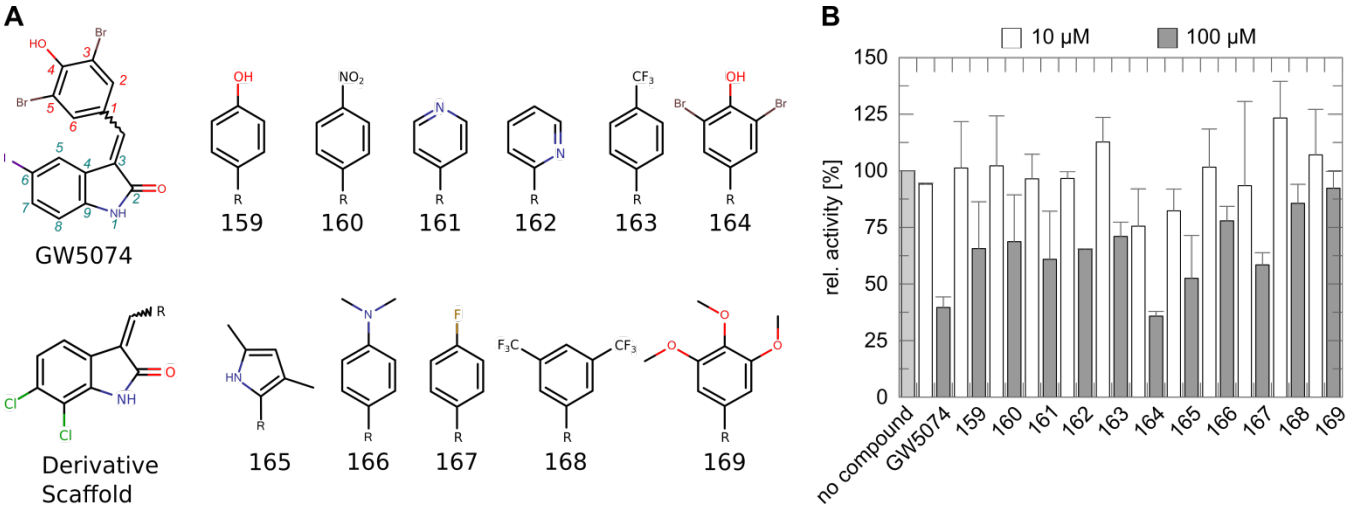

Figure 30: Sirt5 inhibition by GW5074 derivatives. Derivatives of GW5074 with two chlorides instead of one iodine atom on the compounds indole part (A) were tested against Sirt5 desuccinylation activity, revealing electron rich and unbranched phenol substituents to be crucial for enzyme inhibition (B).

Table 12: Sirtuin inhibition by GW5074 and its most potent derivatives UBCS 164, 165 and 167

Compound	Relative activity [%][(a)]							
	GW5074		164		165		167	
	10 µM	100 µM	10 µM	100 µM	10 µM	100 µM	10 µM	100 µM
Sirt1 + p53	77.6 ± 22.5	5.8 ± 1.2	81.6 ± 6.8	6.8 ± 0.2	111.1 ± 22.5	42.7 ± 13.0	107.6 ± 7.9	61.9 ± 12.4
Sirt2 + αTub	89.8 ± 6.1	14.9 ± 8.7	88.7 ± 15.1	13.1 ± 0.3	86.3 ± 19.6	20.0 ± 17.7	66.4 ± 1.1	36.2 ± 4.6
Sirt3 + ACS2	80.1 ± 4.4	44.8 ± 9.8	120.7 ± 3.6	47. 0 ± 2.8	83.5 ± 25.5	68.5 ± 23.0	99.3 ± 35	64.2 ± 8.0
Sirt5 + Prx1	94.1 ± 0.4	39.6 ±4.7	75.5 ± 16.5	35.8 ± 2.1	82.3 ± 9.6	52.5 ± 18.9	93.4 ±37.2	58.4 ± 5.4

a) Reactions in absence of inhibitor are set as 100 % rel. activity for each enzyme/peptide pair

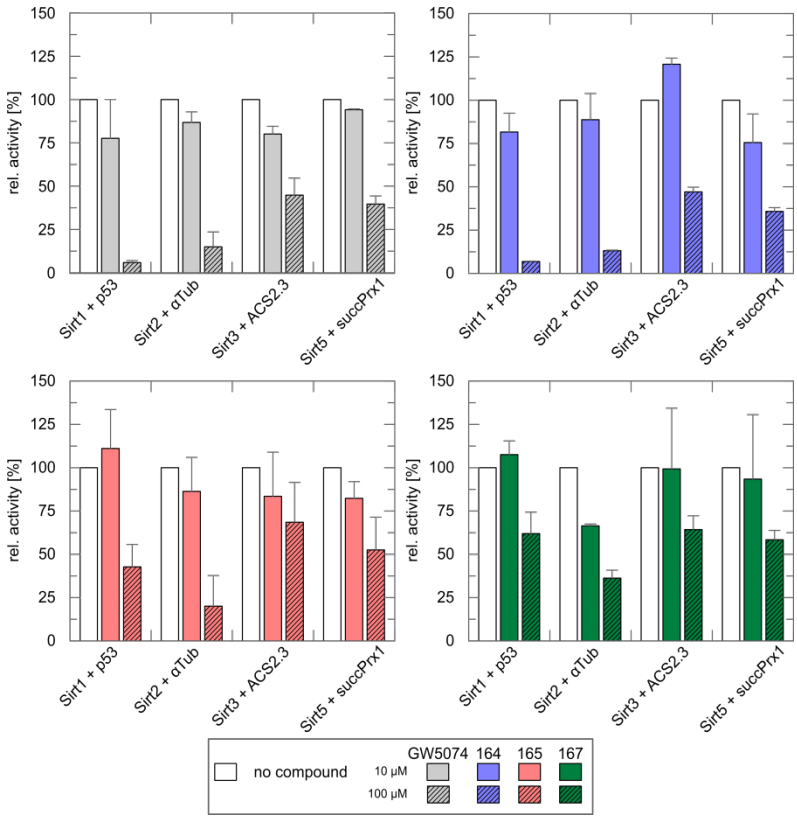

Figure 31: GW5074 and its derivatives are specific inhibitors for non-mitochondrial Sirtuins. Specificity analysis reveals GW5074 as well as its derivatives Compound 6, 7 and 9 to be more active against Sirt1 and Sirt2 and their preferred substrates, p53 and αTub, respectively. In comparison, the two mitochondrial Sirtuins Sirt3 and Sirt5 are less inhibited. However, concerning mitochondrial Sirtuins, desuccinylation of Prx1 by Sirt5 is inhibited slightly better than deacetylation of ACS2.3 by Sirt3. Grey: GW5074; blue: UBCS 164; red: UBCS 165; green: UBCS 167; colored bars: 10 µM compound; colored shaded bars: 100 µM. (Error) bars derived from at least three independent measurements.

3.3.2.3. The difficulty with GW5074 kinetic analyses

Derivatization of GW5074 resulted in no Sirt5 specific compound. Instead, a stronger inhibition of non-mitochondrial Sirtuins was observed, rendering this scaffold still valuable for developing future specific Sirtuin inhibitors. Thus, GW5074 inhibition mechanism was elucidated further in kinetic experiments using Sirt5 and succPrx1, as this combination was already well optimized for GW5074 inhibition analysis. However, since GW5074 is incompatible with the coupled enzymatic assay (designed for microtiter plates, thus allowing for high throughput analyses) the MS-based activity assay was employed, as it does not depend on any further enzymes, which could be inhibited by GW5074 (as the coupled enzyme GDH, see above).

Initially GW5074 was identified as a competitive kinase inhibitor blocking the enzyme's ATP-site and based on the rational that they would block the NAD^+ binding site of Sirtuins, the compound was revealed to be a µM Sirt2 inhibitor while screening possible inhibitory effects of adenosine analogues[156]. Although experiments summarized in Figure 28 were performed

at high NAD^+ concentrations (2.5 mM, cf. section 3.3.1) a profound Sirt5 desuccinylation inhibition by GW5074 was observed. This already indicates the compound to act rather against the peptide substrate.

Therefore, Sirt5 desuccinylation activity was analyzed at different succinylated peptide concentrations and at increasing GW5074 concentrations. For every peptide concentration the increase in deacylated peptide was analyzed over 20 min and afterwards initial rates were calculated and plotted against the respective peptide and GW5074 concentration. As seen in Figure 32 this resulted in a Michaelis-Menten like reaction course, which then could be fitted non-linearly to several inhibition models (competitive inhibition, non-competitive inhibition and mixed type inhibition) using *GraFit7*.

Comparing the three inhibitory models did not support a competitive inhibitory model on the kinetic level, since regression curves for a peptide competition did not fit to the experimental data (Figure 32A). Likewise, both other possible kinetic inhibition models did not fit clearly to the data points: Although the mixed inhibition regression curve fitted rather acceptably to the data points, inhibitory constants exhibited high error rates (Figure 32B). This was also observed for the non-competitive inhibition model (Figure 32C).

3.3.2.4. Competitive binding to Sirt5 between GW5074 and substrate peptide

Since the kinetic analyses were inconclusive, other techniques to elucidate GW5074 inhibitory mechanism were applied. Besides of competing on the kinetic level against any of the two or both Sirt5 substrates, GW5074 could simply bind to and thereby abolish Sirt5 activity – either allosterically or by binding too tight to one of the two substrates sites resulting in a stalled enzyme. Therefore, GW5074 binding to Sirt5 was analyzed in absence and presence of either substrate molecule by microscale thermophoresis (MST). After incubating Sirt5 with increasing concentrations of GW5074 for 30 min the MST of the Sirt5/GW5074 ligands was determined and plotted against the respective inhibitor concentration (Figure 33). This resulted in a K_D value of 24.2 ± 5.7 µM (Table 13), a concentration similar to the IC_{50} value of GW5074 against Sirt5 desuccinylation activity of 19.5 ± 7.3 µM (Table 12).

Competitive binding to Sirt5 between compound and substrate(s) would indicate a competitive inhibition mechanism of GW5074. Thus, compound binding to Sirt5 was analyzed in presence of saturating peptide and/or NAD^+ concentration(s). Interestingly, this resulted in a slightly higher compound affinity to Sirt5 in presence of NAD^+ (K_D of 16.6 ± 5.0 µM, Figure 33). On the contrary, peptide presence weakened compound binding to Sirt5, an effect slightly reversed if both peptide and NAD^+ were present (Table 13). This strongly indicates that the compound acts competitively against the substrate peptide, although this was not observed in kinetic experiments.

A

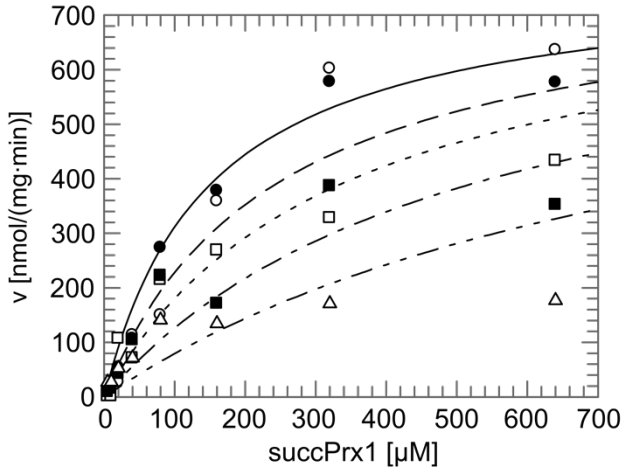

competitive inhibition

Parameter	Value	Std. Error
Vmax	776.2644	91.8001
Km	153.4634	47.1285
Ki	16.8586	5.3623

$$v = \frac{V_{max} \cdot [S]}{K_m \cdot \left(1 + \frac{[I]}{K_i}\right) + [S]}$$

B

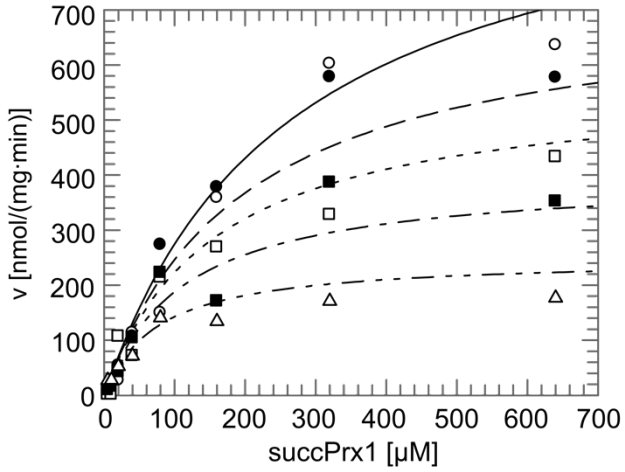

mixed inhibition

Parameter	Value	Std. Error
Vmax	997.9580	110.2368
Km	263.6375	62.1104
Ki	535.8722	764.9149
Ki' value	26.6660	7.0254

$$v = \frac{V_{max} \cdot [S]}{K_m \cdot \left(1 + \frac{[I]}{K_i}\right) + \left(1 + \frac{[I]}{Ki'}\right) \cdot [S]}$$

C

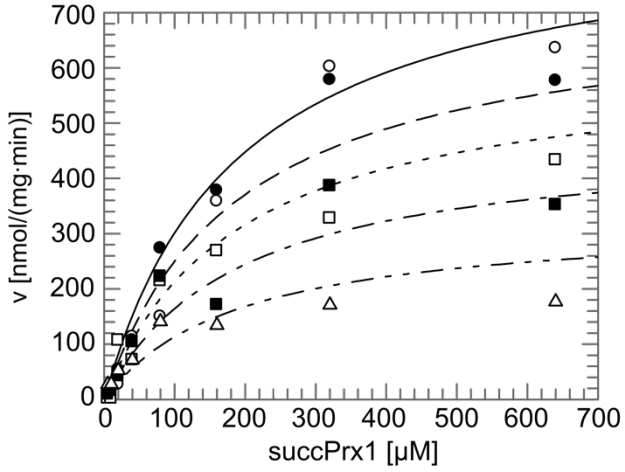

non-competitive inhibition

Parameter	Value	Std. Error
Vmax	871.7875	69.1760
Km	189.2818	34.6836
Ki	48.0104	7.9079

$$v = \frac{V_{max} \cdot [S] \cdot \frac{1}{1 + [I]/K_i}}{K_m + [S]}$$

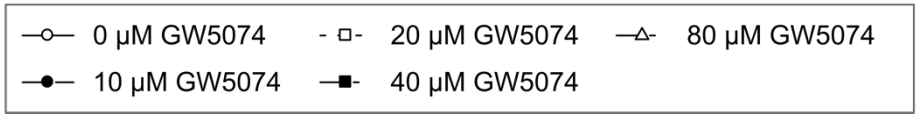

Figure 32: GW5074 does not follow common inhibition kinetics. Using Prx1 as substrate Sirt5 peptide kinetics in presence of increasing GW5074 concentrations fitted neither to a competitive inhibition model (A), to a mixed inhibition model (B), nor to a non-competitive inhibition model (C). MS-based assay using 5 µM Sirt5, 2.5 mM NAD^+ and varying concentrations of succPRx1. Std. Error depicts the error of the non-linear regression from *GraFit7*.

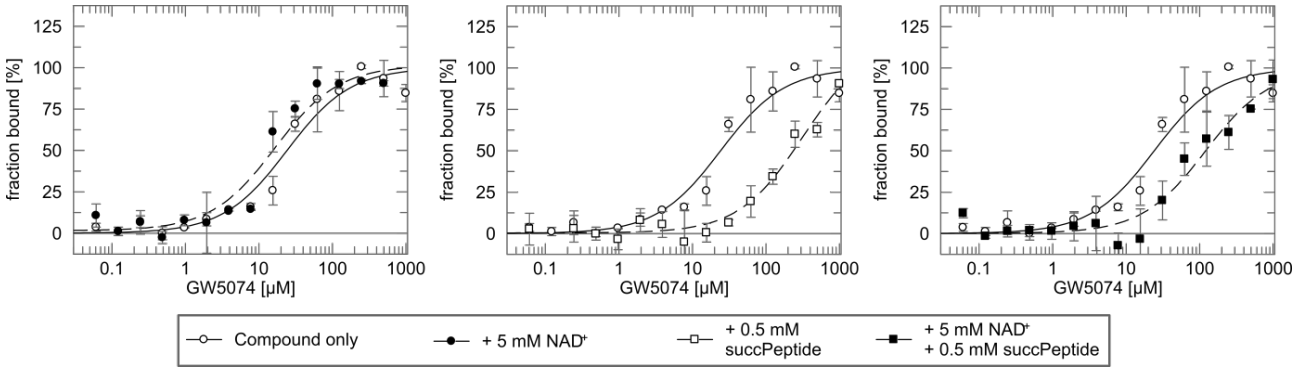

Figure 33: GW5074 binding to Sirt5. Sirt5 binds GW5074 with a K_D of 24.2 ± 5.7 µM. Presence of NAD^+ improves GW5074 affinity slightly whereas peptide presence weakens compound binding – an effect which can be rescued slightly in presence of both Sirt5 substrates.

Table 13: K_D values of GW5074 binding to Sirt3, Sirt5 and Sirt5 R105L determined

Sample	K_D [µM]		
	Sirt3	Sirt5	Sirt5 R105L
Enzyme only	~ 90 [(a)]	24.2 ± 5.7	9.5 ± 3.5
+ NAD^+ [(b)]	~ 70 [(a)]	16.6 ± 5.0	3.2 ± 1.4
+ peptide [(b)]	~ 50 [(a)]	> 250 [(a)]	6.8 ± 2.3
+ peptide & NAD^+ [(b)]	~ 50 [(a)]	>100	11.0 ± 4.7

a) estimated due to missing upper baseline (solubility limit of compound reached)

b) 5 mM NAD^+ and/or 0.5 mM succCPS1 (Sirt5), acACS2 (Sirt3) or acCPS1 (Sirt5 R105L), respectively

3.3.2.5. Acyl specific GW5074 inhibition due to active site amino acid composition?

The MST experiments suggested a competitive binding between peptide and GW5074, although initial kinetic experiments excluded this inhibition model. In order to investigate this behavior further, GW5074 was tested on the likewise mitochondrial Sirtuin Sirt3. Other than Sirt5, Sirt3 is a protein deacetylase and as such the major protein deacetylase within mitochondria. Furthermore, active site amino acid compositions of Sirt3 and Sirt5 are optimized to accommodate either acetylated peptides or succinylated peptides, respectively, which were already found to be involved in distinguishing NAM sensitivity for these two enzymes (cf. section 3.2.2)[126]. With Sirt5 exhibiting differential sensitivities towards GW5074 inhibition of its deacetylation and desuccinylation activity, an inhibition model similar to NAM is imaginable. Thus, GW5074 was tested against Sirt3 accordingly to previous Sirt5 experiments. Comparing GW5074 affinities for Sirt3 and Sirt5 revealed a strong preference for Sirt5, as no distinct K_D value for GW5074 binding to Sirt3 could be determined within the compound's solubility limits. Estimated K_D values for GW5074 binding to Sirt3 ranged above 50 µM (Figure 34, Table 13), thus at least two-fold weaker compared to Sirt5. Furthermore, any substrate presence did not interfere or compete with compound binding (Figure 34).

In order to verify the different active site amino acid composition to be the reason of the different sensitivity of Sirt3 and Sirt5 against GW5074, a Sirt5 R105L variant (cf. sections

1.2.4 & 3.2.2) was analyzed for its GW5074 sensitivity. Binding analysis revealed a general stronger GW5074 binding to Sirt5 R105L (Figure 34) but as for Sirt3 no peptide influence on compound binding could be observed (K_D of 9.5 ± 3.5 µM vs. 6.8 ± 2.3 µM, Table 13). This indicates that R105 within the active site of Sirt5 is crucial for compound binding and peptide competition.

3.3.2.6. GW5074 inhibits Sirt5 irreversibly

Apart from these binding properties, GW5074/peptide competition had to be confirmed during catalysis. Therefore, Sirt5 was incubated with either peptide or compound for 30 min. Then, GW5074 or peptide was added, respectively, and samples were incubated additional 30 min. Then the reaction was started by adding NAD^+. As soon as Sirt5 was incubated with GW5074, no enzymatic activity could be observed (Figure 35). This effect occurred independent of the order of incubation, i.e. independent of whether compound or peptide was added and incubated first. Even if both peptide and GW50074 were incubated simultaneously, Sirt5 was inactive. If no compound was present, Sirt5 exhibited profound desuccinylase activity even after 1 h of incubation. This reveals GW5074 to inhibit Sirt5 irreversibly, possibly by abolishing peptide binding as indicated by the binding analyses.

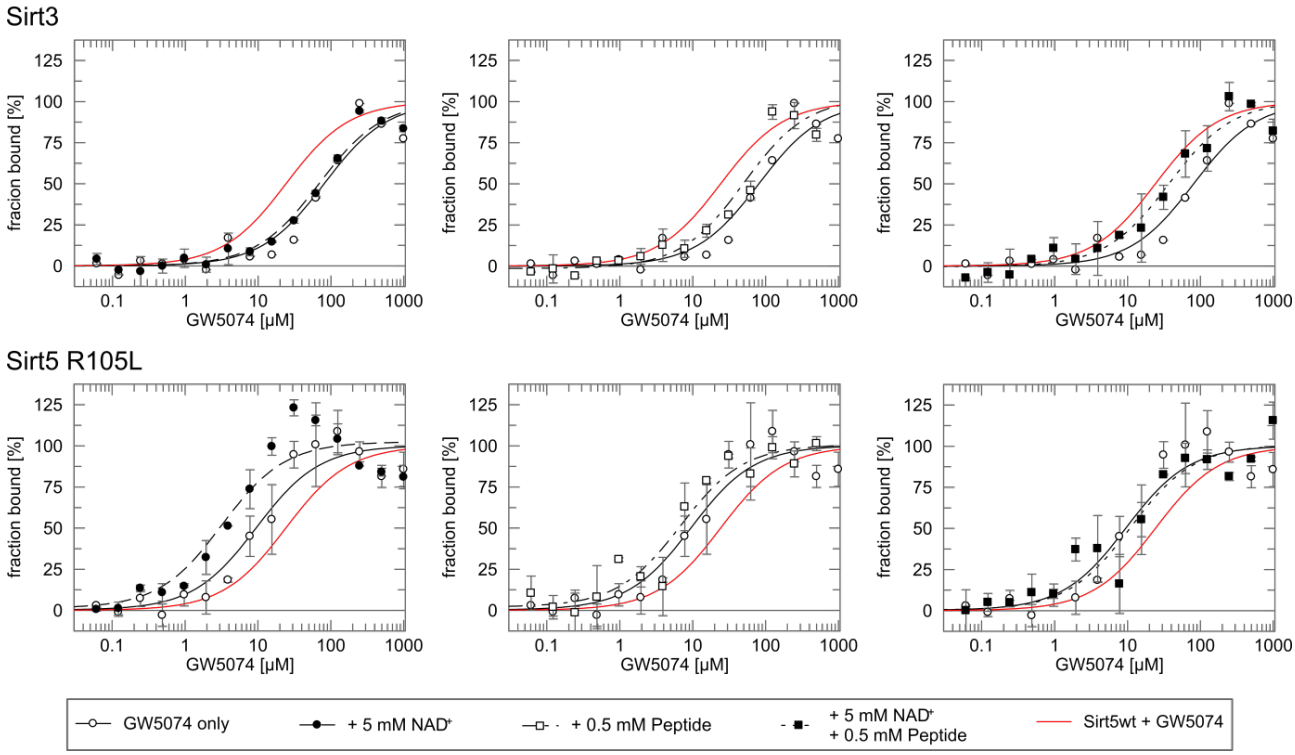

Figure 34: GW5074 binding is dependent on the active site amino acid composition. GW5074 binding to Sirt3 is weaker compared to its binding to Sirt5. Furthermore, presence of NAD^+ and or substrate peptide does not interfere with compound binding significantly (upper panel) while peptide presence weakens GW5074 binding to Sirt5 (Figure 33). Sirt5 R105L binds GW5074 better than the wild type variant but in a Sirt3 like manner: neither one of the two substrates seem to affect compound binding. This indicates R105 being crucial for compound binding and peptide competition for Sirt5.

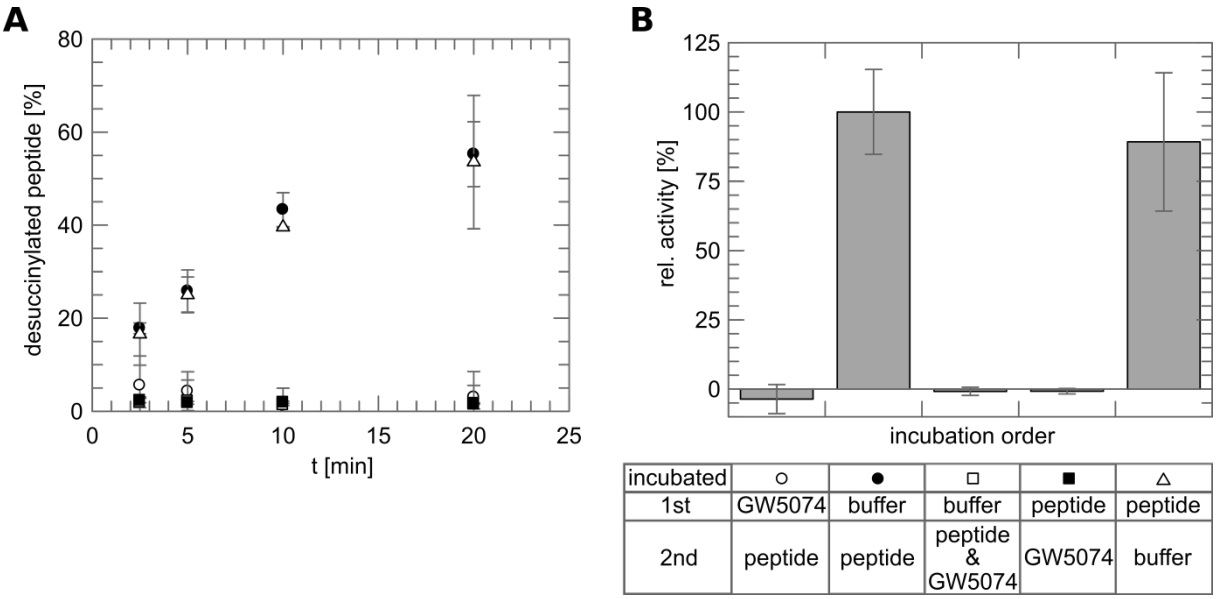

Figure 35: GW5074 stalls Sirt5 irreversibly. Time series experiments after incubating Sirt5 first with GW5074, then with peptide and vice versa before reaction start exhibit the same course as if compound and peptide are incubated simultaneously. Only in absence of GW5074 Sirt5 activity was observed, suggesting the compound to interfere with peptide binding irreversibly. (A) Time course experiment of Sirt5 desuccinylation after different incubation conditions; (B) Relative Sirt5 activity calculated from linear regression of the time course experiment, Sirt5 activity after initial buffer incubation and subsequent peptide incubation before addition of NAD^+ is set to 100 % relative activity.

3.4. Developing Specific Sirtuin Regulators

3.4.1. Inhibitory Lysine Derivatives

Screening known Sirtuin modulators for their effect on Sirt5 revealed the indole GW5074 to be a specific inhibitor regarding the different Sirt5 activities. However, further analyses identified GW5074 to inhibit Sirtuins rather unspecific with a slight Sirt1 preference. Thus, specific Sirt5 inhibitors remain to be identified.

For the development of specific Sirt5 inhibitors, its unique active site amino acid composition could be exploited. Only Sirt5 bears a positively charged amino acid inside its active site (R105), thus succinylated, malonylated or glutarylated substrate lysines can be positioned via salt bridge formation, resulting in a preference towards these substrate acylations[6,31]. Indeed, a substrate peptide analogue that contains a phenyl moiety adjacent to the succinyl carboxy group was shown to inhibit Sirt5. The bulky aromatic group points inside the C-site, thus abolishing NAD^+ binding[34]. However, as already mentioned, inhibitory peptides suffer from several downsides (cf. section 1.3.2.1). In order to overcome the disadvantages of peptide inhibitors (e.g. intracellular degradation), single lysine molecules with presumably inhibitory acylations were synthesized by the collaborating lab of Prof. Antonello Mai (Sapienza University Rome, Figure 36).

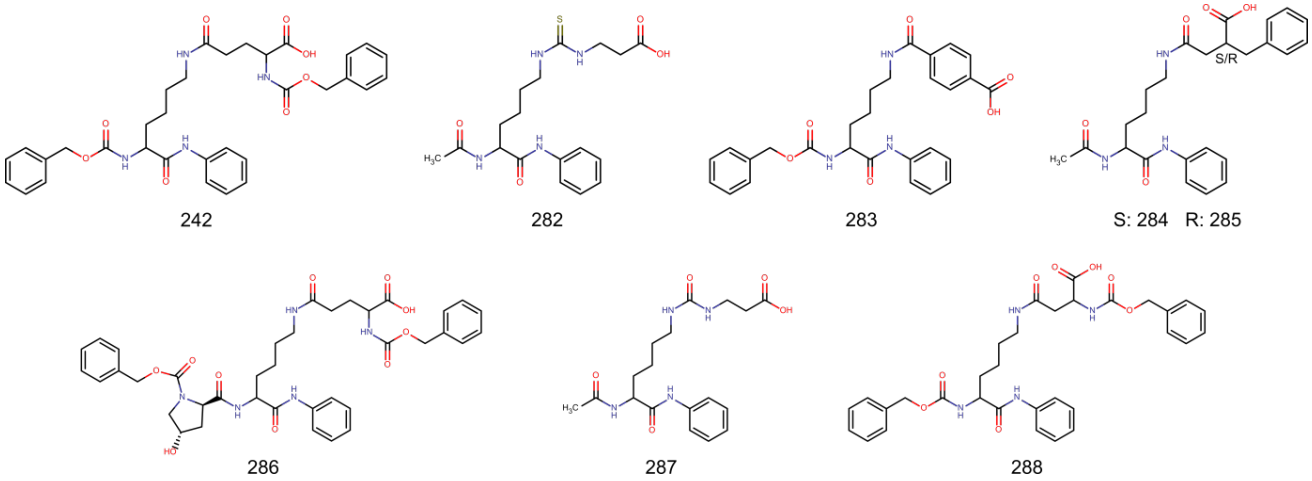

Figure 36: Design of inhibitory Sirt5 compounds based on a single acylated lysine. Based on the presumably inhibitory lysine derivative UBCS 242, which contains a 2-(Z-amino)-glutarylated lysine further, lysine derivatives were designed. The compounds moieties and there expected mode of action are summarized in Table 14.

The compounds were expected to compete with the substrate acylated lysine and in case of UBCS 242 & 286 an additional blocking of the C-site of the NAD^+ binding pocket was predicted. In order to verify their inhibitory effect, 100 µM of each compound were tested against Sirt5 desuccinylation in a fluorometric deacylation assay (Figure 37A). This screen revealed the parent UBCS 242 to reduce Sirt5 activity to 72.8 ± 1.6 % compared to a control reaction without compound. All other lysine derivatives turned out to be comparably or less potent (residual activity of 75 – 90 %, cf. Table 15 for exact values) apart from UBCS 282, which reduced Sirt5 activity to 47.1 ± 10.9 µM at a concentration of 100 µM.

Table 14: List of lysine derivatives tested.

UBCS	Protecting group		Attached acid	Expected mode of action
	N-terminal	C-terminal		
242	Z	Anilino	4S-Z-amino-glutaric acid	Competing substrate lysine & blocking C-site
282	Acetyl		β-alanine linked via carbothioamide	Competing substrate peptide and stalling enzyme
283	Z		1,4-phtalic acid	Competing substrate peptide
284/285	Acetyl		2-benzyl-succinic acid	Competing substrate lysine
286	Z[(a)]		4S-Z-amino-glutaric acid	Competing substrate lysine & blocking C-site
287	Acetyl		β-alanine linked via carboxyamide	Competing substrate lysine
288	Z		3S-Z-amino-succinic acid	Competing substrate lysine & blocking C-site

a) UBCS 286 contains an additional 4-Hydroxyproline N-terminally of the lysine, which was expected to increase compound binding.

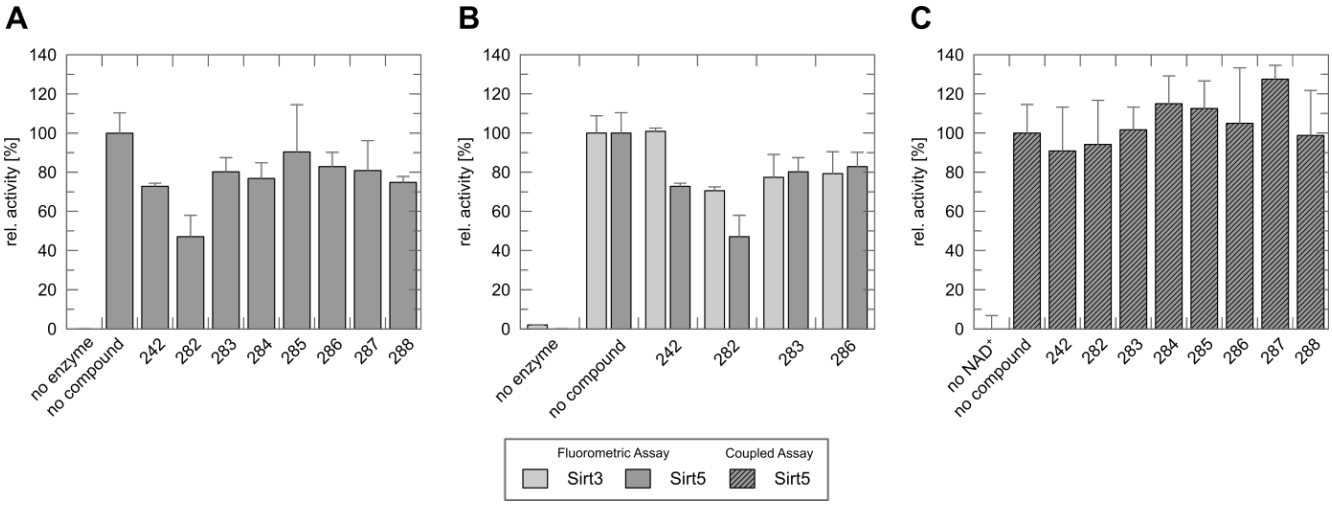

Figure 37: Lysine derivatives as Sirt5 inhibitors. (A) Screening the set of compounds from Figure 37 against Sirt5 desuccinylase activity in a fluorometric assay revealed the parent UBCS 242 and its derivative UBCS 282 to be Sirt5 inhibitors. (B) These compounds turned out to be Sirt5 specific as Sirt3 deacetylation under the same settings is less inhibited by UBSC 242 & 282. However, the weak Sirt5 inhibiting UBCS 283 & 286 are weak Sirt3 inhibitors as well. (C) Using a label free substrate peptide in the coupled enzymatic assay reveals the lysine derivative to be unable to inhibit Sirt5 desuccinylation. Assays were performed using 1.5 µM enzyme, 50 µM succinylated or acetylated FdL peptide or 50 µM succCPS1 peptide, respectively, and 500 µM NAD^+, 100 µM of each compound and a final DMSO concentration of 5 %. Bars represent the mean of at least two independent experiments. Residual activities are summarized in Table 15.

Table 15: Sirtuin activity in presence of lysine derivatives designed as Sirt5 inhibitors.

UBCS	Rel. activity [%]		
	Fluorometric Assay		Coupled Assay
	Sirt3	Sirt5	Sirt5
No enzyme/NAD^+	1.95 ± 0.1	0.0 ± 0.1	0.0 ± 6.8
No Cmpd	100.0 ± 8.8	100.0 ± 10.3	100.0 ± 14.6
242	100.8 ± 1.7	72.8 ± 1.6	90.8 ± 22.4
282	70.6 ± 1.9	47.1 ± 10.9	94.2 ± 22.5
283	77.4 ± 11.6	80.2 ± 7.3	101.7 ± 11.5
284	n.d.	76.8 ± 8.0	115.0 ± 14.1
285	n.d.	90.3 ± 24.2	112.5 ± 14.1
286	79.2 ± 11.3	82.9 ± 7.2	105.0 ± 28.3
287	n.d.	80.8 ± 15.3	127.5 ± 7.1
288	n.d.	74.8 ± 3.0	98.8 ± 23.0

Assays were performed using 1.5 µM enzyme, 50 µM succinylated or acetylated FdL peptide or 50 µM succCPS1 peptide, respectively, and 500 µM NAD^+, 100 µM of each compound and a final DMSO concentration of 5 %.

All Sirtuins bind substrate peptides via β-sheet interaction and accommodate a substrate lysine via a hydrophobic tunnel, thereby positioning the acyl moiety inside the active site; other Sirtuin isoforms might bind the lysine derivatives designed for Sirt5 as well. Therefore, the two best inhibiting UBCS 242 & 282 and the weakly inhibiting UBCS 283 & 286 were

tested against Sirt3 deacetylation accordingly, revealing a reduced inhibitory effect compared to Sirt5 (Figure 37B): while the parent UBCS 242 did not inhibit Sirt3 deacetylation at 100 µM, UBCS 282 reduced Sirt3 activity to 70.6 ± 1.9 %. UBCS 283 and 286 decreased Sirt3 activity in a similar manner as Sirt5 with approximately 80 % residual activity (cf. Table 15 for exact values).

The specificity of the lysine derivatives for Sirt5 inhibition proved their expected mode of action: being derivatives of a glutarylated lysine, both compounds are preferentially bound by the proper deglutarylase Sirt5. On the contrary, the profound deacetylase Sirt3 is less inhibited as it binds and deacylates long and charged acyl moieties to a lesser extend[53]. In order to analyze the compound potency and in order to exclude assay artifacts from using labeled substrate peptides, the panel of lysine derivatives was tested for their inhibitory effect in the coupled enzymatic assay. Using the same settings as for the fluorometric assay, it turned out, that 100 µM of any compound were unable to inhibit Sirt5 desuccinylation of a label free CPS1 peptide (Figure 37C). The label free Sirtuin substrate peptides of 9 – 13 amino acids used in the coupled assay are known to be better Sirtuin substrates compared to the four amino acids spanning fluorescently labeled substrates used in the fluorometric assay. Hence, lysine derivatives act only as proper inhibitors against weak Sirtuin substrates.

For the development of more potent Sirt5 inhibitors based on a single acylated lysine, optimized lysine modifications need to be identified. Since structural data of glutarylated CPS1 and 3S-Z-amino-succinylated CPS1 peptides in complex with zSirt5 is already available (pdb code: 4UUA & 4UTR)[34], UBCS 242, 282, 283 and 286 were modeled into the active site of Sirt5 to gain further insight into binding properties a more potent compound should exhibit. By fitting the chosen compounds into the electron density of the CPS1 peptides of the reference structure and subsequent superposition of Sirt5 bound to a succinylated peptide and NAD^+ (pdb code 3RIY)[31] with the reference zSirt5, a possible position of each compound within the Sirt5 active site could be determined (Figure 38).

Sirt5 favors the deacylation of negatively charged acyl moieties. Different from other Sirtuin isoforms it contains an Arginine (R105 in Sirt5), which positions the carboxy group of the substrate lysine's acyl moiety within the active site (Figure 38A)[31]. Thus, all lysine derivatives were modeled to interact with this specific Arginine residue (Figure 38B – F). This modelling supports the notion that all compounds could act as competitive inhibitors against the substrate's acylated lysine. In addition, UBCS 242 (Figure 38B) as well as UBCS 286 (Figure 38F) point into and thereby block the C-site with their Z group. The C-site harbors the NAM part of the co-substrate NAD^+ during Sirtuin catalysis; hence UBCS 242 & 286 compete with both Sirtuin substrates for active site binding.

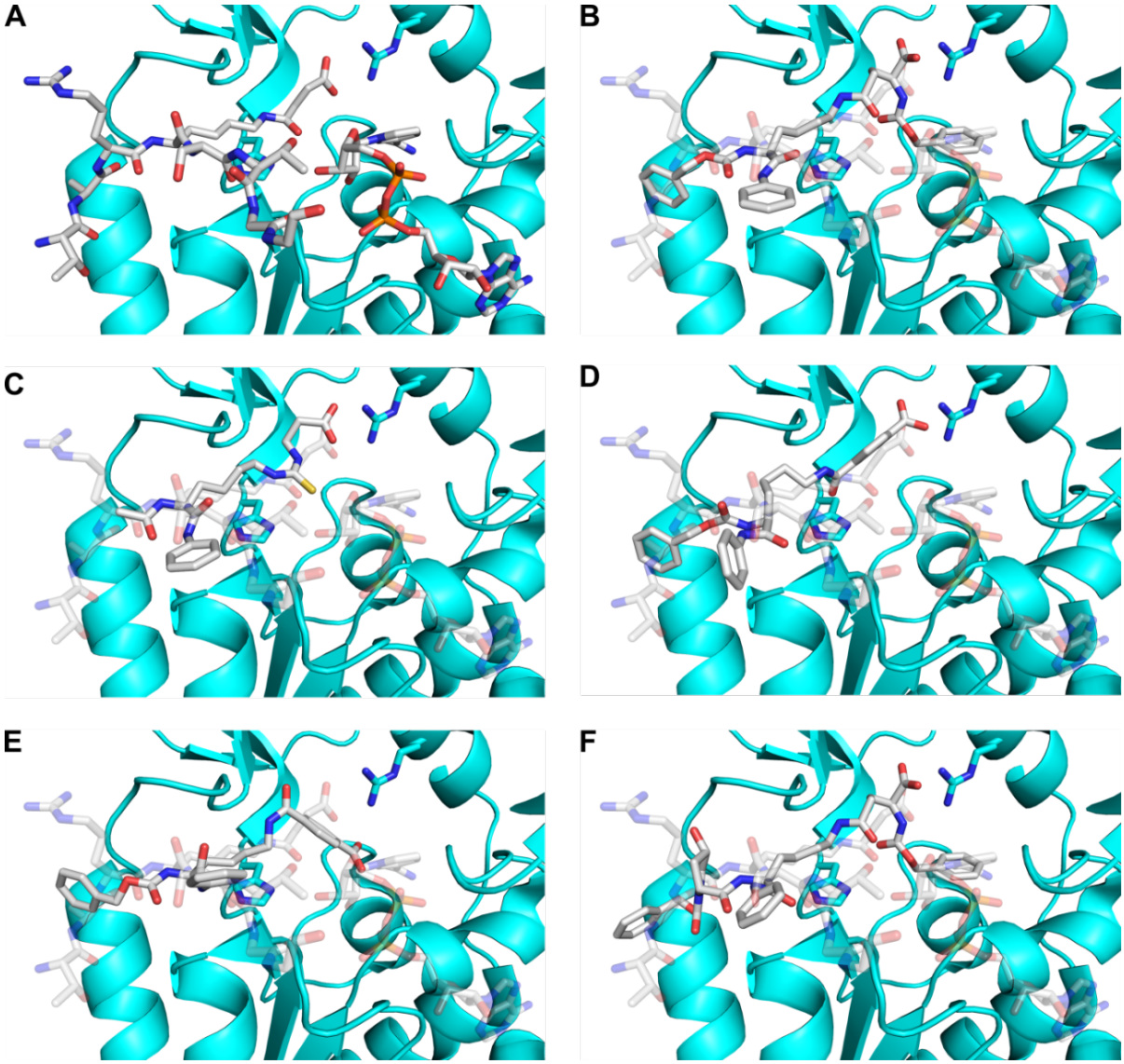

Figure 38: Modelling the lysine derivatives into the active site of Sirt5 suggests their inhibitory mechanism. Comparing the structure of Sirt5 in complex with a succinylated peptide and NAD^+ (A, pdb entry: 3RIY) and models of UBCS 242 (B), 282 (C), 283 (D & E) and 286 (F) reveal UBCS 242 & 286 to compete with both substrate peptide and NAD^+ for binding. UBCS 282 competes only with the substrate peptide and due to its carbothioamide it stalls the enzymatic reaction[157]. For UBCS 283 two binding conformations are possible: it could adopt a salt bridge with the Sirt5 specific active site Arg, thus competing just with the substrate peptide for binding (D). In a different conformation (E), UBCS 283 could point towards the C-site, thus competing with the substrate peptide and hampering NAD^+ binding. Cartoon representation of Sirt5 (cyan) in complex with a succinylated peptide and NAD^+ (A, peptide and NAD^+ as sticks and in B – F transparent as a reference). Models were created by fitting compounds into the electron density of the substrate peptide from the complex structures of zSirt5 in complex with either a glutarylated CPS1 peptide (UBCS 282 & 283) or a 3S-Z-amino-succinylated CPS1 peptide (UBCS 242, 283 & 286, zSirt5 reference structures: 4UUA & 4UTR)[34].

UBCS 282 bears a β-alanine linked via a carbothioamide to the lysine ε-amino group. Resembling a glutarylated lysine, this compound differs from a Sirt5 substrate by the sulfur atom within the carbothioamide. As suggested by the model shown in Figure 38C this sulfur would point towards the ribose of NAD^+, just like the oxygen atom of the substrate lysine's ε-amide bond. Thus, UBCS 282 might form a S-alkylimidate which is more stable compared to the usual O-acylimidate formed during Sirtuin enzymatic reaction[85,157], resulting in a stalled intermediate and blocked Sirt5 enzyme.

For UBCS 283 with its phtalic acid two binding conformations are imaginable: on the one hand, its terminal carboxy group could form a salt bridge with Sirt5 R105 thus competing solely with the substrate's acylated lysine (Figure 38D). However, in order to form this salt bridge, the Lys side chain would have to adopt a highly unfavorable conformation. On the other hand, the phtalic acid moiety could point towards the C-site, a conformation that provides the lysine side chain with more space within the hydrophobic tunnel of the Sirtuin active site (Figure 38E). This would render UBCS 283 a competitive inhibitor against the substrate's acylated lysine and NAD^+. Without structural data for this lysine derivative, the precise inhibitory mode of action of UBCS 283 remains elusive. However, this compound shows little Sirtuin isoform specificity since the deacetylase Sirt3 lacking an active site Arg is equally inhibited by UBCS 283 as the desuccinylase/deglutarylase Sirt5 (Figure 37 and Table 15). Thus, it is possible that Sirt5 is inhibited by the formation of a salt bridge between UBCS 283 and R105, while Sirt3 is inhibited by UBCS 283 adopting another conformation, in which the phtalic moiety points towards the C-site.

3.4.2. 1,4-Dihydropyridines are Specific Sirtuin Activators

3.4.2.1. Specific activation of Sirt3 by 1,4-DHP compounds

With the many beneficial effects of CR and Sirtuin enzymes contributing to these health advantages, Sirtuin activation by STACs are of special pharmacological interest. However, only a few STACs are known for Sirt1 by now (cf. section 1.3). Previously, the 1,4-DHP scaffold was designed based on structural similarity between already known Sirtuin compounds (Figure 7 & Figure 8), resulting in the Sirt1 activating UBCS 125 (Figure 39A)[106].

In order to investigate, whether Sirt3 could be modulated by 1,4-DHP compounds as well, ten derivatives of UBCS 125 were generated by the collaborating lab of Prof. Antonello Mai (Sapienza University Rome) by changing the functional groups at the scaffold's positions 1 and 3 – 5 (Figure 39B). Sirt3 deacetylation activity was analyzed using the coupled continuous assay which circumvents possible artificial chromophore/compound interaction of the FdL-assay but still allows for a higher experimental throughput than the MS-based assay. Sirt3 activity analyses in presence of 10 & 100 µM of UBCS 123 – 133 indeed revealed a twofold activation by the parent compound UBCS 125, consistent with previous reports[106]. UBCS 129, 130, 132 & 133 activated Sirt3 similar to the parent compound, while UBCS 123, 124, 127 & 128 had no or just minor activating effects. Strikingly UBCS 126 & 131 turned out to activate Sirt3 deacetylation ~ 3.5- and 5-fold, respectively (Figure 39C).

In this experimental setup, supposedly Sirtuin modulating compounds might also affect the coupled enzymes NCA and GDH. Thus, control reactions were conducted in which NAM was added to the reaction mixture instead of a substrate peptide. This confirmed that the 1,4-DHP compounds tested acted neither on NCA nor GDH, as no significant difference in NAM consumption was observed (Figure 39D). However, to provide evidence that the compounds activate Sirt3 directly, a MS-based assay in presence of 100 µM UBCS 131 was performed. This again resulted in proper activation of Sirt3 deacetylation activity, which confirms the direct activation of Sirtuins by 1,4-DHP compounds.

The parent compound was initially described to activate Sirt1 better than Sirt2 and Sirt3 in the FdL-assay[106]. In order to analyze the specificity of the panel of 1,4-DHP compounds, UBCS 123 – 133 were tested against further human Sirtuin enzymes. As expected, the parent compound UBCS 125 activated Sirt1 deacetylation of a p53 peptide ~ 2-fold, which was observed for most of the other compounds tested. As for Sirt3, UBCS 128 exhibited no effect on Sirt1. Interestingly, different to Sirt3, UBCS 131 had no significant effect on Sirt1 activity (Figure 40A). Sirt2 dependent deacetylation of an αTub peptide was little affected by all 1,4-DHP compounds tested (Figure 40B). This was observed for Sirt5 desuccinylation activity against succCPS1 as well. Only UBCs 133 had a moderately activating effect of ~ 2.5-fold (Figure 40C).

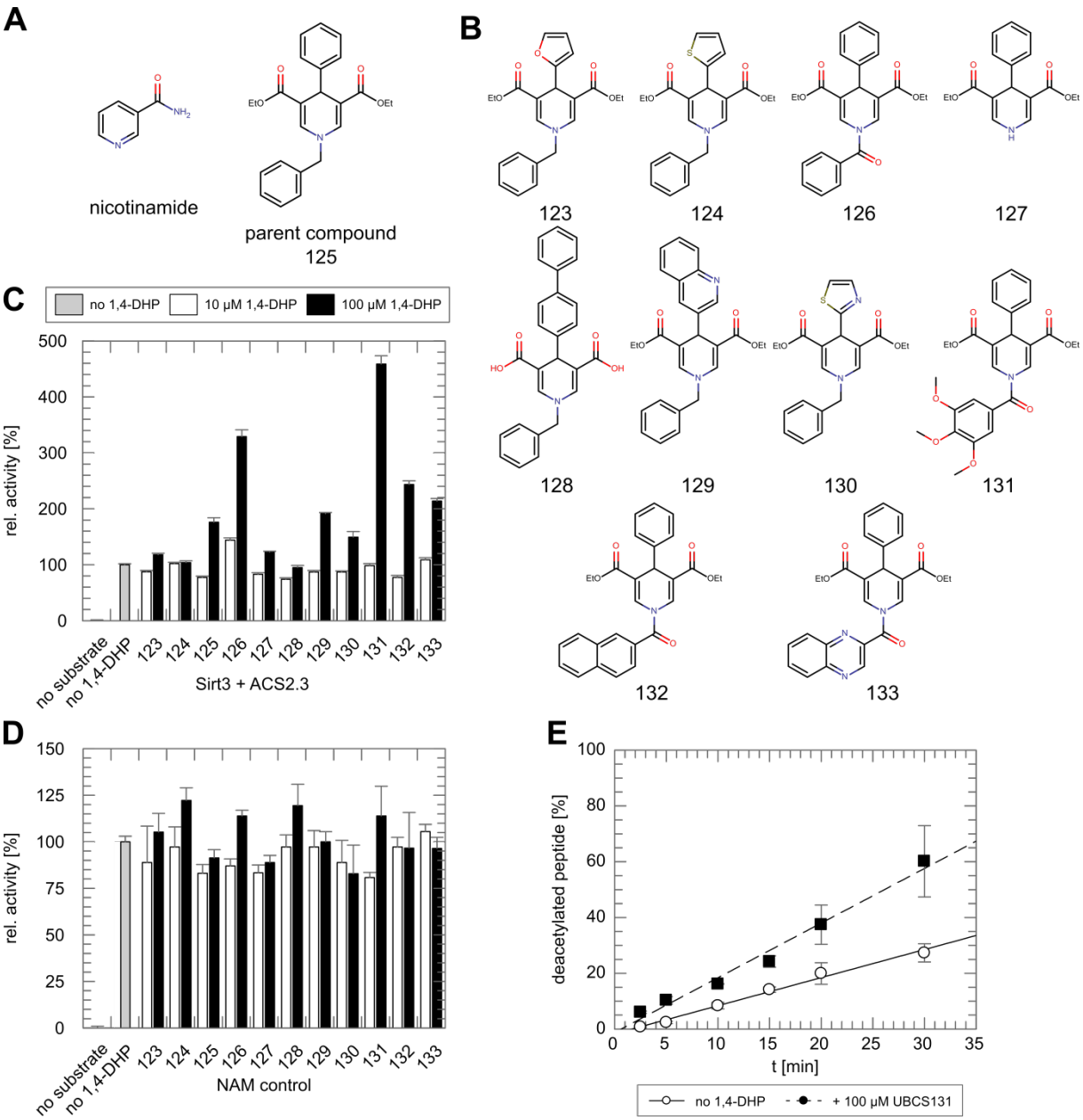

Figure 39: Sirt3 activation by 1,4-DHPs. (A) 1,4-DHP compounds and the parent UBCS 125 are derived from structural similarity towards nicotinamide (NAM) and other Sirtuin modulators (cf. Figure 7). (B) Ten derivatives of UBCS 125 were generated and tested against Sirt3. (C) UBCS 126 & 131 increase Sirt3 deacetylation activity in the coupled continuous assay 3.5 -and 4.5-fold, respectively. (D) Using NAM instead of substrate peptide in the coupled continuous assay reveals no 1,4-DHP effect on the coupled enzymes GDH and NCA. (E) Verification of Sirt3 activation by UBCS 131 using the mass spectrometry based assay. Values and (error) bars are derived from at least three independent experiments. Assays consisted of 1.5 µM Sirt3, 50 µM ACS2.3 or NAM, 100 µM NAD^+ and a final DMSO concentration of 5 %. The MS based assay was supplemented with NCA to avoid NAM accumulation.

Sirt1 activation by resveratrol and other STACs is known to be substrate sequence dependent[108]. To assess, whether this is the case for 1,4-DHP activation as well, the deacetylation of several recently identified Sirt3 substrate peptides[153] was analyzed. As seen in Figure 40D UBCS 131 was able to activate Sirt3 deacetylation activity against any peptide tested. Importantly, even the activity against poor Sirt3 substrate peptides was enhanced in presence of 100 µM UBCS 131 (e.g. AATase and αTub). Thus, 1,4-DHP activation of Sirtuins is substrate sequence independent.

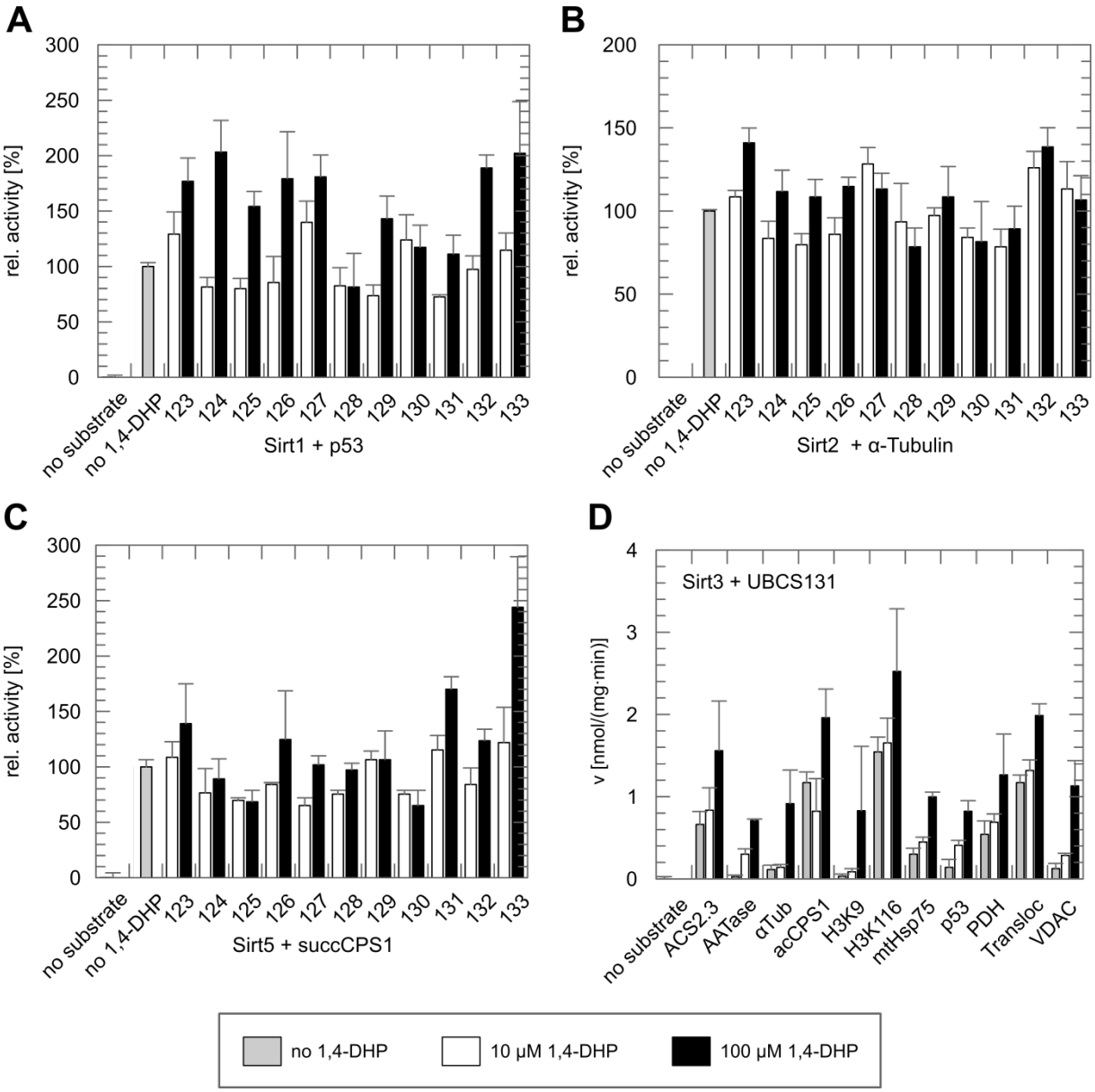

Figure 40: Sirt3 activation by UBCS 126 & 131 is specific and substrate independent. (A) Sirt1 is moderately activated by several 1,4-DHP compound but not by UBCS 131. (B) UBCS 123 – 133 have no significant effect on Sirt2. (C) Sirt5 is activated mildly by UBCS 133. (D) UBCS 131 enhances Sirt3 deacetylation activity towards any substrate. Bars and error bars depict the mean and STDEV from at least three independent experiments. Coupled enzymatic assay in presence of 1.5 µM enzyme, 50 µM substrate peptide, 100 µM NAD^+ and a final DMSO concentration of 5 %.

3.4.2.2. Identification of Sirt5 specific 1,4-DHP compounds

The Sirt3 activating 1,4-DHPs UBCS 126 & 131 significantly enhanced the deacetylation reaction at a concentration of 100 µM (Figure 39C). For a detailed analysis of these compounds and to evaluate their potency, dose response experiments were conducted. As seen in Figure 41A, Sirt3 activity increases with increasing amounts of both UBCS 126 & 131. Although no saturating Sirt3 activity was detected within the solubility limits of each compound, EC_{50} values of 100 – 200 µM can be estimated. In addition, UBCS 131 seems to be more potent than UBCS 126 and likely exhibits a higher efficacy.

Due to their moderate potency, derivatives of UBCS 126 & 131 were synthesized, keeping the bottom (i.e. position 1 of the 1,4-DHP scaffold) benzoyl or 3,4,5-trimethoxybenzoyl moiety fixed and varying the top aromatic group (i.e. position 4 of the activator scaffold). Furthermore, additional benzyl and two 3,4,5-trimethoxy benzyl derivatives were generated, to assess the importance of the carbonyl oxygen on Sirtuin activation by UBCS 126 & 131. In addition, 1,4-DHP compounds with varying bottom aromatic moieties and a fixed top were prepared (Figure 41B). Before they were tested for their effect against Sirt3, it was verified again that the panel of novel compounds would not affect NCA or GDH. Indeed, no modulating effect of the novel derivatives was observed on NAM consumption in the coupled continuous assay control. Only UBCS 333 turned out to inhibit one of the coupled enzymes (Figure 41C).

Having confirmed that the novel 1,4-DHP compounds do not interfere with the coupled continuous assay significantly, their effect against Sirt3 deacetylation activity was analyzed. Surprisingly, out of all 36 compounds tested, only UBCS 366 was able to activate Sirt3 ~ 2.5-fold (Figure 41D), thus being as potent as the parent compound UBCS 125 (Figure 39C).

in addition, the novel compounds were screened for their effect on Sirt1, Sirt2 and Sirt5 activity, which identified UBCS 366 to act as a pan Sirtuin activator (Figure 41E – G). Moreover, several of the 36 novel compounds turned out to activate Sirt5 specifically (Figure 41G). The best activating 1,4 DHPs were UBCS 344, 345, 349 & 350. The latter activated Sirt5 desuccinylation activity already at 10 µM (~2-fold) and ~ 3.5-fold at a concentration of 100 µM. In a dose response experiment an EC_{50} value of ~ 60 µM was observed for UBCS 350, with a 5-fold activation compound concentrations ≥ 200 µM compound (Figure 41H).

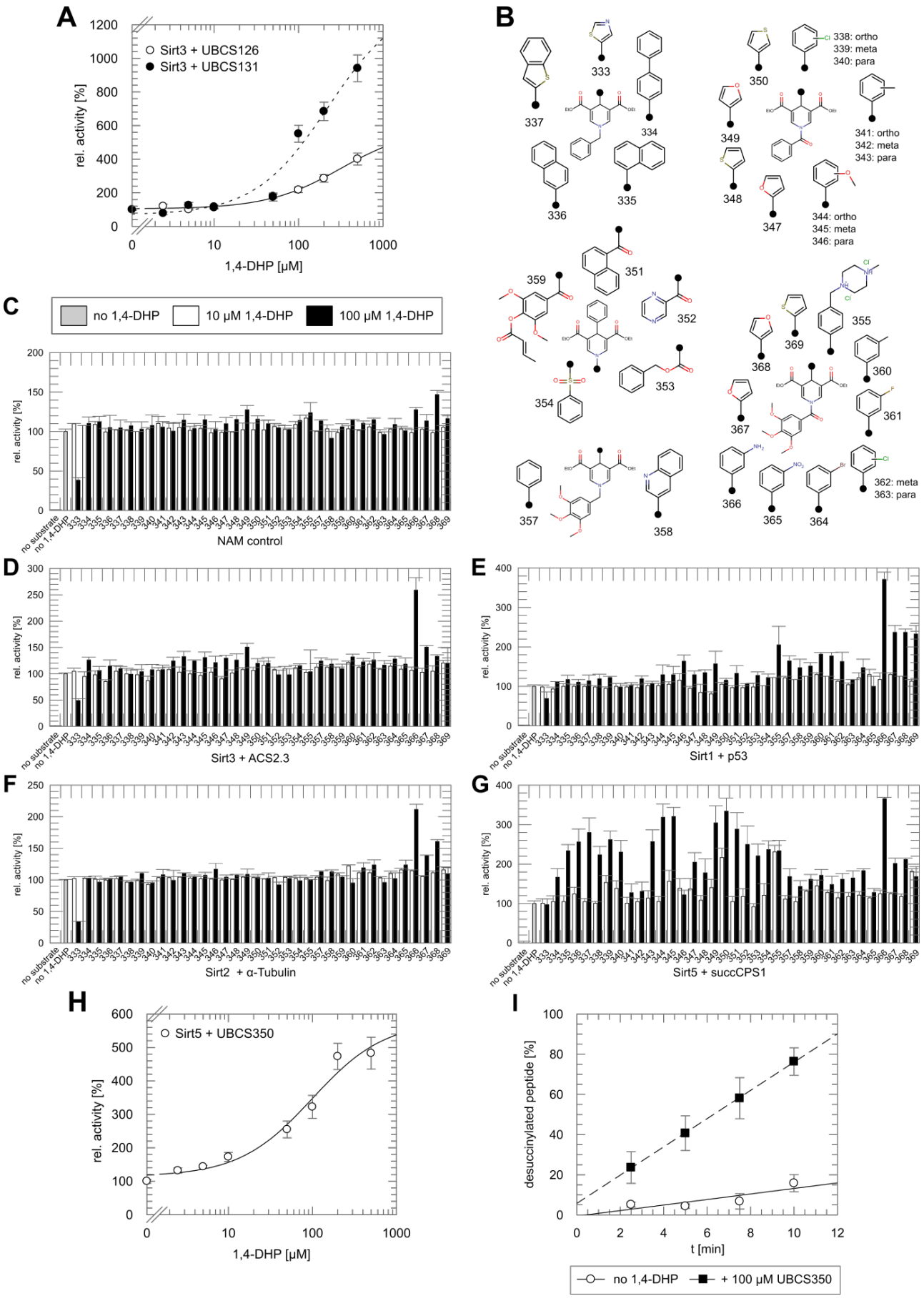

(Figure legend on the following page)

(Figure on the previous page)

Figure 41: Derivatization of UBCS 126 & 131 reveals Sirt5 specific activators. (A) Sirt3 is activated by UBCS 126 & 131 in a dose-dependent manner with estimated EC_{50} values of ~ 100 – 200 µM. (B) Derivatives of UBCS 126 & 131 with fixed bottom Benz(o)yl or 3,4,5-trimethoxy benz(o)yl groups and varying top aromatic groups or with a fixed top phenyl moiety and varying bottom aromatic groups. (C) The novel 1,4-DHP compounds do not interfere with the coupled enzymes NCA and GDH. (D) Sirt3 is activated only by UBCS 366, which also activates Sirt1 (E) and Sirt2 (F). (G) Surprisingly, several novel 1,4-DHP compounds at as Sirt5 specific activators. (H) Similar to UBCS 126 & 131 against Sirt3, UBCS 350 activates Sirt5 dose dependent with an estimated EC_{50} value of 60 µM. (I) Sirt5 activation by UBCS 350 is also observed in the mass spectrometric assay. A & C – H: Coupled enzymatic assays in presence of varying 1,4-DHP concentrations, 1.5 µM enzyme, 50 µM substrate peptide, 100 µM NAD^+ and a final DMSO concentration of 5 %. The MS-based assay with Sirt5 (I) was set up as in Figure 39E. Values and error bars depict the mean and STDEV of at least three independent measurements.

3.4.2.3. 1,4-DHP binding is Sirtuin specific

For the first time, specific activators for Sirt3 and Sirt5 were discovered by analyzing 47 1,4-DHP compounds. Moreover, the specificity of UBCS 131 & 350 and the ability of UBCS 366 to activate any Sirtuin indicated the possibility to customize the 1,4-DHP scaffold towards a specific Sirtuin enzyme by varying the aromatic moieties at positions 1 and 4. In order to validate, if these small alterations indeed mediated the selectivity towards Sirtuins, UBCS 131 & 350 binding to Sirt3 and Sirt5 was analyzed. Therefore, FITC labelled Sirt3 was incubated with increasing amounts of UBCS 131 and analyzed by MST (cf. section 2.4.12), which revealed a proper compound binding with a K_D value of 33.8 ± 8.9 µM (Figure 42A & Table 16). Strikingly, the Sirt5 specific UBCS 350 bound significantly weaker to Sirt3 with an estimated K_D value of ~ 140 µM, which resembled the compound effects on Sirt3 activity (4.5-fold activation by UBCS 131 vs. no activation by UBCS 350, Figure 39C & Figure 41D). A similar behavior was observed in FITC-Sirt5 binding studies: while the 3.5-fold activating UBCS 350 (Figure 41G) exhibited a K_D value of 18.3 ± 0.9 µM (Figure 42B & Table 16), UBCS 131 bound Sirt5 with a K_D of 72.4 ± 11.1 µM (1.9-fold activation of Sirt5, Figure 40C). This indicates, that the 1,4-DHP selectivity towards Sirtuins is mediated by their affinity towards distinct Sirtuin enzymes. This affinity can be modulated by small variations of the 1,4-DHP scaffold and resembles the effects observed in activity analyses (cf. sections 3.4.2.1 & 3.4.2.2).

Table 16: Dissociation constants for UBCS 131 & 350 to Sirt3 and Sirt5.

Titration	K_D [µM]	
	Sirt3	Sirt5
UBCS 131	33.8 ± 8.9	72.4 ± 11.1
UBCS 350	~140 µM	18.3 ± 0.9
1,4-DHP[(a)] + 0.5 mM peptide [(b)]	17.1 ± 5.1	23.6 ± 5.4
1,4-DHP[(a)]+ 5 mM NAD^+	70.2 ± 27.1	27.8 ± 6.6

a) Binding studies in presence of peptide/NAD^+ were only performed for Sirt3/UBCS 131 and Sirt5/UBCS 350

b) ACS2.3 (Sirt3) or succCPS1 (Sirt5)

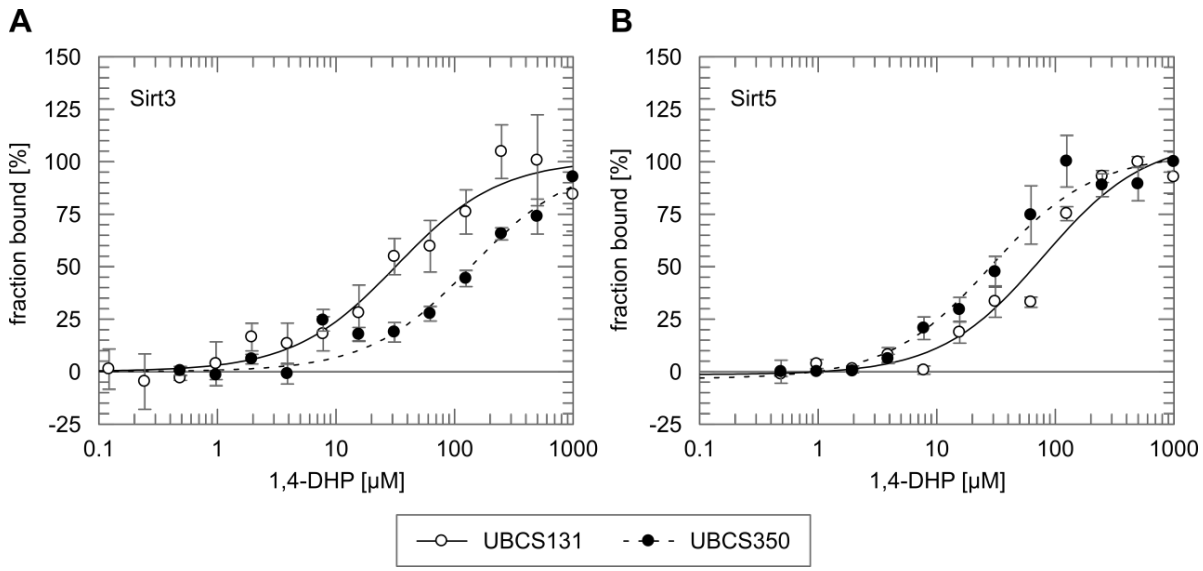

Figure 42: Specific 1,4-DHP binding to Sirtuins. (A) The Sirt3 selective activator UBCS 131 binds stronger (K_D of 33.8 ± 8.9 µM) to Sirt3 than the Sirt5 specific activator UBCS 350 (K_D of ~140 µM), resembling the compounds' effect on Sirt3 activity (4.5 fold activation vs. no activation, Figure 39C & Figure 41D). (B) A similar trend is observed for Sirt5, which binds its specific activator UBCS 350 with a K_D of 18.3 ± 1.0 µM (3.5 fold activation, Figure 40C & Figure 41G) and UBCS 131 with a K_D of 72.4 ± 11.1 µM (1.9 fold activation). MST binding analysis using 10 nM FITC labelled Sirtuin and varying ligand concentrations in absence or presence of 0.5 mM 1,4-DHP and a final DMSO concentration of 10%. Values and error bars denote the mean and STDEV of at least four independent measurements.

3.4.2.4. Sirtuin/1,4-DHP crystallization trials

For a detailed understanding of both 1,4-DHP specificity and their activation mechanism, the crystallization of a Sirtuin/1,4-DHP complex was aimed. Prior to setting up crystals, an optimized crystallization sample was determined by MST binding studies. The binding affinity of UBCS 131 towards Sirt3 ranged around 30 µM and was just slightly improved, if saturating concentrations of substrate peptide were present (K_D of 17.1 ± 5.1 µM, Figure 43A & Table 16). Presence of NAD^+, however, had a slight negative impact on UBCS 131 binding (K_D of 70.2 ± 27.1 µM, Figure 43B & Table 16). In contrast, the UBCS 350 affinity towards Sirt5 of ~ 20 µM was not influenced by the presence of peptide or NAD^+ (K_D values of 23.6 ± 5.4 µM and 27.8 ± 6.6 µM, respectively, Figure 43C & D, Table 16).

The affinity studies suggested proper binding of UBCS 131 & 350 to Sirt3 and Sirt5, respectively, already in absence of any further ligand. Moreover, a slightly improved UBCS 131 binding to Sirt3 in presence of substrate peptide was observed. Thus, Sirt3 co-crystallization experiments with UBCS 131 in absence and presence of substrate peptide, NAD^+ or substrate peptide & ADPr were performed using factorial screens. In order to gain a complex structure of Sirt5 and UBCS 350, *D. rerio* zSirt5 was used, as it exhibits an improved crystallization behavior (cf. section 3.3.2.1) and was stimulated by UBCS 350 similar to its human homologue (Figure A 4). Crystals were obtained from several conditions and for both Sirtuins. The majority of crystals grew from Sirtuin/peptide/1,4-DHP setups and

could be optimized for their buffer pH and precipitant concentration (Table 17, Figure 44). In order to ensure compound binding within the crystals, the cryo-protectant was supplemented with saturating 1,4-DHP concentrations (1 – 2 mM compound, which is the solubility limit of 1,4-DHP compounds in the used final DMSO concentration of 10 %). However, no electron density for either one of the 1,4-DHP compounds could be observed. MST experiments confirmed proper compound binding even in absence of any Sirtuin substrate. Nevertheless, UBCS 131 & 350 might act by stabilizing a Sirtuin conformation, which is only established during catalysis and/or by stabilizing a reaction intermediate or a transition state. Therefore, Sirt3/ACS2.2 and zSirt5/succCPS1 crystals were extensively soaked in cryo-protectant solution containing saturating concentrations of substrate peptide, NAD^+ or ADPr and the respective 1,4-DHP (up to 24 h and using saturating concentrations of every ligand). Still, all structures derived from these crystals contained no density for any 1,4-DHP compound, even after 24 h of soaking.

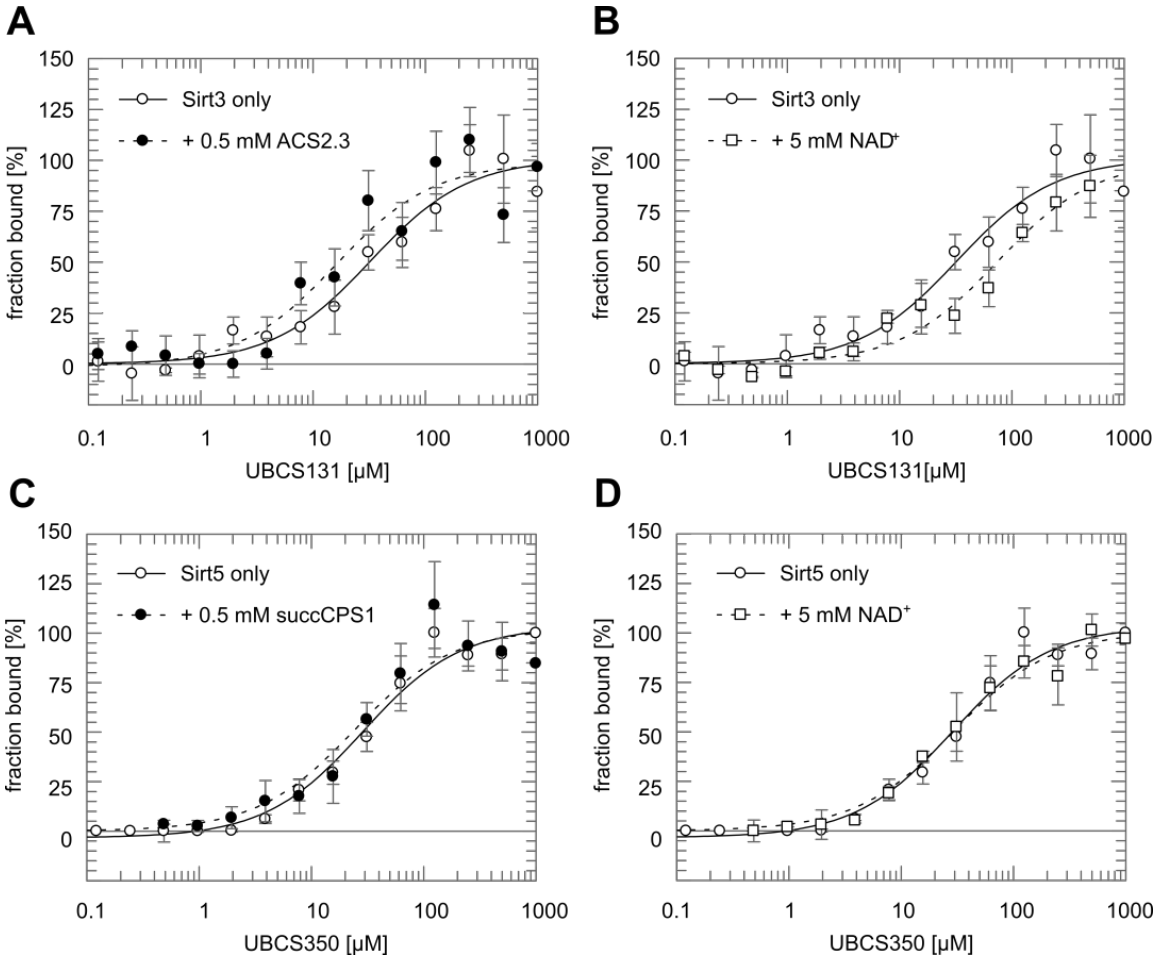

Figure 43: 1,4-DHP binding to Sirtuins is unaffected by substrate presence. UBCS 131 exhibits low micromolar affinity towards Sirt3 in absence and presence of ACS2.3 peptide (A) and NAD^+ (B). This behavior is likewise seen for Sirt5 and UBCS 350 (C & D). MST binding analysis using 10 nM FITC labelled Sirtuin and varying 1,4-DHP concentrations in absence or presence of 0.5 mM peptide or 5 mM NAD^+ and a final DMSO concentration of 10%. Values and error bars denote the mean and STDEV of at least four independent measurements. Data for Sirt3 vs. UBCS 131 and Sirt5 vs. UBCS 350 are taken from Figure 43 for comparison reasons. K_D values are summarized in Table 16.

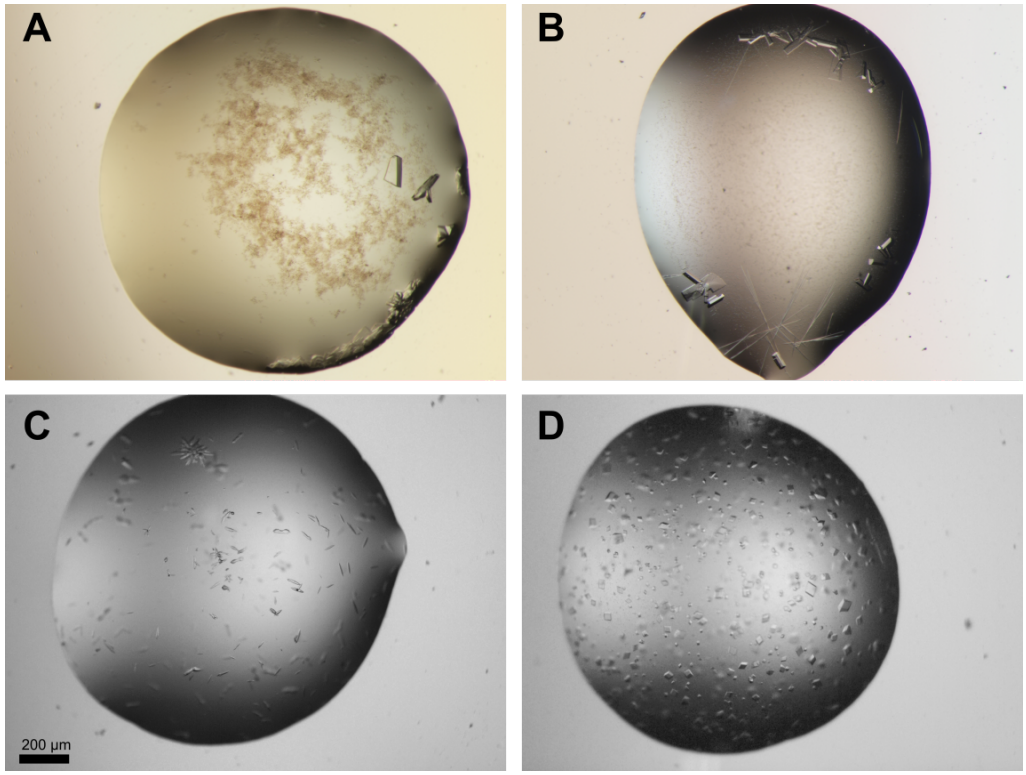

Figure 44: Sirtuin crystallization in presence of 1,4-DHP compounds. Exemplary crystals from co-crystallization trials of Sirt3 (A & B) or zSirt5 (C & D) and UBCS 131 or UBCS 350, respectively. Proteins crystallized as rods (A & B), needles (C) or bi-pyramidal (D). A: co-crystallization of UBCS 131 and Sirt3 in 1 M LiCl; 0.1 M MES, pH 6.0; 20 % (w/v) PEG 6000; B: co-crystallization of Sirt3, ACS2.2 and UBCS 131 in 0.2 M $(NH_4)_2SO_4$; 0.1 M Bis-Tris, pH 5.5; 20 % PEG 3350; C: co-crystallization of zSirt5, succCPS1 and UBCS 350 in 0.1 M HEPES, pH 7.5; 20 % (w/v) PEG 3350; D: co-crystallization of zSirt5, succCPS1 and UBCS 350 in 1.4 M Citrate; 0.1 M Hepes, pH 7.5.

Table 17: Overview of crystallization trials to determine the 1,4-DHP activation mechanism.

	Crystallization condition	Setup	Reproducible/ Optimizable	Diffracting	Structure
Sirt3	1 M LiCl; 0.1 M MES, pH 6.0; 20 % (w/v) PEG 6000	Sirt3 & UBCS 131	yes	yes	apo structure, no compound density
	0.2 M $(NH_4)_2SO_4$; 0.1 M Bis-Tris, pH 5.5; 20 % PEG 3350	Sirt3, ACS2.2 & UBCS131	yes	yes	peptide in active site, ADPr visible if soaked with NAD^+ or ADPr, no compound density
zSirt5	0.1 M HEPES, pH 7.5; 20 % (w/v) PEG 3350	zSirt5, succCPS1 & UBCS 350	yes	yes	apo structure, PEG molecule in active site, no compound density
	1.4 M Citrate; 0.1 M Hepes, pH 7.5	zSirt5, succCPS1 & UBCS 350	yes	yes	apo structure, no compound density
	0.2 M NaThiocyanate; 20 % (w/v) PEG 3350	zSirt5, succCPS1 & UBCS 350	-	-	-
	0.1 M Citrate, pH 5.5; 40 % (w/v) PEG 3350	zSirt5, succCPS1 & UBCS 350	-	-	-
	0.1 M Citric acid, pH 5.0; 2.4 M $(NH_4)_2SO_4$	zSirt5, succCPS1 & UBCS 350	-	-	-
	0.2 M $MgCl_2$, 0.1 M Tris/HCl, pH 8.5; 30 % (w/v) PEG 4000	zSirt5, succCPS1 & UBCS 350	-	-	-

Crystallization experiments consisted of 5 – 10 mg/ml Sirtuin and 1 – 2 mM 1,4-DHP ± 1 mM peptide and/or 5 mM ADPr/NAD^+, 10 % DMSO; crystals diffracted at BESSY beamline 14.1 to 2 – 3.5 Å

Ligand binding to Sirtuins in presence of 1,4-DHPS

Although both UBCS 131 & 350 exhibited affinities in the low micromolar range towards Sirt3 and Sirt5, respectively (Table 16), no Sirtuin/1,4-DHP complex structure was obtained. Binding analyses already indicated that the Sirtuin substrates do not affect compound binding. However, presence of 1,4-DHP compounds might improve substrate binding to Sirtuins and therefore enhance Sirtuin activity. Thus, ACS2.3 binding to FITC-Sirt3 in absence and presence of UBCS 131 was analyzed in further MST experiments. This resulted in an enhanced peptide K_D in presence of 0.5 mM UBCS 131 (K_D of 16.4 ± 2.8 µM vs. 4.6 ± 1.4 µM, Table 18 & Figure 45A). Due to fluorescence artifacts the effect of UBCS 131 on NAD^+ binding could not be analyzed in MST experiments (Figure A 5). Thus, the effect of UBCS 131 on binding of NAM and ADPr was analyzed, as these two molecules would bind to similar sites of Sirt3 (C-site and the groove between the two Sirtuin domains, respectively). Interestingly, ADPr binding to Sirt3 was slightly improved in presence of UBCS 131 (K_D of 454.9 ± 193.8 vs. 130.8 ± 32.8 µM, Figure 45B & Table 18) as well. On the contrary, the surprisingly strong affinity of NAM towards Sirt3 (K_D of 6.4 ± 2.6 µM) was not affected by UBCS 131 (K_D of 3.8 ± 1.8 µM, Figure 45C & Table 18). This indicated that 1,4-DHP compounds might stabilize the closed conformation of Sirtuins. The closed conformation is formed when the substrate peptide and NAD^+ interact with both Sirtuin domains, which causes the two domains to move towards each other. On the contrary, NAM as a single molecule binds only within the C-site, which is deep inside the smaller domain. Hence, its presence would not result in the conformational change which establishes the closed conformation supposedly stabilized by 1,4-DHPs.

To support the hypothesis that the 1,4-DHP compounds stabilized the closed conformation of Sirtuins, the effect of UBCS 350 on substrate (analogue) binding to FITC-Sirt5 was analyzed as well. Surprisingly, neither succCPS1 binding nor ADPr binding to Sirt5 was significantly affected by 0.5 mM UBCS 350 (Figure 45D & E, Table 18). As for Sirt3, UBCS 350 had no influence on NAM binding to Sirt5 (Figure 45F & Table 18).

Table 18: K_D values of Sirtuin ligands in absence or presence of 1,4-DHP compounds

	1,4-DHP[(a)]	K_D [µM]		
		Peptide[(b)]	ADPr	NAM
Sirt3	-	16.4 ± 2.8	454.9 ± 193.4	6.4 ± 2.6
	+	4.6 ± 1.4	130.8 ± 32.8	3.8 ± 1.8
Sirt5	-	56.9 ± 10.6	247.8 ± 52.7	60.5 ± 13.6
	+	62.8 ± 12.2	528. ± 133.5	222.6 ± 67.6

a) Sirt3 ± 0.5 mM UBCS 131, Sirt5 ± 0.5 mM UBCS 350

b) ACS2.3 in case of Sirt3, succCPS1 in case of Sirt5

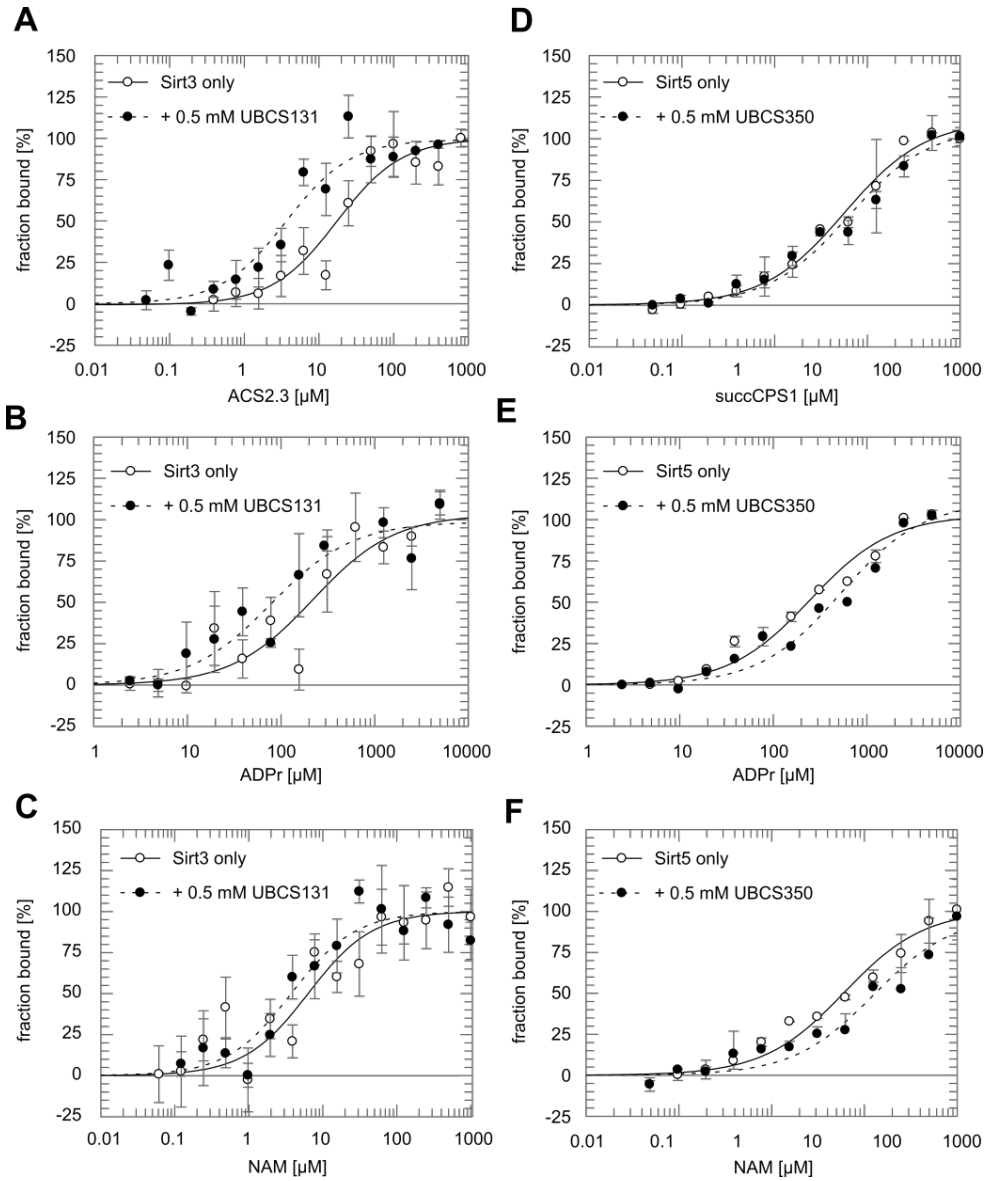

Figure 45: Peptide binding to Sirt3 is slightly increased in presence of 1,4-DHP compounds. ACS2.3 binding to Sirt3 is slightly improved in presence of 0.5 mM UBCS 131 (A), while the NAD^+ mimicking ligands ADPr (B) and NAM (C) exhibit no changes in their Sirt3 affinity. For Sirt5, presence of UBCS 350 has no effect on succCPS1 (D), ADPr (E) and NAM (F) binding. MST binding analysis using 10 nM FITC labelled Sirtuin and varying ligand concentrations in absence or presence of 0.5 mM 1,4-DHP and a final DMSO concentration of 10%. Values and error bars denote the mean and STDEV of at least four independent measurements. All K_D values are summarized in Table 18.

3.4.2.5. Sirtuin kinetics in presence of 1,4-DHP compounds

Although the affinity studies indicated proper compound binding, crystallization attempts did not result in a Sirtuin/1,4-DHP complex. The MST studies also indicated a slightly improved UBCS 131 binding to Sirt3 in presence of substrate peptide and vice versa. However, this effect was only observed for Sirt3 and could not be reproduced for Sirt5/UBCS 350.

As the mechanism of Sirtuin activation by 1,4-DHP compounds could not be elucidated using these two different approaches, the effect of UBCS 131 and UBCS 350 in Sirt3 and Sirt5

kinetics was analyzed. Sirtuin activity depends on two different substrates. Hence, one of the Sirtuin substrates has to be present in a fixed and saturating concentration during kinetic experiments, while the concentration of the other substrate varies.

As expected, Sirt3 peptide and NAD^+ kinetics in presence of high concentrations of NAD^+ (2 mM, Figure 46A) or ACS2.3 (0.4 mM, Figure 46B), respectively, resulted in comparable v_{max} values in both substrate titrations experiments (Table 19). Likewise, obtained K_m values matched already reported values[82,158]. Strikingly, kinetic experiments in presence of 200 µM UBCS 131 resulted in a ~ 2-fold increased v_{max} value in both substrate titrations (Figure 46A & B). Interestingly, the K_m value for NAD^+ seemed to be unaffected by UBCS 131, while the peptide K_m increased (Table 19). Surprisingly, the kinetic curves also revealed, that in presence of 200 µM UBCS 131 2 mM NAD^+ or 0.4 mM peptide are not sufficient to reach saturation in ACS2.3 and NAD^+ titrations, respectively. This renders conclusions about the differential effect on the substrates' K_m values difficult.

Considering the different results between Sirt3 and Sirt5 during 1,4-DHP affinity studies, the astounding effect of UBCS 131 on Sirt3 v_{max} had to be validated using Sirt5 and UBCS 350. Importantly, while Sirt5 peptide and NAD^+ kinetics in absence of 1,4-DHP compound matched previous reports[34,82] and resulted in comparable v_{max} values, presence of 200 µM UBCS 350 resulted in a ~ 2-fold increased v_{max} for both substrates (Figure 46C & D, Table 19). As for the Sirt3 kinetics, UBCS 350 affected the K_m values for the two Sirt5 substrates differently. But in contrast to UBCS 131 and Sirt3, UBSC 350 presence decreased the K_m value for succCPS1 2-fold, while it increased the K_m for NAD^+ 2-fold as well (Table 19).

All curves derived from the kinetic experiments exhibit little differences within a concentration range up to 100 – 200 µM of each substrate, which might be caused by the detection limit of the coupled continuous assay (10 – 20 µM of the substrate, internal lab experience). Due to this low resolution below 100 – 200 µM substrate, significant and reproducible effects of the 1,4-DHP activators on K_m are difficult to observe. But still, Sirtuin v_{max} is significantly improved in presence of 1,4-DHP compounds, possibly by enhancing k_{cat} of the enzymatic reaction (cf. section 4.2.4).

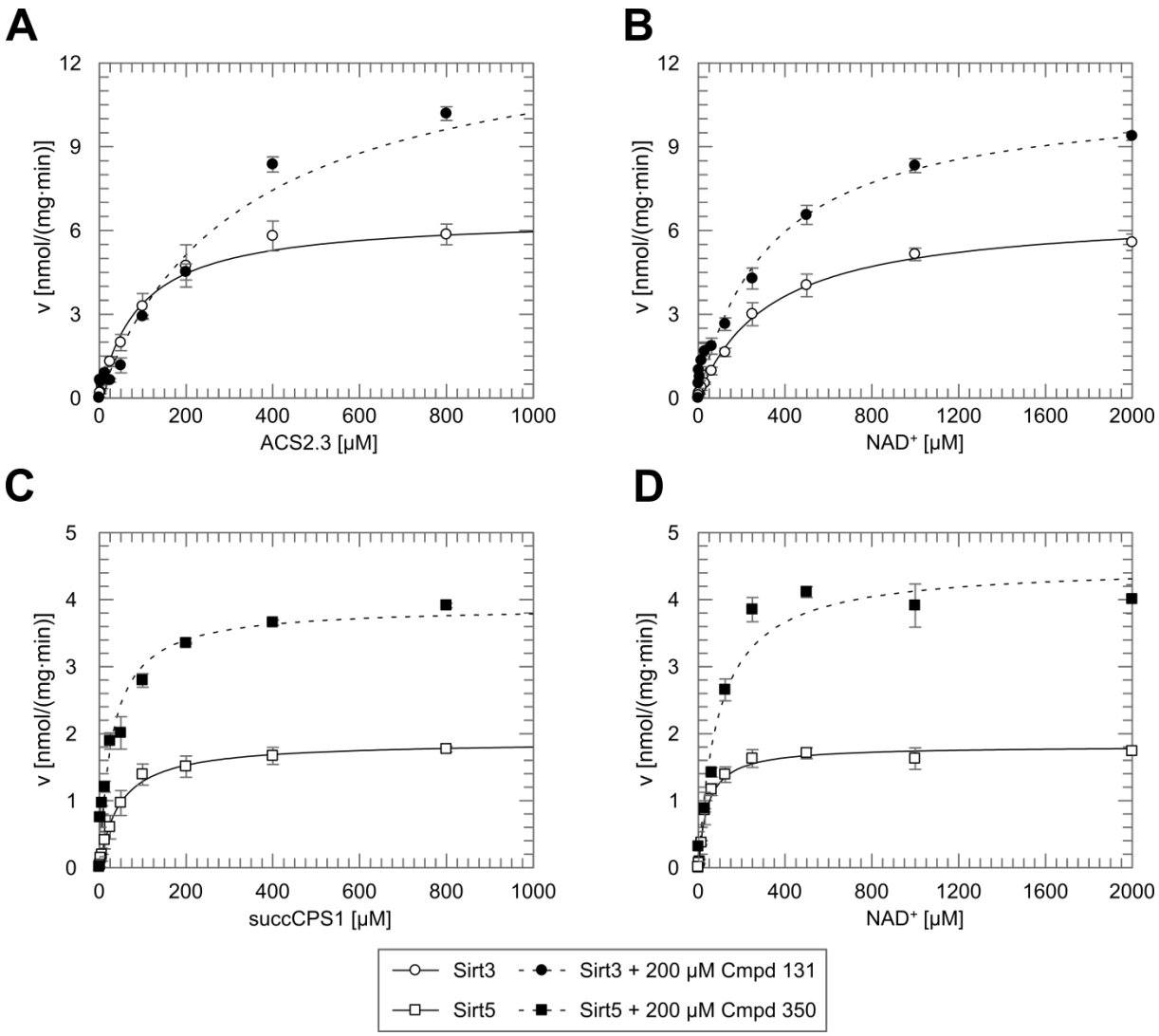

Figure 46: 1,4-DHP compounds increase Sirtuin v_{max}. UBCS 131 doubles Sirt3 v_{max} during peptide (A) and NAD^+ titration (B), while K_m is unaffected. This effect is observed for Sirt5 activation by UBCS 350 as well (C & D). Coupled enzymatic assay in presence of varying peptide or NAD^+ concentrations, 1.5 µM enzyme, 2 mM NAD^+ or 400 µM substrate peptide, respectively, in absence or presence of 200 µM 1,4-DHP and a final DMSO concentration of 5 %. Values and error bars depict the mean and STDEV of at least three independent measurements. Kinetic constants are summarized in Table 19.

Table 19: Kinetic constants for Sirt3 and Sirt5 in presence of UBCS 131 & 350, respectively.

	1,4-DHP[(b)]	Peptide kinetic[(a)]		NAD^+ kinetic	
		K_m [µM]	v_{max} [nmol/(min·mg)]	K_m [µM]	v_{max} [nmol/(min·mg)]
Sirt3	-	106.2 ± 28.5	6.50 ± 0.22	389.2 ± 132.3	6.64 ± 0.16
	+	313.7 ± 24.6	13.58 ± 0.93	369.3 ± 84.0	10.93 ± 0.73
Sirt5	-	68.7 ±19.7	1.89 ± 0.04	45.5 ± 4.0	1.82 ± 0.06
	+	28.8 ± 1.6	3.90 ± 0.17	91.6 ± 9.2	4.51 ± 0.27

a) ACS2.3 was used as Sirt3 substrate, succCPS1 was used for Sirt5

b) ± 200 µM UBCS 131 (Sirt3) or UBCS 350 (Sirt5)

4. Discussion

4.1. Physiological Sirtuin Modulation

4.1.1. Sirtuin Posttranslational Modifications

So far, only a few Sirtuin PTMs and their effects on these enzymes were characterized. These PTMs were identified within large-scale proteomic approaches that aimed to identify a certain kind of PTM within a certain tissue or cell line by mass spectrometry[1,122,149]. Therefore, samples routinely undergo an enrichment step, which increases the amount of modified proteins/peptides prior to MS analyses, e.g. by using TiO_2 to enrich phosphorylated peptides after the tryptic digest[149].

Here, a Sirtuin focused approach was pursued. First, Sirtuins were enriched from crude extracts for a subsequent identification of any PTM possibly present. Initially, native Sirtuin purification from bovine liver mitochondria was aimed. This was believed to introduce the least possible artifacts compared to cultivated eukaryotic cells as protein source. Indeed, native bovine Sirt5 could be enriched by the use of Blue Sepharose as purification resin. But although this resin turned out to enrich Sirtuins from mitochondrial extracts, too large amounts of starting material would have been necessary for proper PTM analysis by mass spectrometry both in terms of protein amount and sample purity (cf. section 3.1.1.1).

Likewise, immunopurification from bovine tissue did not result in proper protein amounts and purity (cf. section 3.1.1.2). Instead, human cultured cells allowed for a high yielding protein purification. Transient overexpression of affinity tagged Sirtuins indeed resulted in the identification of several PTMs on four different Sirtuins (Table 4). Cultured cells might differ in their protein modifications compared to native tissues. However, among the identified PTMs two acylation sites matched observations from previous studies, in which Sirt5 acK112 and Sirt5 acK203 were reported[88,159]. This indicates that the identified PTMs from cultured cells also reside in native tissue.

Interestingly, the identified Sirt7 phosphoT263 aligned with possible PTM sites in further Sirtuins (Figure 18): Sirt4 S255, which was already identified to be phosphorylated[149], Sirt6 S210 and Sirt5 CDLC 242 – 245, with the latter being a possible target of redox regulation. A structural alignment of Sirt1, Sirt5 and Sirt6 (pdb entries 4I5I, 3RIY and 3K35, respectively) reveals Sirt6 S210 and thus probably Sirt7 T263, for which no structural data is available, to be part of a β-strand of the Rossmann domain (Figure 47A). Sirt6 S210 points towards a neighboring α-helix thus stabilizing the Rossmann-fold. If modified, the phosphorylation would introduce a bulky and charged moiety, which might destabilize this domain. In addition, Sirt6 S210 resides in a β-strand that ends in a turn involved in NAD^+ binding. Thus phosphorylation of this site should affect the enzymatic activity as well, e.g. by changing the NAD^+ affinity. Indeed, the enzymatic activity of murine Sirt1 is increased, if S434 within this turn is phosphorylated[160].

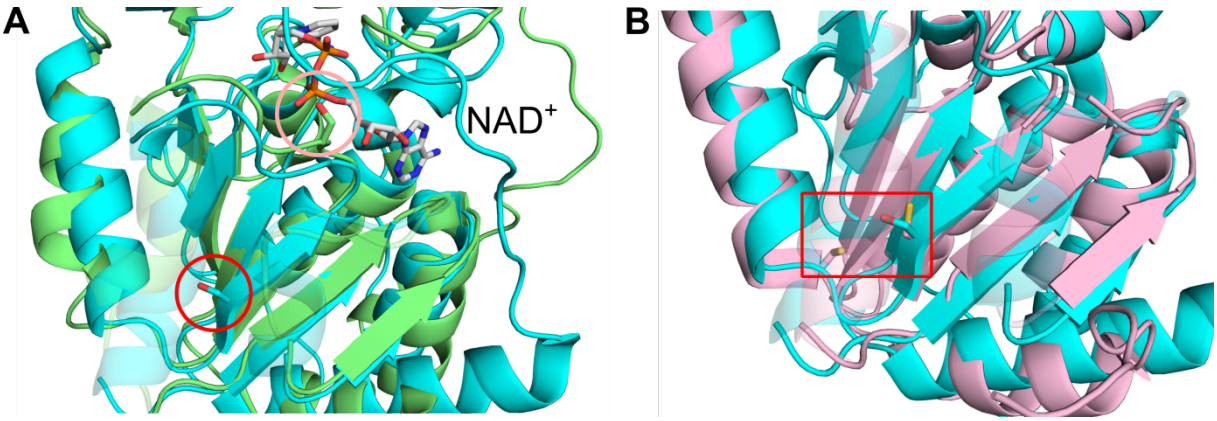

Figure 47: Structural alignments indicate a possible role of the putative conserved PTM site in Sirtuins. Sequence alignment of all human Sirtuins already revealed Sirt7 T263, which was identified as phosphorylation site, to align with an already reported phosphorylation site in Sirt4 (S255)[149] but also with a CXXC motif in Sirt5 (CDLC 242 – 245) and with Sirt6 S210 (Figure 18). (A) Structural alignment of Sirt1 (green) and Sirt6 (cyan) indicate a regulatory role of Sirt6 S210 (red circle) and thus Sirt7 T263. Phosphorylation of S422 (black circle)[160] activates Sirt1. This site is located to a turn between the two Sirtuin domains. To the turns N-terminus ends a β-strand, which in case of Sirt6 the possible phosphorylation site S210. (B) In addition, Sirt6 S210 (cyan) corresponds to Sirt5 CDLC 242 – 245 (pink), suggesting possible redox regulation of Sirt5 (red rectangle). *pymol* was used for structural alignment of Sirt1 (green), Sirt5 (pink) and Sirt6 (cyan) (pdb codes: 4I5I, 3RIY and 3K35, respectively)[31,161]. Sirtuins are represented as cartoons, highlighted PTMs are represented in sticks and colored by atom. NAD^+ from 3RIY in sticks and colored by atom (O: red, S: yellow).

This might be mediated by an increased acADPr release due to the opposing charges of pS434 and the ADPr backbone (Figure 47A, S434 in mouse Sirt1 corresponds to S422 in human Sirt1). However, in case of Sirt6 S210D did not affect NAD^+ binding but resulted in an increased peptide K_m. Furthermore, this variant was dramatically destabilized compared to the wt variant. This indicates that the phosphorylation site reported for Sirt1 just affects the substrate binding and might leave the Rossmann-fold little affected. On the contrary, the putative conserved phosphorylation site in Sirt6 affects the Rossmann-fold domain which subsequently affects in an increased peptide K_m.

In contrast to Sirt4, Sirt6 and Sirt7, this putative conserved site corresponds to a CXXC motif in Sirt5 (CDLC 242 – 245, Figure 47B). Within mitochondria, this motif might be targeted by oxygenases or simply by ROS which eventually could result in disulfide bridge formation. A disulfide bridge between the opposing C242 and C245 would move the neighboring α-helix and β-strand towards each other. It will be interesting to see, whether and how this would affect Sirt5.

For human Sirt7 no soluble construct is available, which could be used for the characterization of pT263 and its effect on enzyme activity and/or stability. Thus, the effect of this putative conserved PTM site had to be analyzed using Sirt4 and Sirt6, which can be purified after heterologous expression from *E. coli.* Indeed, Sirt6 S210D exhibited a reduced thermal stability, which could be caused by a destabilized Rossmann-fold domain. A

destabilized Rossmann-fold domain could negatively affect NAD^+ binding, presence of this co-substrate stabilized Sirt6 (Figure 22A). On the contrary, the S210D exchange had a negative effect on Sirt6 peptide kinetics (Figure 25B). Interestingly, Sirt4 S255D seemed to be dramatically destabilized as well, since this variant can be overexpressed in *E. coli* but in contrast to Sirt4wt fully precipitates after cell lysis (M. Pannek, personal communication). However, in order to confirm that this is a conserved effect, a soluble Sirt7wt and Sirt7 T263D variant have to be tested as well in combination with a thorough analysis of this putative site in cell-based assays. However, in initial experiments performed by the collaborating lab of Prof. Katrin Chua (Stanford University) both reduced activities and stabilities for Sirt6 S210D and Sirt7 T263D were observed in HEK 293T cells (Winnie Zheng, personal communication).

Different to Sirt6 and Sirt7, for Sirt5 predominantly acylation sites were identified. These modifications affected Sirt5 stability and peptide K_m as well. Cell-based data have to confirm a physiological relevance for these modifications yet. In addition, it would be interesting to see, if Sirt5 acylation sites might be Sirtuin targets as well. During CR mitochondrial metabolism is upregulated by Sirtuin activity. As this results in elevated levels of acylated Coenzyme A, the non-enzymatical acylation of proteins, including mitochondrial Sirtuins, might increase as well[11,12]. Thus, Sirtuins might target each other in order to maintain their active state and thereby maintain upregulation of e.g. TCA, β-oxidation and amino acid degradation during CR.

4.1.2. Sirtuin Regulation by Cellular Ligands

So far, only the AROS protein was described as physiological Sirtuin regulator by interacting and thereby activating Sirt1[89]. NAD^+ and NAM were also reported to act as physiological Sirtuin regulators[19,91]. However, these molecules are Sirtuin co-substrate and product, respectively, thus a change in Sirtuin activity upon changing NAD^+/NAM levels is not surprising.

NAM inhibition was not characterized for all Sirtuin enzymes. Especially its effect on the two different Sirt5 activities was not known. Surprisingly, using MS based Sirtuin activity assay[125,126] in combination with improved substrates[31,153] NAM was found to act differently against the two different Sirt5 activities (Figure 26A). This is probably caused by the unique amino acid composition within the active site of Sirt5. Only the active site of Sirt5 contains an arginine, which aids positioning the substrate's succinylated lysine[31]. However, if an acetylated substrate binds to Sirt5, this arginine is free to adopt further conformations, e.g. into the direction of C-pocket bound NAM. Thus, the inhibitor would be repelled, which would explain why Sirt5 deacetylation activity is insensitive towards NAM inhibition (Figure 26B).

Still, nothing is known about further Sirtuin modulating physiological ligands. Running Sirtuin reactions within protein depleted ML resulted in proper inhibition of Sirt3 deacetylation and Sirt5 desuccinylation activity, which was caused by inhibitory amounts of NAM inside the mitochondrial lysate (Figure 27). Protein and NAM depleted ML had no effect on Sirtuin activity at all. This suggests that no further physiological small molecule Sirtuin modulator is present inside mitochondria. However, Sirtuin affecting ligands might reside in different cellular compartments. Thus, mammalian cells could be fractionated and could be tested for the presence of Sirtuin regulating components. In addition, those fractions could be pre-cleared from NAD^+ and NAM by NAD^+ hydrolase and NCA treatment, respectively. Then, all proteins could be cleared by boiling the respective cellular fractions as it was performed with the ML experiments.

Incubation of heterologous expressed and still tagged Sirtuins in NAD^+/NAM-depleted cellular extracts might be another approach to identify physiological relevant small molecule modulators or regulatory proteins. After they are recovered and carefully washed, effects on Sirtuin activity could be monitored using the direct MS-assay. If modulating effects are observed, the binding partner could be identified using mass spectrometry or in case of a small molecule ligand by NMR.

4.2. Pharmacological Sirtuin Modulation

4.2.1. Specificity of Sirtuin Modulators

Although several Sirtuin modulators were already described, they were tested only against two or three different Sirtuin enzymes. Since proper assays and substrates are available by now, a thorough specificity analysis of these already reported compounds is possible. Interestingly, the specificity analysis of several already reported Sirt1 and Sirt2 regulators (Table 10) revealed no significant effect on the two Sirt5 activities. Only the pan-Sirtuin inhibitor Suramin was able to inhibit Sirt5 deacetylation activity but not its desuccinylation activity. GW5074, which was previously reported as Sirt2 inhibitor GW5074[156] acted vice versa by inhibiting only Sirt5 desuccinylation activity. The differential effects of Suramin might be caused by its competitive mode of action: it binds to the NAD^+ and the peptide binding site (Figure 48) and thus competes for Sirt5 binding with both substrates. However, succinylated substrates bind stronger to Sirt5 compared to acetylated substrates due to salt bridge formation with R105 (Figure 26B). Suramin might bind with a similar or even higher affinity to Sirt5 compared to acetylated peptides but with a weaker affinity compared to succinylated peptides. This might cause the reduced sensitivity of Sirt5 desuccinylation activity towards the competitive inhibitor Suramin.

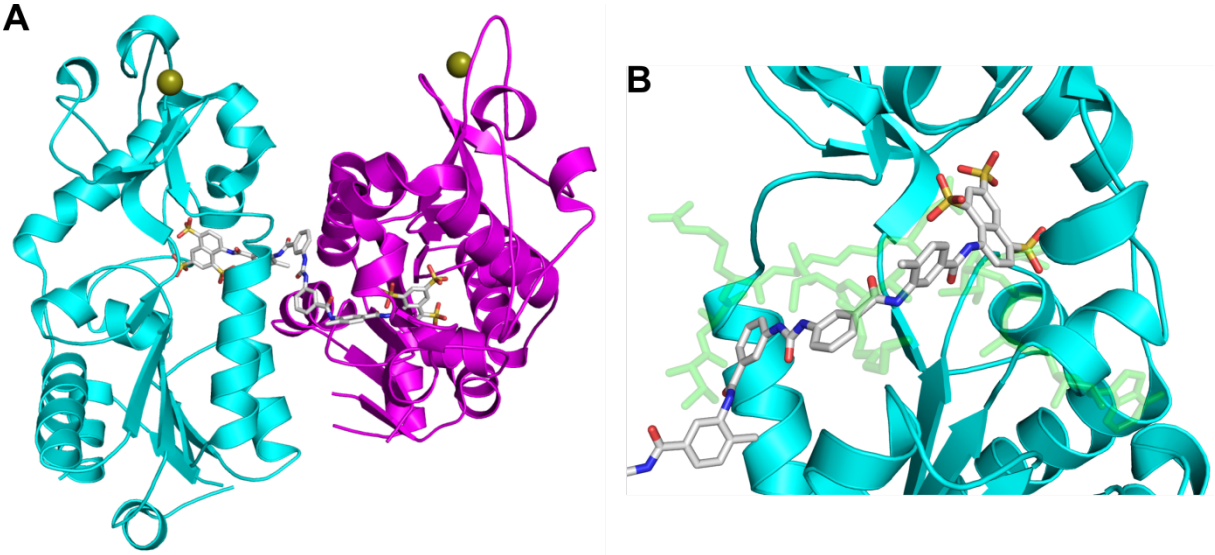

Figure 48: Sirtuin inhibition by Suramin. (A) The symmetric Suramin molecule binds toe the active site of two Sirtuin enzymes. (B) The Suramin binding site overlaps with the NAD^+ and peptide binding site. Thus, it acts as competitive inhibitor for both Sirtuin substrates. Cartoon representation of Sirt5 (cyan & magenta) in complex with Suramin (in sticks and colored by elements, N: blue, O: red, S: yellow; pdb entry: 2NYR)[101]. NAD^+ and succPeptide (both as sticks colored in green) are modelled inside the active site by superposition of the Sirt5/NAD^+/succPeptide complex (pdb entry: 3RIY)[31].

4.2.2. GW5074 Inhibitory Mechanism

GW5074 was initially described as kinase inhibitor[154], found to inhibit GDH[155] and later on it was identified to inhibit Sirt2[156]. As a nucleotide analogue, the compound is believed to inhibit kinases by blocking their active site and Sirtuins by blocking their C-site, thus competing with either ATP or NAD^+, respectively. Docking analysis supported the NAD^+ competition model since a GW5074 related compound could bind to the C-site of apo Sirt2[162]. Yet, no experimental data corroborated the GW5074/NAD^+ competition model.

The various analyses performed here shown for the first time that NAD^+ has no negative but rather a slight positive effect on GW5074 binding to Sirt5. On the contrary, peptide presence weakens compound affinity. This rather supports a model in which GW5074 acts against the substrate peptide, probably by exploiting the charged acyl moiety as the Sirt5 deacetylation activity is hardly inhibited by this compound (see below). Furthermore, Sirt5 incubation with GW5074 abolishes enzymatic activity completely, even if Sirt5 was pre-incubated with peptide. This could indicate an inhibitory mechanism, in which the compound covalently modifies and thereby inhibits Sirt5.

Modifying the substituents of GW5074 did not result in an improved inhibitor. Analyzing the effects of several GW5074 derivatives revealed that the indole part of the compound scaffold is of little importance: UBCS 164 and GW5074, which only differ by their indole halogen substituents, exhibited similar inhibitory potentials. On the contrary, replacing the phenolic substituents weakened the inhibitor's potency. Nevertheless, evaluating the less potent

compounds revealed small unbranched electron-rich substituents in para and meta position to be favorable for inhibition. GW5074 as well as UBCS 164 bear on both of these positions electron-rich substituents (Figure 31 A). Thus, one possibility that might yield in a more potent inhibitor would be the replacement of the hydroxyl moiety with bromine, in order to introduce more electrons to the para position. Moreover, all meta and para substituents could be altered to iodine atoms, which would further increase the electron density.

Furthermore, affinity studies revealed a similar binding behavior of GW5074 to Sirt5 R105L and Sirt3. Inhibitor binding to these Sirtuins was not affect by substrate presence in contrast to Sirt5. This strongly suggests Sirt5 R105 is crucial for the differential Sirt5 sensitivity towards this compound: in wt Sirt5 the negative charged succLys faces the positive charged R105, thus forming a salt bridge which causes the enzyme's preference for succinylated substrates. In GW5074 the phenol is substituted with two bromines and with a hydroxyl group. With these three moieties, the phenol part is highly electron-rich, which therefore might compete with a succinylated lysine for Sirt5 binding. Replacing these moieties weakens inhibitory function, which supports this competition model. This would also explain why Sirt5 deacetylation activity is not inhibited by this compound. Furthermore, this binding seems to be so strong that it abolishes peptide binding completely as no Sirt5 desuccinylation activity can be observed if peptide and compound are pre-incubated before catalysis. This suggests a competitive inhibition model against substrate peptides for GW5074 against Sirt5 desuccinylase but not deacetylase activity, caused by an interaction between Sirt5 R105 and electron-rich moieties at the compounds phenolic part.

However, whether peptide and GW5074 compete indeed for the same binding site or whether the compound acts allosteric thereby preventing peptide binding still remains elusive: despite missing positively charged active site amino acids (corresponding to Sirt5 R105) GW5074 exhibited a strong preference for nuclear Sirtuins over mitochondrial Sirtuins. Thus the compound can inhibit Sirtuins independent of an active site Arg (as it is the case in Sirt5). Nevertheless, only selected Sirtuin/substrate pairs have been tested. GW5074's specificity for Sirt1/p53 could be based on either a higher affinity towards the enzyme or based on substrate properties. Even different binding sites on different Sirtuins are imaginable. Testing other Sirt1 substrates could reveal the compound's specificity and could provide further clues about its inhibitory mechanism. Furthermore, it is tempting to speculate that keeping the phenolic part of the compound and changing the indolic substituents or even replacing the indole part by other aromatic groups or fusing it to an acylated lysine derivative (cf. section 4.2.3) would improve this specificity. These changes could even reduce off target effects (e.g. kinase and GDH inhibition).

Taken together, GW5074 is demonstrated to be rather a Sirt1 specific inhibitor, competitive against substrate peptides. Unbranched electron-rich substituents in meta and para position

of the compounds phenol part improve inhibition whereas changes on the indole part did not affect the compound's potency. These results indicate that GW5074 can be used as lead for more potent and specific Sirtuin inhibitors by introducing more electron rich substituents to the phenol ring and by altering the indole moiety, respectively.

4.2.3. Lysine Derivatives as Specific Sirtuin Inhibitors

Sirt5 binds its succinylated substrate via β-sheet like interaction (Figure 49A) in addition to the salt bridge between the acyl and R105[31]. The NAM part of NAD^+ on the other hand is accommodated via hydrogen bond formation and hydrophobic interaction inside the C-site (Figure 49D). A closer look at the modelled compounds (Figure 49) indicates that all compounds except for UBCS 286 probably lack the β-sheet like interaction (Figure 49B & C). This probably results in low binding affinities and eventually in the observed low inhibitory properties (Figure 37). In case of UBCS 242 & 286, a Z moiety would point into the C-site (Figure 49E). Thus, these compounds would not just compete with the substrate peptide for Sirt5 binding, but also with NAD^+ for C-site binding.

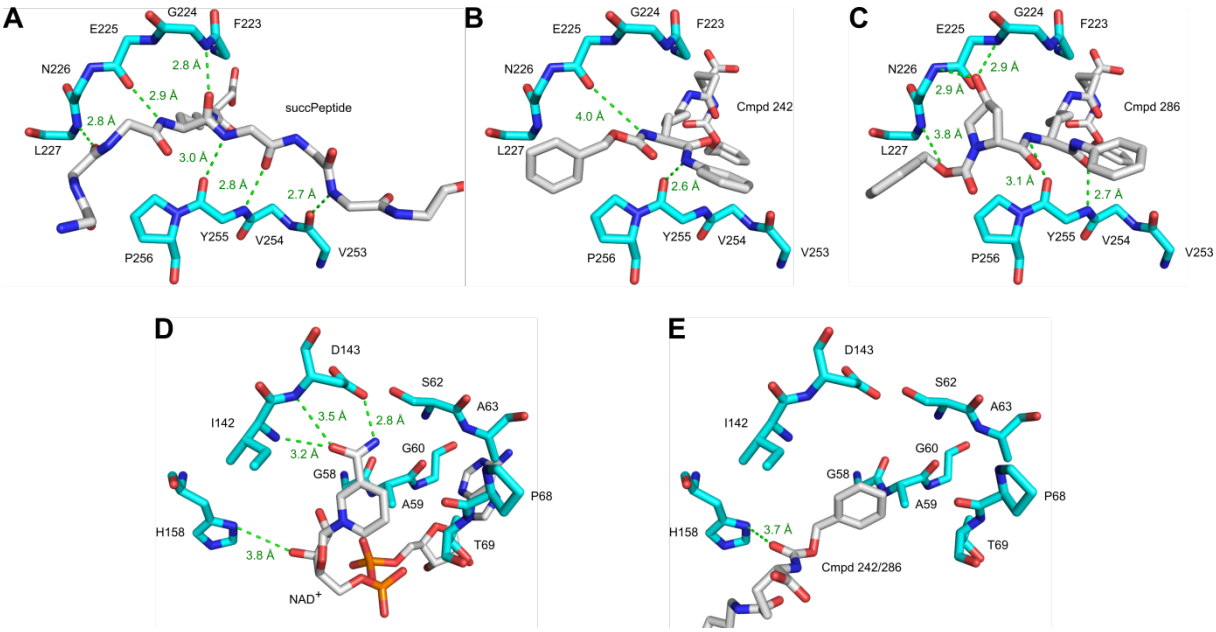

Figure 49: Lysine derivative binding to Sirt5. In case of Sirt5, the substrate's peptide chain backbone interacts with nine Sirt5 amino acids (A). All lysine derivatives tested (in particular the modelled UBCS 242, 282 & 286; B) lack most of these interactions, only UBCS 286 forms almost the same amount of hydrogen bonds as the native substrate peptide (C). Since UBCS 242 & 286 compete for peptide and NAD^+ binding (D & E), these compounds might lose inhibitory potency as the Z-moiety lacking UBCs 282 inhibits Sirt5 best. Stick representation of Sirt5 models from Figure 38. Substrate binding aa of Sirt5 in cyan, aa side chains removed except for succLys in A, C-site aa and H158 in D & E. Distances of possible hydrogen bonds are depicted in green.

This is reflected by their lower inhibitory potency compared to UBCS 282. This compound lacks any moiety that could point into the C-site, but might form a stalled intermediate thereby inhibiting Sirt5[163]. These binding features suggest UBCS 286 to be improved by replacing the Z moiety pointing into the C-site by a NAM related group, which should improve compound binding. However, UBCS 282 is already more potent than UBCS 286 although it lacks β-sheet like interaction with Sirt5. Therefore, introducing 4-hydroxyproline N-terminally to the modified lysine should improve UBCS 282 binding, thus enhancing the formation of the stalled intermediate and thereby improving Sirt5 inhibition.

4.2.4. 1,4-Dihydropyridine Activation of Sirtuins

The 1,4-DHP scaffold turned out to be a promising activating scaffold, despite it was designed based on structural similarities between Sirtuin inhibitors[106]. Interestingly, small changes at position 1 and 3 – 5 of the compound scaffold can change both the compounds effect as its specificity: a cyclopropane, a phenyl or a phenylethyl moiety at position 1 in combination with a carboxy group or a carboxamide at positions 3 & 5 render these compounds Sirtuin inhibitors[106] whereas benz(o)yl and ethoxy moieties turn these compounds into activating compounds. In addition, varying the moiety at position 4 seems to mediate the activator specificity between different Sirtuin enzymes. Strikingly, the activating effect on Sirtuins seems to be independent of the substrate used. So far, Sirtuin modulation by small molecule compounds occurred only using specific enzyme/substrate combinations[108]. Furthermore, depending on the Sirtuin/substrate combination, compounds acted either as activators (e.g. Resveratrol against Sirt1/p53)[108] or inhibitor (e.g. Resveratrol against Sirt3/ACS2)[109]. Due to this, it was assumed that Sirtuin modulating compounds had to be tailored for a specific effect and towards a distinct enzyme/substrate pair[109]. Adversely, the (substrate) specificity screens presented here suggest that 1,4-DHP based compounds can be designed to enhance the deacylation activity of a specific Sirtuin against all of its substrates.

4.2.4.1. 1,4-DHP compound properties for Sirt3 activation

Comparing the structure of all 47 1,4-DHP compounds indicates that a phenyl substituent at position 4 of the activator scaffold is beneficial for Sirt3 activation. Compounds with significant activation effects share this group, whereas compounds with little to no activating effect share a furan, thiophen, biphenyl or naphthalene moiety. UBCS 129 & 130 with a quinoline or a thiazole group, respectively, enhance Sirt3 activity similar to the parent compound. This might be caused by the stronger delocalization of the π-electrons within the thiazole ring compared to the furan or thiophen ring of UBCS 123 & 124. More critical for Sirt3 activation seems to be the aromatic substituent at position 1 of the activator scaffold.

The parent compound UBCS 125 with its benzyl moiety activates Sirt3 less compared to UBCS 126 which contains a benzoyl group at the same position. Increasing the aromatic ring system to naphthalene or quinalzoline (UBCS 132 & 133) extending the linker between 1,4-DHP scaffold and the aromatic group (UBCS 353) weakens the activating effect. The best activating compound UBCS 131 contained a benzoyl moiety with three methoxy residues which increase the compounds aromaticity by supplying further π-electrons and should also increase the compound's solubility. Interestingly, UBCS 357 with a 3,4,5-trimethoxybenzyl at position 1 exhibits no activating effect. This indicates that the carbonyl oxygen might be crucial for Sirt3 activation. However, substituting the phenyl moiety with additional functional groups (e.g. UBCS 360 – 369) while keeping the trimethoxy benzoyl moiety fixed, abolished the activating effect on Sirt3. Only UBCS 366 with its aminophenyl group activates Sirt3 similar to UBCS 126. This suggests that the combination of a trimethoxybenzoyl at position 1 and a phenyl moiety at position 4 of the 1,4-DHP scaffold are optimal for Sirt3 activation.

4.2.4.2. 1,4-DHP effects on other Sirtuins

Only Sirt3 is activated by UBCS 131 with minor effects on Sirt5. In case of Sirt1 and Sirt2 no effect of UBCS 131 was observed. Analyzing the effects of all 47 1,4-DHP compounds on Sirt1, Sirt2 and Sirt5 did not result in a similar specific Sirtuin/activator pair as for Sirt3 and UBCS 131.

Several compounds were able to activate Sirt1 moderately (~ 2-fold activation). Strikingly, 1,4-DHP derivatives that contained a benzoyl group at position 1 had no effect on Sirt1, except for UBCS 126. However, 3,4,5-trimethoxybenzoyl compounds acted as Sirt1 activators only in combination with a positively charged moiety at position 4 of the 1,4-DHP scaffold (UBCS 355 and 366) or in combination with a compact aromatic substituent (UBCS 367-369). Moreover, UBCS 123 and 124 with compact ring systems at position 4 and a benzyl moiety at position 1 were able to activate Sirt1. This indicates that for Sirt1 activation either compact or hydrophilic/positively charged moieties are necessary at position 4 while different substituents at position 1 are tolerable, with the exception of benzoyl moieties, which generally extinguish the activating effect.

Most Sirt5 activating 1,4-DHP compounds share a carbonylated residue at position 1. While the pan-Sirtuin activator UBCS 366 bears a trimethoxy benzoyl moiety, the best Sirt5 activators contain the less aromatic benzoyl residue at this position. Out of these, UBCS 344, 345 and 350 were the best Sirt5 activating compounds. UBCS 338 – 343 & 349 are weaker or no Sirt5 activators. This suggests that position 4 of the 1,4-DHP scaffold needs to be substituted with aromatic systems of a defined shape and aromaticity: methylated phenyl residues have minor or no effect on Sirt5 as well as chlorated phenyl moieties. However, a methoxy substituent in ortho and meta position seems to be just the appropriate feature for

proper Sirt5 activation: it contains an oxygen atom which is smaller than chlorine and more electronegative than a carbon atom. This is supported by UBCS 350 activating Sirt5 slightly better compared to UBCS 349, which contains a less aromatic furan ring instead of a thiophen moiety. Furthermore, meta position of the heteroatom enhances the activating effect, as UCBS 349 & 350 are better Sirt5 activators than UBCS 347 & 348.
Interestingly, UBCS 366 activated all Sirtuins tested. With its trimethoxy benzoyl at position 1 it contains a carbonyl moiety crucial for Sirt5 activation, the trimethoxy benzoyl moiety as a whole is important for Sirt3 activation. In addition it contains an anilinophenyl residue at position 4, a large aromatic ring system that also contains a charged functional group important for Sirt1 activation. The combination of these two substituents at position 1 and 4 is generally beneficial, as it is the only Sirt2 activating 1,4-DHP compound.

4.2.4.3. Specificity of 1,4-DHP compounds

The specificity analyses lacked the three human Sirtuins Sirt4, Sirt6 and Sirt7. Since for Sirt4 no profound *in vivo* deacylation activity is reported and since no soluble Sirt7 construct is available yet, these two Sirtuins were not included in the specificity analyses. Sirt6 is described to target myristoylated substrates both *in vivo* and *in vitro* (e.g. TNFα)[32,53]. Also in this study Sirt6 demyristoylase activity was observed (cf. section 3.2.1.2) in presence of either 100 µM peptide or NAD^+ concentrations above 1 mM. For the analysis of the activating effect of 1,4-DHP compounds, limiting amounts of each substrate were used (50 µM peptide and 100 µM NAD^+). Despite each of the limiting substrate concentrations ranged above the determined Sirt6 K_m values (Table 8 & Table 9), no Sirt6 activity was observed when both substrates were limited (not shown). In contrast to all other Sirtuin/substrate pairs analyzed, the Sirt6 construct used might tolerate only one limited substrate at once. The Sirt6 construct and/or the myrTNFα substrate peptide might need to be optimized as well to obtain a similar behavior as for all other Sirtuin/substrate pairs in the coupled continuous assay. However, cell-based assays that monitor e.g. the acylation level of known endogenous Sirtuin substrates should reveal, whether the 1,4-DHP compounds act specific and whether off-targets exist. Still, the specificity analyses included human Sirt1 – 3 and human Sirt5 in combination with robust substrate peptides derived from their *in vivo* targets (Table A 1). Hence, the 47 1,4 DHP compounds were tested against the majority of the human Sirtuin enzymes including differently acylated substrates. This already allows for a good estimation about the specificity of the compounds tested, i.e. UBCS 366 acting as pan-Sirtuin activator, while UBCS 124 acts Sirt1 specific, and UBCS 131 & 350 being specific and strong activators of Sirt3 and Sirt5, respectively.

4.2.4.4. Mechanism of Sirtuin activation by 1,4-DHP compounds

The precise mechanism of Sirtuin activation by 1,4-DHP and the basis of their specificity remain elusive. No Sirtuin/1,4-DHP complex structure could be obtained and binding effects were not comparable between Sirt3 and Sirt5. Nevertheless, the MST analyses revealed compound affinities to their respective Sirtuin target that were in good agreement with the specificity data observed during the activity analyses.

Some information about the activation mechanism of 1,4-DHP compounds can be drawn from the kinetic experiments. No clear effect on the substrates' K_m was observed. This was probably caused by the low data resolution at very low substrate concentrations, which are close to the signal limit of the coupled continuous assay. Importantly, presence of UBCS 131 & 350 increased Sirt3 and Sirt5 v_{max} significantly for both substrates. As the Sirtuin enzymatic mechanism is quite complex (Figure 5 & Figure 50), 1,4-DHP compounds can target several steps of this mechanism, which would finally result in an increased v_{max}.

At the beginning of the Sirtuin enzymatic mechanism, the substrates are bound in a sequential non-ordered manner (Figure 50). 1,4-DHP compounds might aid in the formation of the Sirtuin/substrates complex by enhancing its formation or by reducing its dissociation, which finally might result in an improved v_{max}. However, this would be accompanied by an improved K_m. Therefore, the MS-based assay could be used to unravel K_m effects during kinetic analyses, as this assay is more sensitive in terms of data resolution despite being more elaborate compared to the coupled assay.

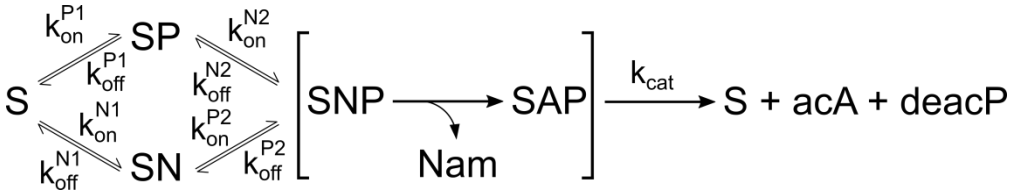

Figure 50: Schematic mechanism of Sirtuin catalysis. In general, the substrates (P: peptide/protein; N: NAD^+) bind sequentially to the Sirtuin (S) eventually resulting in the enzyme substrate complex (SNP). The rapid and reversible nicotinamide (Nam) release converts NAD^+ into ADPr (A), which forms an alkylimidate with the substrate acyl moiety and eventually resulting in a bicyclic intermediate. Resolving this intermediate comprises the rate limiting step of the Sirtuin reaction and results in free enzyme, the acylated ADPr (acA) and the deacylated peptide/protein (deacP).

Once both substrates are bound, the reversible release of NAM occurs and subsequently an alkylimidate between the remaining ADPr and the acylated substrate lysine is formed. Eventually, this alkylimidate forms a bicyclic intermediate. Hydrolysis of this intermediate comprises the rate limiting step of the Sirtuin reaction[86], which finally results in a deacylated lysine and acylated ADPr. 1,4-DHP activators might enhance the hydrolysis of the bicyclic intermediate which would eventually result in an improved v_{max} value. Use of thioacylated substrate peptides might confirm, whether the 1,4-DHP compounds enhance this step. The

bicyclic intermediates derived from S-alkylimidates are much more stable compared to regular O-alkylimidates[86], which results in very little product formation. If the compounds target the hydrolysis of this intermediate, thioacylated substrates should be consumed and S-acyl-ADPr as well as deacylated peptide should be produced much faster in presence of 1,4-DHP compounds, maybe even close to rates observed with regular acylated substrates.
Such experiments should be accompanied by further structural approaches as only a complex structure might provide insight into the activating mechanism and might indicate possible compound optimization strategies. Recently, promising strategies were reported for obtaining Sirt1 and Sirt2 structures in complex with a bound small molecule compound[29,164]. Thus, co-crystallization of Sirt1 in combination with UBCS 124 or UBCS 366 might result in a complex structure. As Sirt2 is also activated by UBCS 366, this combination might be used to obtain a complex structure as well. In addition, Sirtuin homologues from bacteria, yeast or archaea could be tested, as e.g. Sir2Tm, Hst2 and Sir2-Af2 are known for their robust crystallization behavior[26,28,104].

4.3. Perspectives on Sirtuin Modulation Approaches

4.3.1. Regulatory Strategies Based on Physiological Ligands

The results presented here indicate many strategies for Sirtuin specific regulation. These enzymes can be affected both by pharmacological and physiological ligands and PTMs. Modifications on distinct sites may affect these enzymes differently, as suggested by the PTM mimicking mutational studies. However, PTM regulation of Sirtuins as an approach in pharmacological research is hampered as the triggers and Sirtuin modifying enzymes need to be identified first. Secondly, small molecule compounds targeting these modifying enzymes would be needed in such approaches. Since Sirtuin modifying enzymes will probably modify further proteins, this strategy might eventually end in many off-targets and side effects.
Still, physiological interaction partners might be an approach to regulate Sirtuins specifically. However, it is not well understood whether Sirtuins act on their own or as a part of multi-protein complexes. *S. cerevisiae* Sir2 is known to be part of a multimeric transcriptional silencing complex[165]. For human Sirtuins, interaction partners are not well characterized. Only AROS is described to enhance Sirt1 activity, but this interaction is not vital for Sirt1 activity *in vivo*[89]. Should further interacting proteins reside within cells that are crucial for Sirtuin activity *in vivo*, disruption of such complexes might be a further strategy in pharmacological Sirtuin regulation. In addition, physiological Sirtuin small molecule ligands might be promising leads for pharmacological research. Although no further Sirtuin modulating small molecules were observed in ML besides NAM, further cellular

compartments might contain Sirtuin interacting molecules. Once identified, they could be used as parent scaffold in order to develop further Sirtuin regulating compounds.
Besides the identification of physiological Sirtuin modulating compounds in mammalian organisms, the search for Sirtuin regulating ligands could be expanded to further organisms. The stilbene Resveratrol is found in e.g. grapes and known to affect mammalian Sirtuin activity (cf. section 1.3). *Magnolia sp*. extracts, which are used in traditional Chinese medicine, contain e.g. Honokiol. This lignan was recently reported to stimulate Sirt3 activity in cell based assays[166]. Although this effect is not characterized in direct and label-free Sirtuin assays yet, it suggests that further plants might contain Sirtuin regulating metabolites.

4.3.2. Pharmacological Small Molecule Regulators

Many approaches aimed to identify small molecule regulators for pharmacological Sirtuin modulation. Interestingly, during high throughput screens not only the grape stilbene Resveratrol but also the inhibitor Suramin was discovered[80]. Introduced by the Bayer Company in 1916 as *Germanin* to treat sleeping sickness, it took almost 100 years until Suramin was identified to inhibit Sirtuins. Whether the antiparasitic effect of Suramin is indeed due to trypanosomal Sirtuin inhibition[167] or due to synergistic effects is still not known. However, NAM and Salermide were already shown to inhibit trypanosomal Sirtuins[168,169]. This suggests, that some therapeutics are already in use, which might not be characterized well enough for their cellular targets and thereby might not be linked to Sirtuin regulation yet. Further high throughput compound screens against human Sirtuins might identify compounds already in therapeutic use, which could be exploited as scaffold for novel Sirtuin regulators.
Nevertheless, the specificity analysis of available Sirtuin modulating compounds revealed known Sirt1 and Sirt2 regulators not to act against Sirt5. Only the indole GW5074, which was described to inhibit Sirt2[156], turned out to inhibit several Sirtuins with a slight preference for Sirt1. Derivatization of this compound revealed that its phenolic part is crucial for inhibition. It is tempting to speculate, if derivatization of its indole part might be able to mediate Sirtuin specificity and reduce off-target effects[155,156].
Using substrate acyl analogues seems to be a promising strategy for Sirtuin inhibition. Inhibitory peptides containing modifications on the lysine's acyl are already reported[34,163]. Here, lysine derivatives containing inhibitory acyl modifications are indicated as promising leads for Sirtuin specific inhibition. This might overcome disadvantages observed for peptide based pharmacological modulators (cf. 1.3.2).
The most promising scaffold for pharmacological targeting of Sirtuins characterized here, is the 1,4-DHP scaffold. Initially it was designed based on Sirtuin inhibitors. However, benz(o)yl and 3,4,5-trimethoxybenzyol groups at position 1 in combination with an ethoxy moiety at positions 3 & 5 of the scaffold turn these compounds into proper and efficient Sirtuin

activators. Thus, adjusting the distinct substituents of the 1,4-DHP scaffold might allow for the development of STACs specific for one of the seven Sirtuin enzymes. 1,4-DHP compounds are indicated to act in cell-based assays in a Sirtuin dependent manner as well (Mai et al., 2009; Valente et al., 2016; Neha Garg, Lab of Prof. David Sinclair at Harvard Medical School, personal communication)[106,119]. Thus, it will be exciting to see how these compounds behave during the next steps of pharmaceutical research (e.g. determination of their biostability, strategies for drug delivery and effects in rodents) and whether the results provided in this study might contribute to the development of a novel class of therapeutics in the treatment of metabolic and age-related diseases.

5. References

1. Kim, S. C. *et al.* Substrate and Functional Diversity of Lysine Acetylation Revealed by a Proteomics Survey. *Mol. Cell* **23,** 607–618 (2006).
2. Guan, K. L. & Xiong, Y. Regulation of intermediary metabolism by protein acetylation. *Trends Biochem. Sci.* **36,** 108–116 (2011).
3. Tan, M. *et al.* Identification of 67 histone marks and histone lysine crotonylation as a new type of histone modification. *Cell* **146,** 1016–1028 (2011).
4. Rardin, M. J. *et al.* Label-free quantitative proteomics of the lysine acetylome in mitochondria identifies substrates of SIRT3 in metabolic pathways. *Proc. Natl. Acad. Sci.* **110,** 6601–6606 (2013).
5. Rardin, M. J. *et al.* SIRT5 regulates the mitochondrial lysine succinylome and metabolic networks. *Cell Metab.* **18,** 920–933 (2013).
6. Tan, M. *et al.* Lysine glutarylation is a protein posttranslational modification regulated by SIRT5. *Cell Metab.* **19,** 605–617 (2014).
7. Weiss, M. S. & Schulz, G. E. Structure of porin refined at 1.8 ?? resolution. *J. Mol. Biol.* **227,** 493–509 (1992).
8. Cappadocia, L. *et al.* Structural and Functional Characterization of the Phosphorylation-Dependent Interaction between PML and SUMO1. *Structure* **23,** 126–138 (2015).
9. Choudhary, C., Weinert, B. T., Nishida, Y., Verdin, E. & Mann, M. The growing landscape of lysine acetylation links metabolism and cell signalling. *Nat. Rev. Mol. Cell Biol.* **15,** 536–550 (2014).
10. Hirschey, M. D. & Zhao, Y. Metabolic Regulation by Lysine Malonylation, Succinylation, and Glutarylation. *Mol. Cell. Proteomics* **14,** 2308–2315 (2015).
11. Wagner, G. R. & Payne, R. M. Widespread and enzyme-independent N??-acetylation and N??-succinylation of proteins in the chemical conditions of the mitochondrial matrix. *J. Biol. Chem.* **288,** 29036–29045 (2013).
12. Wagner, G. & Hirschey, M. D. Nonenzymatic Protein Acylation as a Carbon Stress Regulated by Sirtuin Deacylases. *Mol. Cell* **54,** 5–16 (2014).
13. Simic, Z., Weiwad, M., Schierhorn, A., Steegborn, C. & Schutkowski, M. The ε-Amino Group of Protein Lysine Residues Is Highly Susceptible to Nonenzymatic Acylation by Several Physiological Acyl-CoA Thioesters. *Chembiochem* (2015). doi:10.1002/cbic.201500364
14. Moniot, S., Weyand, M. & Steegborn, C. Structures, substrates, and regulators of mammalian Sirtuins - opportunities and challenges for drug development. *Front. Pharmacol.* **3 FEB,** 16 (2012).
15. Frye, R. A. Phylogenetic Classification of Prokaryotic and Eukaryotic Sir2-like Proteins. *Biochem. Biophys. Res. Commun.* **273,** 793–798 (2000).
16. Hirschey, M. D. Old enzymes, new tricks: Sirtuins are NAD +-dependent De-acylases. *Cell Metab.* **14,** 718–719 (2011).
17. Gertz, M. & Steegborn, C. Function and regulation of the mitochondrial Sirtuin isoform Sirt5 in Mammalia. *Biochim. Biophys. Acta - Proteins Proteomics* **1804,** 1658–1665 (2010).
18. Suenkel, B. & Steegborn, C. in *Methods in Enzymology* **573,** 183–208 (2016).
19. Houtkooper, R. H., Pirinen, E. & Auwerx, J. Sirtuins as regulators of metabolism and healthspan. *Nat. Rev. Mol. Cell Biol.* **13,** 225–238 (2012).
20. Guarente, L. Calorie restriction and sirtuins revisited. *Genes Dev.* **27,** 2072–2085 (2013).
21. Sebastián, C. *et al.* The histone deacetylase SIRT6 Is a tumor suppressor that controls cancer metabolism. *Cell* **151,** 1185–1199 (2012).
22. Barber, M. F. *et al.* SIRT7 links H3K18 deacetylation to maintenance of oncogenic transformation. *Nature* **487,** 1–7 (2012).
23. Tsai, Y.-C., Greco, T. M., Boonmee, a., Miteva, Y. & Cristea, I. M. Functional Proteomics Establishes the Interaction of SIRT7 with Chromatin Remodeling Complexes and Expands Its Role in Regulation of RNA Polymerase I Transcription. *Mol. Cell. Proteomics* **11,** M111.015156-M111.015156 (2012).
24. Tsai, Y.-C., Greco, T. M. & Cristea, I. M. Sirtuin 7 plays a role in ribosome biogenesis and protein synthesis. *Mol. Cell. Proteomics* **13,** 73–83 (2014).
25. Dryden, S. C., Nahhas, F. A., Nowak, J. E., Goustin, A.-S. & Tainsky, M. A. Role for human SIRT2 NAD-dependent deacetylase activity in control of mitotic exit in the cell cycle. *Mol. Cell. Biol.* **23,** 3173–85 (2003).
26. Zhao, K., Chai, X., Clements, A. & Marmorstein, R. Structure and autoregulation of the yeast Hst2 homolog of Sir2. *Nat. Struct. Biol.* **10,** 864–871 (2003).
27. Hawse, W. F. & Wolberger, C. Structure-based mechanism of ADP-ribosylation by sirtuins. *J. Biol. Chem.* **284,** 33654–33661 (2009).
28. Avalos, J. L., Bever, K. M. & Wolberger, C. Mechanism of sirtuin nhibition by nicotinamide: Altering the NAD + cosubstrate specificity of a Sir2 enzyme. *Mol. Cell* **17,** 855–868 (2005).
29. Dai, H. *et al.* Crystallographic structure of a small molecule SIRT1 activator-enzyme complex. *Nat. Commun.* **6,** 7645 (2015).
30. Moniot, S., Schutkowski, M. & Steegborn, C. Crystal structure analysis of human Sirt2 and its ADP-ribose complex. *J. Struct. Biol.* **182,** 136–143 (2013).
31. Du, J. *et al.* Sirt5 Is a NAD-Dependent Protein Lysine Demalonylase and Desuccinylase. *Science (80-.).* **334,** 806–809 (2011).
32. Jiang, H. *et al.* SIRT6 regulates TNF-α secretion through hydrolysis of long-chain fatty acyl lysine. *Nature* **496,** 110–3 (2013).

33. Jin, L. *et al.* Crystal structures of human SIRT3 displaying substrate-induced conformational changes. *J. Biol. Chem.* **284,** 24394–24405 (2009).
34. Roessler, C. *et al.* Chemical probing of the human sirtuin 5 active site reveals its substrate acyl specificity and peptide-based inhibitors. *Angew. Chemie - Int. Ed.* **53,** 10728–10732 (2014).
35. Schwer, B., Bunkenborg, J., Verdin, R. O., Andersen, J. S. & Verdin, E. Reversible lysine acetylation controls the activity of the mitochondrial enzyme acetyl-CoA synthetase 2. *Proc. Natl. Acad. Sci. U. S. A.* **103,** 10224–10229 (2006).
36. Schlicker, C. *et al.* Substrates and Regulation Mechanisms for the Human Mitochondrial Sirtuins Sirt3 and Sirt5. *J. Mol. Biol.* **382,** 790–801 (2008).
37. Nakagawa, T., Lomb, D. J., Haigis, M. C. & Guarente, L. SIRT5 Deacetylates Carbamoyl Phosphate Synthetase 1 and Regulates the Urea Cycle. *Cell* **137,** 560–570 (2009).
38. Haigis, M. C. *et al.* SIRT4 Inhibits Glutamate Dehydrogenase and Opposes the Effects of Calorie Restriction in Pancreatic ?? Cells. *Cell* **126,** 941–954 (2006).
39. Laurent, G. *et al.* SIRT4 coordinates the balance between lipid synthesis and catabolism by repressing malonyl CoA decarboxylase. *Mol. Cell* **50,** 686–698 (2013).
40. Sebastiań, C., Satterstrom, F. K., Haigis, M. C. & Mostoslavsky, R. From sirtuin biology to human diseases: An update. *J. Biol. Chem.* **287,** 42444–42452 (2012).
41. Radak, Z. *et al.* Redox-regulating sirtuins in aging, caloric restriction, and exercise. *Free Radic. Biol. Med.* **58,** 87–97 (2013).
42. Smith, B. C. & Denu, J. M. Acetyl-lysine analog peptides as mechanistic probes of protein deacetylases. *J. Biol. Chem.* **282,** 37256–37265 (2007).
43. Utani, A. Laminin ??3 chain-derived peptide promotes keratinocyte migration and wound closure: Clustering of syndecan-4 and integrin ??1. *Seikagaku* **82,** 327–331 (2010).
44. Eskandarian, H. A. *et al.* A role for SIRT2-dependent histone H3K18 deacetylation in bacterial infection. *Science* **341,** 1238858 (2013).
45. Vaquero, A. *et al.* SirT2 is a histone deacetylase with preference for histone H4 Lys 16 during mitosis. *Genes Dev.* **20,** 1256–1261 (2006).
46. Schwer, B., North, B. J., Frye, R. A., Ott, M. & Verdin, E. The human silent information regulator (Sir)2 homologue hSIRT3 is a mitochondrial nicotinamide adenine dinucleotide-dependent deacetylase. *J. Cell Biol.* **158,** 647–657 (2002).
47. Finley, L. W. S. *et al.* Succinate dehydrogenase is a direct target of sirtuin 3 deacetylase activity. *PLoS One* **6,** e23295 (2011).
48. Cheng, Y. *et al.* Interaction of Sirt3 with OGG1 contributes to repair of mitochondrial DNA and protects from apoptotic cell death under oxidative stress. *Cell Death Dis.* **4,** e731 (2013).
49. He, W., Newman, J. C., Wang, M. Z., Ho, L. & Verdin, E. Mitochondrial sirtuins: Regulators of protein acylation and metabolism. *Trends Endocrinol. Metab.* **23,** 467–476 (2012).
50. Lin, Z. F. *et al.* SIRT5 desuccinylates and activates SOD1 to eliminate ROS. *Biochem. Biophys. Res. Commun.* **441,** 191–195 (2013).
51. Peng, C. *et al.* The First Identification of Lysine Malonylation Substrates and Its Regulatory Enzyme. *Mol. Cell. Proteomics* **10,** M111.012658-M111.012658 (2011).
52. Gertler, A. A. & Cohen, H. Y. SIRT6, a protein with many faces. *Biogerontology* **14,** 629–639 (2013).
53. Feldman, J. L., Baeza, J. & Denu, J. M. Activation of the protein deacetylase SIRT6 by long-chain fatty acids and widespread deacylation by Mammalian Sirtuins. *J. Biol. Chem.* **288,** 31350–31356 (2013).
54. Verdin, E., Hirschey, M. D., Finley, L. W. S. & Haigis, M. C. Sirtuin regulation of mitochondria: Energy production, apoptosis, and signaling. *Trends Biochem. Sci.* **35,** 669–675 (2010).
55. Giblin, W., Skinner, M. E. & Lombard, D. B. Sirtuins: Guardians of mammalian healthspan. *Trends Genet.* **30,** 271–286 (2014).
56. Warburg, O. H. Uben den Stoffwechsel der Tumoren. *Klin. Wochenschr.* **4,** 534–536 (1926).
57. Blumenthal, E. Z. On the origin of cancer. *Med. Hypotheses* **46,** 581–583 (1996).
58. Someya, S. *et al.* Sirt3 mediates reduction of oxidative damage and prevention of age-related hearing loss under Caloric Restriction. *Cell* **143,** 802–812 (2010).
59. Osborne, B., Cooney, G. J. & Turner, N. Are sirtuin deacylase enzymes important modulators of mitochondrial energy metabolism? *Biochim. Biophys. Acta - Gen. Subj.* **1840,** 1295–1302 (2014).
60. Finley, L. W. S. *et al.* SIRT3 Opposes Reprogramming of Cancer Cell Metabolism through HIF1?? Destabilization. *Cancer Cell* **19,** 416–428 (2011).
61. Nakagawa, T. & Guarente, L. Urea cycle regulation by mitochondrial sirtuin, SIRT5. *Aging (Albany NY)* **1,** 578–581 (2009).
62. Liu, B. *et al.* SIRT5: A safeguard against oxidative stress-induced apoptosis in cardiomyocytes. *Cell. Physiol. Biochem.* **32,** 1050–1059 (2013).
63. Jais, A. *et al.* Heme oxygenase-1 drives metaflammation and insulin resistance in mouse and man. *Cell* **158,** 25–39 (2014).
64. Peck, B. *et al.* SIRT inhibitors induce cell death and p53 acetylation through targeting both SIRT1 and SIRT2. *Mol. Cancer Ther.* **9,** 844–855 (2010).
65. Chen, Y. *et al.* Sirtuin-3 (SIRT3), a therapeutic target with oncogenic and tumor-suppressive function in cancer. *Cell Death Dis* **5,** e1047 (2014).
66. Körner, S. *et al.* Differential sirtuin expression patterns in amyotrophic lateral sclerosis (ALS) postmortem tissue: Neuroprotective or neurotoxic properties of sirtuins in ALS? *Neurodegener. Dis.* **11,** 141–152 (2013).
67. Lu, W., Zuo, Y., Feng, Y. & Zhang, M. SIRT5 facilitates cancer cell growth and drug resistance in non-

small cell lung cancer. *Tumour Biol.* **35,** 10699–10705 (2014).
68. Lee, S. H. & Min, K. J. Caloric restriction and its mimetics. *BMB Rep.* **46,** 181–187 (2013).
69. McCay, C. M., Crowell, M. F. & Maynard, L. A. The effect of retarded growth upon the length of life span and upon the ultimate body size. *J. Nutr.* **5,** 63–79. DOI: (1935).
70. McDonald, R. B. & Ramsey, J. J. Honoring Clive McCay and 75 years of calorie restriction research. *J. Nutr.* **140,** 1205–10 (2010).
71. Fontana, L. & Partridge, L. Promoting health and longevity through diet: From model organisms to humans. *Cell* **161,** 106–118 (2015).
72. Weindruch, R., Walford, R. L., Fligiel, S. & Guthrie, D. The retardation of aging in mice by dietary restriction: longevity, cancer, immunity and lifetime energy intake. *J. Nutr.* **116,** 641–654 (1986).
73. Soare, A., Weiss, E. P. & Pozzilli, P. Benefits of caloric restriction for cardiometabolic health, including type 2 diabetes mellitus risk. *Diabetes. Metab. Res. Rev.* **30,** 41–47 (2014).
74. Donato, A. J. *et al.* Life-long caloric restriction reduces oxidative stress and preserves nitric oxide bioavailability and function in arteries of old mice. *Aging Cell* **12,** 772–783 (2013).
75. Srivastava, S. & Haigis, M. C. Role of Sirtuins and Calorie Restriction in Neuroprotection : Implications in Alzheimer ' s and Parkinson ' s Diseases. *Curr. Pharm. Des.* **17,** 3418–3433 (2011).
76. Haigis, M. C. & Sinclair, D. a. Mammalian Sirtuins: Biological Insights and Disease Relevance. *Annu. Rev. Pathol.* **5,** 253–295 (2010).
77. Guarente, L. Diverse and dynamic functions of the Sir silencing complex. *Nat. Genet.* **23,** 281–285 (1999).
78. Kaeberlein, M., McVey, M. & Guarente, L. The SIR2/3/4 complex and SIR2 alone promote longevity in Saccharomyces cerevisiae by two different mechanisms. *Genes Dev.* **13,** 2570–2580 (1999).
79. Lin, S. J., Defossez, P. a & Guarente, L. Requirement of NAD and SIR2 for life-span extension by calorie restriction in Saccharomyces cerevisiae. *Science* **289,** 2126–2128 (2000).
80. Howitz, K., Bitterman, J. & Cohen, H. Small molecule activators of sirtuins extend Saccharomyces cerevisiae lifespan. *Nature* **425,** 191–196 (2003).
81. Wood, J. G. *et al.* Sirtuin activators mimic caloric restriction and delay ageing in metazoans. *Nature* **430,** 686–689 (2004).
82. Sauve, A. A., Wolberger, C., Schramm, V. L. & Boeke, J. D. The biochemistry of sirtuins. *Annu. Rev. Biochem.* **75,** 435–465 (2006).
83. Sanders, B. D., Jackson, B. & Marmorstein, R. Structural basis for sirtuin function: What we know and what we don't. *Biochim. Biophys. Acta - Proteins Proteomics* **1804,** 1604–1616 (2010).
84. Schutkowski, M., Fischer, F., Roessler, C. & Steegborn, C. New assays and approaches for discovery and design of Sirtuin modulators. *Expert Opin Drug Discov* **9,** 183–199 (2014).
85. Sauve, A. A. Sirtuin chemical mechanisms. *Biochim. Biophys. Acta - Proteins Proteomics* **1804,** 1591–1603 (2010).
86. Smith, B. C. & Denu, J. M. Mechanism-based inhibition of Sir2 deacetylases by thioacetyl-lysine peptide. *Biochemistry* **46,** 14478–14486 (2007).
87. Flick, F. & Lüscher, B. Regulation of sirtuin function by posttranslational modifications. *Front. Pharmacol.* **3 FEB,** 29 (2012).
88. Lundby, A. *et al.* Proteomic Analysis of Lysine Acetylation Sites in Rat Tissues Reveals Organ Specificity and Subcellular Patterns. *Cell Rep.* **2,** 419–431 (2012).
89. Kim, E. J., Kho, J. H., Kang, M. R. & Um, S. J. Active Regulator of SIRT1 Cooperates with SIRT1 and Facilitates Suppression of p53 Activity. *Mol. Cell* **28,** 277–290 (2007).
90. Lakshminarasimhan, M. *et al.* Molecular architecture of the human protein deacetylase Sirt1 and its regulation by AROS and resveratrol. *Biosci. Rep.* **33,** 395–404 (2013).
91. Lin, H., Su, X. & He, B. Protein lysine acylation and cysteine succination by intermediates of energy metabolism. *ACS Chem. Biol.* **7,** 947–960 (2012).
92. Bitterman, K. J., Anderson, R. M., Cohen, H. Y., Latorre-Esteves, M. & Sinclair, D. A. Inhibition of silencing and accelerated aging by nicotinamide, a putative negative regulator of yeast Sir2 and human SIRT1. *J. Biol. Chem.* **277,** 45099–45107 (2002).
93. Yuan, H. & Marmorstein, R. Structural basis for sirtuin activity and inhibition. *J. Biol. Chem.* **287,** 42428–42435 (2012).
94. Sauve, A. A., Moir, R. D., Schramm, V. L. & Willis, I. M. Chemical activation of Sir2-dependent silencing by relief of nicotinamide inhibition. *Mol. Cell* **17,** 595–601 (2005).
95. Kiviranta, P. H. *et al.* N ε-Thioacetyl-Lysine-Containing Tri-, Tetra-, and Pentapeptides as SIRT1 and SIRT2 Inhibitors. *J. Med. Chem.* **52,** 2153–2156 (2009).
96. He, B., Du, J. & Lin, H. Thiosuccinyl peptides as Sirt5-specific inhibitors. *J. Am. Chem. Soc.* **134,** 1922–1925 (2012).
97. He, B., Hu, J., Zhang, X. & Lin, H. Thiomyristoyl peptides as cell-permeable Sirt6 inhibitors. *Org. Biomol. Chem.* **12,** 7498–502 (2014).
98. Cen, Y. Sirtuins inhibitors: The approach to affinity and selectivity. *Biochim. Biophys. Acta - Proteins Proteomics* **1804,** 1635–1644 (2010).
99. Chen, L. Medicinal chemistry of sirtuin inhibitors. *Curr. Med. Chem.* **18,** 1936–46 (2011).
100. Suzuki, T. *et al.* Identification of a cell-active non-peptide sirtuin inhibitor containing N-thioacetyl lysine. *Bioorganic Med. Chem. Lett.* **19,** 5670–5672 (2009).
101. Schuetz, A. *et al.* Structural Basis of Inhibition of the Human NAD+-Dependent Deacetylase SIRT5 by Suramin. *Structure* **15,** 377–389 (2007).
102. Trapp, J. *et al.* Structure-activity studies on suramin analogues as inhibitors of NAD +-dependent histone

deacetylases (sirtuins). *ChemMedChem* **2,** 1419–1431 (2007).
103. Outeiro, T. F. *et al.* Sirtuin 2 inhibitors rescue alpha-synuclein-mediated toxicity in models of Parkinson's disease. *Science* **317,** 516–519 (2007).
104. Gertz, M. *et al.* Ex-527 inhibits Sirtuins by exploiting their unique NAD+-dependent deacetylation mechanism. *Proc. Natl. Acad. Sci. U. S. A.* **110,** E2772-81 (2013).
105. Suzuki, T., Imai, K., Nakagawa, H. & Miyata, N. 2-Anilinobenzamides as SIRT inhibitors. *ChemMedChem* **1,** 1059–1062 (2006).
106. Mai, A. *et al.* Study of 1,4-dihydropyridine structural scaffold: Discovery of novel sirtuin activators and inhibitors. *J. Med. Chem.* **52,** 5496–5504 (2009).
107. Maurer, B. *et al.* Inhibitors of the NAD+-dependent protein desuccinylase and demalonylase sirt5. *ACS Med. Chem. Lett.* **3,** 1050–1053 (2012).
108. Lakshminarasimhan, M., Rauh, D., Schutkowski, M. & Steegborn, C. Sirt1 activation by resveratrol is substrate sequence-selective. *Aging (Albany. NY).* **5,** 151–154 (2013).
109. Gertz, M. *et al.* A Molecular Mechanism for Direct Sirtuin Activation by Resveratrol. *PLoS One* **7,** e49761 (2012).
110. Park, S. J. *et al.* Resveratrol ameliorates aging-related metabolic phenotypes by inhibiting cAMP phosphodiesterases. *Cell* **148,** 421–433 (2012).
111. Chung, J. H. Using PDE inhibitors to harness the benefits of calorie restriction: Lessons from resveratrol. *Aging (Albany. NY).* **4,** 144–145 (2012).
112. Milne, J. *et al.* Small molecule activators of {SIRT1} as therapeutics for the treatment of type 2 diabetes. *Nature* **450,** 712–716 (2007).
113. Minor, R. K. *et al.* SRT1720 improves survival and healthspan of obese mice. *Sci. Rep.* **1,** 70 (2011).
114. Mitchell, S. J. *et al.* The SIRT1 activator SRT1720 extends lifespan and improves health of mice fed a standard diet. *Cell Rep.* **6,** 836–843 (2014).
115. Mercken, E. M. *et al.* SRT2104 extends survival of male mice on a standard diet and preserves bone and muscle mass. *Aging Cell* **13,** 787–796 (2014).
116. Hubbard, B. P. *et al.* Evidence for a common mechanism of SIRT1 regulation by allosteric activators. *Science* **339,** 1216–9 (2013).
117. Jin, L. *et al.* Biochemical characterization, localization, and tissue distribution of the longer form of mouse SIRT3. *Protein Sci.* **18,** 514–525 (2009).
118. Nguyen, G. T. T., Schaefer, S., Gertz, M., Weyand, M. & Steegborn, C. Structures of human sirtuin 3 complexes with ADP-ribose and with carba-NAD+ and SRT1720: Binding details and inhibition mechanism. *Acta Crystallogr. Sect. D Biol. Crystallogr.* **69,** 1423–1432 (2013).
119. Valente, S. *et al.* 1,4-Dihydropyridines Active on the SIRT1/AMPK Pathway Ameliorate Skin Repair and Mitochondrial Function and Exhibit Inhibition of Proliferation in Cancer Cells. *J. Med. Chem.* **59,** 1471–1491 (2016).
120. Beausoleil, S. A. *et al.* Large-scale characterization of HeLa cell nuclear phosphoproteins. *Proc. Natl. Acad. Sci. U. S. A.* **101,** 12130–5 (2004).
121. Brill, L. M. *et al.* Phosphoproteomic analysis of human embryonic stem cells. *Cell Stem Cell* **5,** 204–13 (2009).
122. Gauci, S. *et al.* Lys-N and trypsin cover complementary parts of the phosphoproteome in a refined SCX-based approach. *Anal. Chem.* **81,** 4493–4501 (2009).
123. Hsu, P. P. *et al.* The mTOR-regulated phosphoproteome reveals a mechanism of mTORC1-mediated inhibition of growth factor signaling. *Science* **332,** 1317–22 (2011).
124. Park, J. *et al.* SIRT5-Mediated Lysine Desuccinylation Impacts Diverse Metabolic Pathways. *Mol. Cell* **50,** 919–930 (2013).
125. Suenkel, B. *Modulation of Sirtuin Activity*. (2011).
126. Fischer, F. *et al.* Sirt5 Deacylation Activities Show Differential Sensitivities to Nicotinamide Inhibition. *PLoS ONE* **7,** e45098 (2012).
127. North, B. J. *et al.* Is an NAD ⁺ -Dependent Tubulin Deacetylase. *Mol. Cell* **11,** 437–444 (2003).
128. Bradford, M. M. A rapid and sensitive method for the quantitation of microgram quantities of protein utilizing the principle of protein-dye binding. *Anal. Biochem.* **72,** 248–254 (1976).
129. Laemmli, U. K. Cleavage of structural proteins during the assembly of the head of bacteriophage T4. *Nature* **227,** 680–685 (1970).
130. Jerabek-Willemsen, M., Wienken, C. J., Braun, D., Baaske, P. & Duhr, S. Molecular Interaction Studies Using Microscale Thermophoresis. *Assay Drug Dev. Technol.* **9,** 342–353 (2011).
131. Seidel, S. A. I. *et al.* Label-free microscale thermophoresis discriminates sites and affinity of protein-ligand binding. *Angew. Chemie - Int. Ed.* **51,** 10656–10659 (2012).
132. Crowther, G. J. *et al.* Buffer Optimization of Thermal Melt Assays of Plasmodium Proteins for Detection of Small-Molecule Ligands. *J. Biomol. Screen.* **14,** 700–707 (2009).
133. Smith, B. C., Hallows, W. C. & Denu, J. M. A continuous microplate assay for sirtuins and nicotinamide-producing enzymes. *Anal. Biochem.* **394,** 101–109 (2009).
134. Michaelis, L. & Menten, M. L. Die Kinetik der Invertinwirkung. *Biochem. Z.* **49,** 333–369 (1913).
135. Turan, T. & Karakas, M. The effect of trade openness and income on the size of a government. *Transylvanian Rev. Adm. Sci.* **2016,** 164–178 (2016).
136. MacLean, B. *et al.* Skyline: An open source document editor for creating and analyzing targeted proteomics experiments. *Bioinformatics* **26,** 966–968 (2010).
137. Kabsch, W. Xds. *Acta Crystallogr. Sect. D Biol. Crystallogr.* **66,** 125–132 (2010).
138. Krug, M., Weiss, M. S., Heinemann, U. & Mueller, U. XDSAPP: A graphical user interface for the

convenient processing of diffraction data using XDS. *J. Appl. Crystallogr.* **45,** 568–572 (2012).
139. Vagin, A. & Teplyakov, A. Molecular replacement with MOLREP. *Acta Crystallogr. Sect. D Biol. Crystallogr.* **66,** 22–25 (2010).
140. Sanders, B. D., Zhao, K., Slama, J. T. & Marmorstein, R. Structural Basis for Nicotinamide Inhibition and Base Exchange in Sir2 Enzymes. *Mol. Cell* **25,** 463–472 (2007).
141. Vagin, A. A. *et al.* REFMAC5 dictionary: Organization of prior chemical knowledge and guidelines for its use. *Acta Crystallogr. Sect. D Biol. Crystallogr.* **60,** 2184–2195 (2004).
142. The CCP4 suite: Programs for protein crystallography. *Acta Crystallogr. Sect. D Biol. Crystallogr.* **50,** 760–763 (1994).
143. Winn, M. D. *et al.* Overview of the CCP4 suite and current developments. *Acta Crystallogr. Sect. D Biol. Crystallogr.* **67,** 235–242 (2011).
144. Emsley, P. & Cowtan, K. Coot: Model-building tools for molecular graphics. *Acta Crystallogr. Sect. D Biol. Crystallogr.* **60,** 2126–2132 (2004).
145. Schüttelkopf, A. W. & Van Aalten, D. M. F. PRODRG: A tool for high-throughput crystallography of protein-ligand complexes. *Acta Crystallogr. Sect. D Biol. Crystallogr.* **60,** 1355–1363 (2004).
146. Park ', H.-J. *et al.* Purification and characterization of a NADH oxidase from the thermophile Thermus thermophilus HB8. *Eur. J. Biochem* **205,** 881–885 (1992).
147. Smith, J. S. *et al.* in *Methods in Enzymology* (ed. Chandan K. Sen, L. P.) **353,** 282–300 (Academic Press, 2002).
148. Fomenko, D. E. & Gladyshev, V. N. Identity and functions of CxxC-derived motifs. *Biochemistry* **42,** 11214–11225 (2003).
149. Yu, L. R. *et al.* Improved titanium dioxide enrichment of phosphopeptides from HeLa cells and high confident phosphopeptide identification by cross-validation of MS/MS and MS/MS/MS spectra. *J. Proteome Res.* **6,** 4150–4162 (2007).
150. Weinert, B. *et al.* Acetyl-Phosphate is a critical determinant of Lysine Acetylation in E.coli. *Mol. Cell* **51,** 265–272 (2013).
151. Weinert, B. T. *et al.* Lysine succinylation is a frequently occurring modification in prokaryotes and eukaryotes and extensively overlaps with acetylation. *Cell Rep.* **4,** 842–851 (2013).
152. Kawahara, T. L. A. *et al.* SIRT6 Links Histone H3 Lysine 9 Deacetylation to NF-??B-Dependent Gene Expression and Organismal Life Span. *Cell* **136,** 62–74 (2009).
153. Rauh, D. *et al.* An acetylome peptide microarray reveals specificities and deacetylation substrates for all human sirtuin isoforms. *Nat. Commun.* **4,** 2327 (2013).
154. Lackey, K. *et al.* The discovery of potent cRaf1 kinase inhibitors. *Bioorganic Med. Chem. Lett.* **10,** 223–226 (2000).
155. Li, M., Smith, C. J., Walker, M. T. & Smith, T. J. Novel inhibitors complexed with glutamate dehydrogenase: Allosteric regulation by control of protein dynamics. *J. Biol. Chem.* **284,** 22988–23000 (2009).
156. Trapp, J. *et al.* Adenosine mimetics as inhibitors of NAD+-dependent histone deacetylases, from kinase to sirtuin inhibition. *J. Med. Chem.* **49,** 7307–7316 (2006).
157. Zhou, Y. *et al.* The bicyclic intermediate structure provides insights into the desuccinylation mechanism of human sirtuin 5 (SIRT5). *J. Biol. Chem.* **287,** 28307–28314 (2012).
158. Roessler, C., Tüting, C., Meleshin, M., Steegborn, C. & Schutkowski, M. A Novel Continuous Assay for the Deacylase Sirtuin 5 and Other Deacetylases. *J. Med. Chem.* **58,** 7217–7223 (2015).
159. Hebert, A. S. *et al.* Calorie Restriction and SIRT3 Trigger Global Reprogramming of the Mitochondrial Protein Acetylome. *Mol. Cell* **49,** 186–199 (2013).
160. Gerhart-Hines, Z. *et al.* The cAMP/PKA Pathway Rapidly Activates SIRT1 to Promote Fatty Acid Oxidation Independently of Changes in NAD +. *Mol. Cell* **44,** 851–863 (2011).
161. Zhao, X. *et al.* The 2.5 ?? crystal structure of the SIRT1 catalytic domain bound to nicotinamide adenine dinucleotide (NAD+) and an indole (EX527 analogue) reveals a novel mechanism of histone deacetylase inhibition. *J. Med. Chem.* **56,** 963–969 (2013).
162. Huber, K. *et al.* Novel 3-arylideneindolin-2-ones as inhibitors of NAD+-dependent histone deacetylases (sirtuins). *J. Med. Chem.* **53,** 1383–1386 (2010).
163. Zang, W., Hao, Y., Wang, Z. & Zheng, W. Novel thiourea-based sirtuin inhibitory warheads. *Bioorganic Med. Chem. Lett.* **25,** 3319–3324 (2015).
164. Rumpf, T., Gerhardt, S., Einsle, O. & Jung, M. Seeding for sirtuins: Microseed matrix seeding to obtain crystals of human Sirt3 and Sirt2 suitable for soaking. *Acta Crystallogr. Sect. Struct. Biol. Commun.* **71,** 1498–1510 (2015).
165. Imai, S., Armstrong, C. M., Kaeberlein, M. & Guarente, L. Transcriptional silencing and longevity protein Sir2 is an NAD-dependent histone deacetylase. *Nature* **403,** 795–800 (2000).
166. Pillai, V. B. *et al.* Honokiol blocks and reverses cardiac hypertrophy in mice by activating mitochondrial Sirt3. *Nat. Commun.* **6,** 6656 (2015).
167. Religa, A. A. & Waters, A. P. Sirtuins of parasitic protozoa: In search of function(s). *Mol. Biochem. Parasitol.* **185,** 71–88 (2012).
168. Soares, M. B. P. *et al.* Anti-Trypanosoma cruzi activity of nicotinamide. *Acta Trop.* **122,** 224–229 (2012).
169. Moretti, N. S. *et al.* Characterization of Trypanosoma cruzi Sirtuins as Possible Drug Targets for Chagas Disease. *Antimicrob. Agents Chemother.* **59,** 4669–4679 (2015).

6. Appendix

6.1. Peptides and Oligonucleotide Primers used

Table A 1: Substrate peptides, their amino acid sequence and their corresponding Sirtuin isoform used for *in vitro* experiments.

Peptide	Sequence	Derived from	Substrate peptide for
AATase	VFLP-acK-PTWG	Alcohol acetyltransferase	Sirt3
ACS2.2[(a)]	TRSG-acK-VMRRL	Acetyl-CoA synthetase 2	
ACS2.3	TRSG-acK-VMR		
αTub	MPSD-acK-TIG	α-Tubulin	Sirt2
acCPS1	FKRGVL-acK-EYGVKV	Carbamoylphosphate synthetase 1	Sirt5
succCPS1lg[(b)]	FKRGVL-succK-EYGVKV		
succCPS1	RGVL-succK-EYGV		
H3K9	TKQTAR-acK-STGGKA	Histone 3	Sirt6
H3K116	IHA-acK-RVT		Hst2
mtHsp75	RYTLHY-acK-TDAPLN	Mitochondrial Heat shock protein 75	Sirt3
p53	RHK-acK-LMFK	p53	Sirt1
PDH	KADQLY-acK-QKFIRG	Pyruvate dehydrogenase	Sirt3
acPrx1	SKEYFS-acK-QK	Peroxiredoxin	Sirt5
succPrx1	SKEYFS-succK-QK		
myrTNFα	EALPK-myrK-YGG	Tumor necrosis factor α	Sirt6
Transloc	ARDEGG-acK-AFFKGA	ADP/ATP translocase	Sirt3
VDAC	ARDVFT-acK-GYGFGL	Voltage dependent anion channel	

a) ACS2.2 was used for crystallization experiments

b) succCPS1lg was used for crystallization experiments

Table A 2: Vector specific primers used for two step mutagenesis and colony PCR

Primer	Vector	Restriction site used on vector	Sequence
T7 fw	pET 19b	Nde I (pET19b)	TAATACGACTCACTATAGGG
T7 rev	pET 151 D/TOPO[(a)]	Xho I (pET19b)	CTAGTTATTGCTCAGCGGT
pQE for	pQE 80L	Xho I	GTATCACGAGGCCCTTTCGTCT
pQE rev		Hind III	CATTACTGGATCTATCAACAGGAG
CmR-rv		Nhe I / Hind III	CTATACGTAGTTTGCTGGTTAAAATAGTG
pcDNA fw	pcDNA 3.1 +	Bam HI	GGCTAACTAGAGAACCCACTG
pcDNA rev		Xba I	GGCAACTAGAAGGCACAGTC

a) pET 151 D/TOPO contains no restriction site that could be used for ligation

Table A 3: Oligonucleotide Primers used for site directed mutagenesis.

Sirtuin	Mutation	Primer	T_m [°C]
Sirt4	S255A	Forward: 5' GTAAAAGAAGCCGACGCCCTCTTGGTGGTG 3' Reverse: 5' CACCACCAAGAGGGCGTCGGCTTCTTTTAC 3'	78.9
	S255D	Forward: 5' GTAAAAGAAGCCGACGACCTCTTGGTGGTG 3' Reverse: 5' CACCACCAAGAGGTCGTCGGCTTCTTTTAC 3'	78.1
Sirt5	K45A	Forward: 5' ATGGCAGATTTTCGAGCGTTTTTTGCAAAAGCA 3' Reverse: 5' TGCTTTTGCAAAAAACGCTCGAAAATCTGCCAT 3'	79.3
	K45Q	Forward: 5' ATGGCAGATTTTCGACAGTTTTTTGCAAAAGCA 3' Reverse: 5' TGCTTTTGCAAAAAACTGTCGAAAATCTGCCAT 3'	77.0
	K49A	Forward: 5' CGAAAGTTTTTTGCAGCAGCAAAGCACATAGTC 3' Reverse: 5' GACTATGTGCTTTGCTGCTGCAAAAAACTTTCG 3'	76.0
	K49Q	Forward: 5' CGAAAGTTTTTTGCACAAGCAAAGCACATAGTC 3' Reverse: 5' GACTATGTGCTTTGCTTGTGCAAAAAACTTTCG 3'	74.6
	K79A	Forward: 5' GGAGGTTATTGGAGAGCATGGCAAGCCCAGGAC 3' Reverse: 5' GTCCTGGGCTTGCCATGCTCTCCAATAACCTCC 3'	81.4
	K79Q	Forward: 5' GGAGGTTATTGGAGACAATGGCAAGCCCAGGAC 3' Reverse: 5' GTCCTGGGCTTGCCATTGTCTCCAATAACCTCC 3'	80.0
	K112A	Forward: 5' GAGGTCATGGGGAGCGCGGAGCCCAACGCCGGG 3' Reverse: 5' CCCGGCGTTGGGCTCCGCGCTCCCCATGACCTC 3'	92.6
	K112Q	Forward: 5' GAGGTCATGGGGAGCCAGGAGCCCAACGCCGGG 3' Reverse: 5' CCCGGCGTTGGGCTCCTGGCTCCCCATGACCTC 3'	90.2
	S185A	Forward: 5' ATTTGTCCAGCTTTAGCAGGAAAAGGTGCTCCA 3' Reverse: 5' TGGAGCACCTTTTCCTGCTAAAGCTGGACAAAT 3'	77.3
	S185D	Forward: 5' ATTTGTCCAGCTTTAGACGGAAAAGGTGCTCCA 3' Reverse: 5' TGGAGCACCTTTTCCGTCTAAAGCTGGACAAAT 3'	77.3
	K203A	Forward: 5' AGCATCCCAGTTGAGGCACTTCCCCGGTGTGAA 3' Reverse: 5' TTCACACCGGGGAAGTGCCTCAACTGGGATGCT 3'	84.4
	K203Q	Forward: 5' AGCATCCCAGTTGAGCAACTTCCCCGGTGTGAA 3' Reverse: 5' TTCACACCGGGGAAGTTGCTCAACTGGGATGCT 3'	83.1
	C245A	Forward: 5' GTAAAAGAAGCCGACGCCCTCTTGGTGGTG 3' Reverse: 5' CACCACCAAGAGGGCGTCGGCTTCTTTTAC 3'	74.4
Sirt6	S45A	Forward: 5' GGTCTGGCAGTCTGCCAGTGTGGTGTTC 3' Reverse: 5' GAACACCACACTGGCAGACTGCCAGACC 3'	78.3
	S45D	Forward: 5' GGTCTGGCAGTCTGACAGTGTGGTGTTCC 3' Reverse: 5' GGAACACCACACTGTCAGACTGCCAGACC 3'	77.3
	S210A	Forward: 5' GAACGCCGACCTGGCCATCACGCTGG 3' Reverse: 5' CCAGCGTGATGGCCAGGTCGGCGTTC 3'	84.1
	S210D	Forward: 5' GAACGCCGACCTGGACATCACGCTGGG 3' Reverse: 5' CCCAGCGTGATGTCCAGGTCGGCGTTC 3'	83.1
	T294A	Forward: 5' CCCGCCCGCCCGCACCCAAGCTGGA 3' Reverse: 5' TCCAGCTTGGGTGCGGGCGGGCGGG 3'	89.6
	T294D	Forward: 5' GGAGCGGCCCACCGCACCTGCCCCCCACAG 3' Reverse: 5' CTCCAGCTTGGGATCGGGCGGGCGGG 3'	87.2
	S338A	Forward: 5' GGAGCGGCCCACCGCACCTGCCCCCCACAG 3' Reverse: 5' CTGTGGGGGGCAGGTGCGGTGGGCCGCTCC 3'	92.0
	S338D	Forward: 5' GAGCGGCCCACCGATCCTGCCCCCCA 3' Reverse: 5' GTGGGGGGCAGGATCGGTGGGCCGCTC 3'	88.1 87.9
Sirt7	T224A	Forward: 5' CAGACAGGCCGGGCCTGCCACCAGTG 3' Reverse: 5' ACTTGTGGCAGGCCCGGCCTGTCTgG 3'	66.6/62.9
	T224D	Forward: 5' CCAGACAGGCCGGGACTGCCACCAGTG 3' Reverse: 5' ACACTTGTGGCAGTCCCGGCCTGTCTG 3'	62.9
	T267A	Forward: 5' CCAGCAGAGCAGACGCCATCCTGTGTCTAG 3' Reverse: 5' CTAGACACAGGATGGCGTCTGCTCTGCTGG 3'	78.9
	T267D	Forward: 5' CCAGCAGAGCAGACGACATCCTGTGTCTAG 3' Reverse: 5' CTAGACACAGGATGTCGTCTGCTCTGCTGG 3'	76.2

6.2. Supplemental Data

6.2.1. GW5074 inhibition of zSirt5 & Hst2

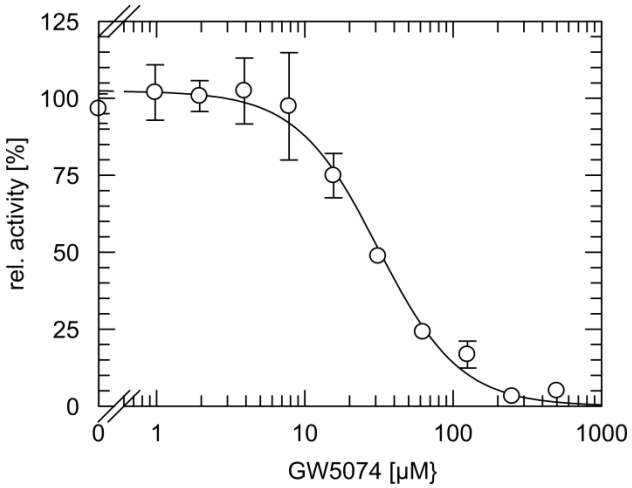

Figure A 1: GW5074 inhibition of zSirt5. GW5074 inhibits zSirt5 from *D. rerio* similar to human Sirt5 with an IC_{50} value of 31.2 ± 2.5 µM.

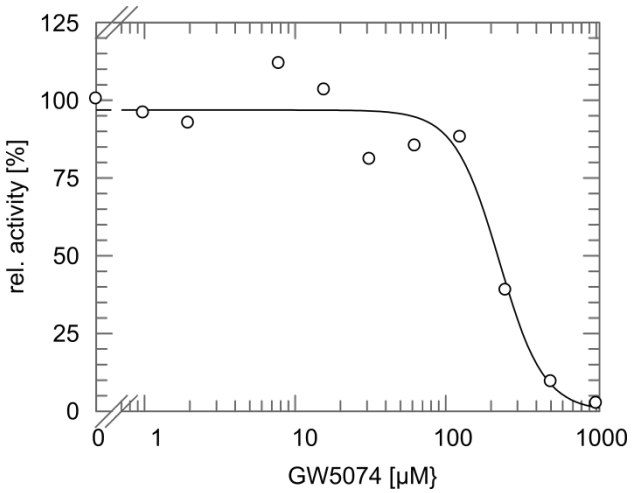

Figure A 2: GW5074 inhibition of Hst2. *S. cerevisiae* Hst2, which readily crystallizes in presence of different ligands, is less inhibited by GW5074 compared to the different Sirt5 homologues (IC_{50} of 226.4 ± 27.4 µM).

6.2.2. GW5074 bound to a Sirt3/ADPr complex

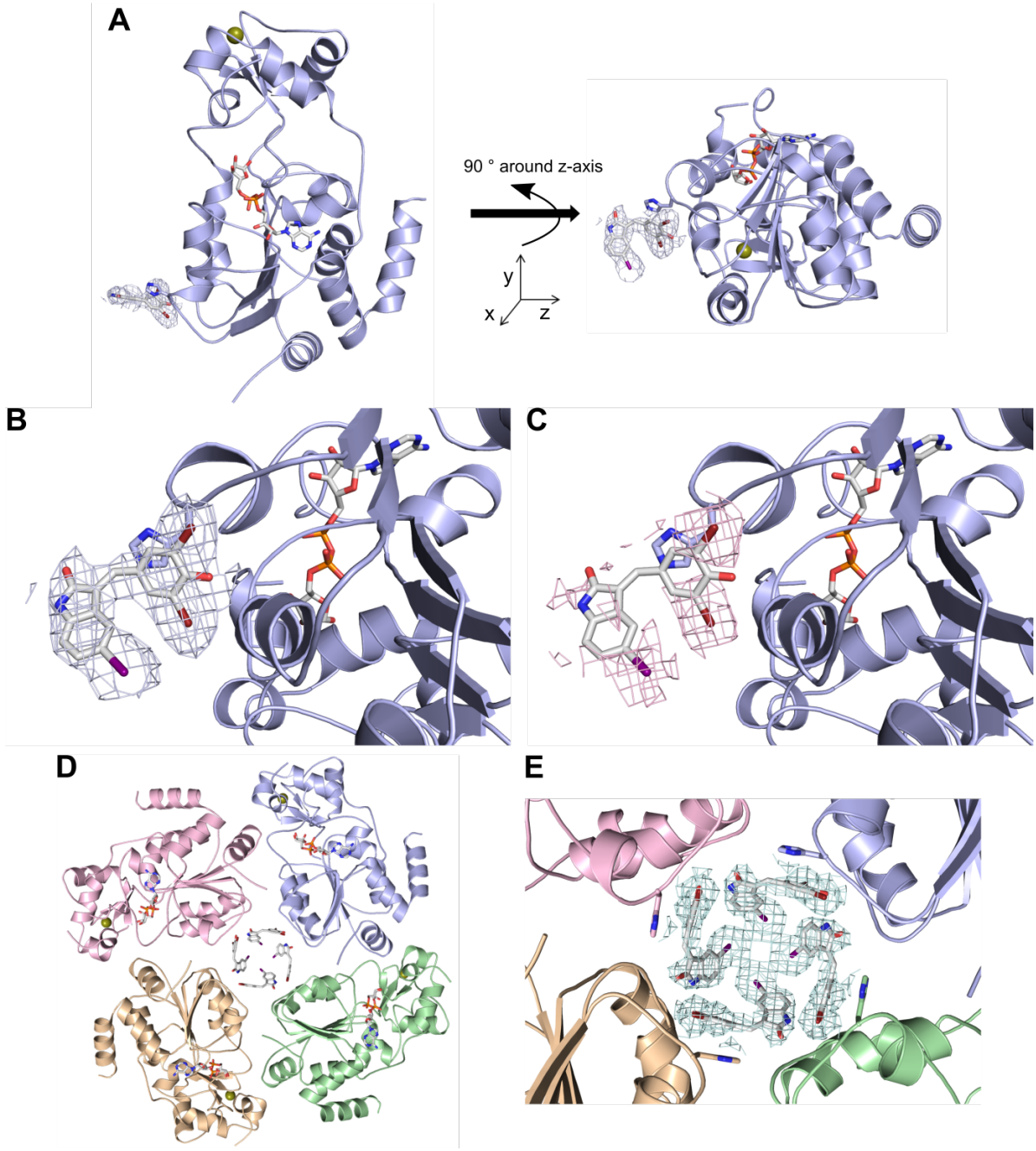

Figure A 3: Sirt3 in complex with ADPr and GW5074. (A) Overall structure of Sirt3 with bound Zn^{2+} in complex with ADPr. GW5074 is located to the bottom part of the Rossmann-fold domain close to His354. The asymmetric unit contains one of each molecule. (B) Sigma weighted density map ($2F_O$-F_C) to locate GW5074 at the bottom of the Sirt3 Rossmann-fold domain. (C) Anomalous difference map verifies the location of the bromine (dark red) and iodine (purple) atoms of GW5074. (D & E) GW5074 is located to the symmetry axis between four Sirt3 copies. While compound's indole iodine points towards the axis, its phenyl part is in close proximity to Sirt3 H354. Cartoon representation of Sirt3 (light blue, symmetry models in light green, red and orange), Zn^{2+} as sphere (olive) and GW5074 & ADPr as sticks colored by element (Br: dark red, I: purple, N: blue, O: red, P: orange). Meshes in light blue denotes the Sigma weighted difference density map at a Sigma level of 1, meshes in light red denote the anomalous difference map at a Sigma level of 1. Data collection and refinement statistics are listed in Table A 4.

Table A 4: Data collection and refinement statistics for the complex structure of Sirt3/ADPr/GW5074[(a)]

Data collection[(b)]	
Space group	I*422*
Unit cell: *a*, *b*, *c* [Å] / α, β, γ [°]	100.1, 100.1, 131.4 / 90, 90, 90
Wavelength [Å]	0.917050
Resolution [Å]	42.37 – 3.00 (3.16 – 3.00)
Reflections Unique Reflections	74129 (10457) 12797 (1837)
R_{meas} [%]	25.8 (112.3)
$I/\sigma[I]$	7.45 (1.76)
$CC_{1/2}$ Completeness [%]	98.2 (65.9) 99.9 (100.0)
Redundancy	5.8 (5.7)
Refinement[(b)]	
Resolution [Å]	3.0
No. reflections	6644
R_{work} / R_{free}	20.56 / 28.37
No. atoms	
Sirt3	2088
ADPr	36
GW5074	21
B factors	
Sirt3	50.4
ADPr	49.4
GW5074	41.5
R.m.s deviations	
Bond lengths [Å]	0.0109
Bond angles [°]	1.7810

a) since GW5074 binding was caused by a crystallization artifact, the refinement process was not completed (e.g. waters and ions were not put into the model)

b) values for the outermost resolution shell in brackets

6.2.3. Rel. activity values for all 1,4-DHP experiments

Table A 5: NAM consumption in presence of 10 µM or 100 µM 1,4-DHP in the coupled continuous assay.

UBCS	10 µM 1,4-DHP		100 µM 1,4-DHP	
	Rel. Activity [%]	STDEV	Rel. Activity [%]	STDEV
No 1,4-DHP	0	0.97		
No substrate	100	3.08		
123	88.89	19.57	105.28	10.02
124	97.22	10.87	122.22	6.84
125	83.05	4.73	91.34	4.38
126	86.97	3.84	113.89	3.16
127	83.33	4.2	88.89	3.77
128	97.22	6.52	119.44	11.43
129	97.22	8.82	100	5.43
130	88.89	11.93	82.81	15.44
131	80.71	2.85	113.89	15.99
132	97.22	5.2	96.54	19.24
133	105.56	3.8	96.44	6.02
333	109.89	0.42	38.47	3.16
334	107.78	0	110.31	8.14
335	109.04	3.8	112.84	6.58
336	99.55	4.43	105.24	15.35
337	102.08	0.63	104.82	9.92
338	101.45	1.27	107.35	4.97
339	100.18	0	103.13	9.14
340	103.35	1.9	107.78	13.22
341	110.31	8.98	105.67	6.91
342	104.4	6.91	100.6	9.87
342	105.24	6.33	114.53	7.5
343	101.45	5.06	103.98	6.33
344	103.98	3.8	114.95	6.13
345	98.28	5.7	102.71	9.83
350	98.92	2.53	109.89	8.05
351	99.55	0.63	115.37	4.79
352	102.29	8.47	127.61	5.49
353	102.29	8.47	115.79	4.22
354	102.08	12.03	109.89	4.76
355	106.51	3.8	104.82	3.61
357	102.71	5.06	102.71	1.46
358	109.04	3.8	114.11	6.6
359	117.27	3.67	123.92	12.86
360	100.5	0.5	113.54	1.33
361	103.51	5.01	91.48	8.78
362	98.5	4.28	106.02	3.92
363	103.51	3.92	114.54	0.87
364	101.5	1	110.53	2.79
365	106.02	3.62	115.04	2.19
366	98.5	3.92	96.49	3.13
367	103.01	2.19	113.54	8.07
368	98.5	3.05	146.88	5.3
369	105.52	2.3	116.55	4.94

Coupled continuous assay using 50 µM NAM instead of Sirtuin substrate peptide. Values and errors are derived from at least three independent measurements. All values were normalized to a control reaction without 1,4-DHP.

Table A 6: Sirt1 deacetylation of p53 substrate peptide in presence of 10 µM or 100 µM 1,4-DHP.

UBCS	10 µM 1,4-DHP		100 µM 1,4-DHP	
	Rel. Activity [%]	STDEV	Rel. Activity [%]	STDEV
No 1,4-DHP	0.02	1.72		
No substrate	100	3.45		
123	129.14	20	176.83	21.03
124	81.46	8.58	203.32	28.48
125	79.87	9.2	154.12	13.37
126	85.43	23.46	179.1	42.58
127	139.74	19.1	180.8	19.87
128	82.45	16.41	81.46	30.26
129	73.51	9.73	143.05	20.36
130	123.84	22.63	117.22	19.87
131	72.38	2.07	110.98	17.23
132	97.35	12.14	188.75	11.92
133	114.57	15.41	202.26	46.57
333	98.27	4.56	68.97	16.98
334	93.1	4.56	110.34	1.72
335	100	6.9	117.24	10.77
336	100	4.56	110.34	6.9
337	100	4.56	113.79	15.03
338	98.27	3.45	118.96	12.07
339	94.83	3.45	122.41	2.99
340	100	7.51	98.27	9.12
341	98.27	4.56	101.72	7.9
342	96.55	7.9	118.96	7.51
342	101.72	5.97	106.89	5.97
343	101.72	5.97	129.3	25.04
344	105.17	6.22	129.3	20.97
345	115.51	16.44	163.78	15.8
350	94.83	4.56	129.3	9.6
351	84.48	20.32	134.47	6.9
352	81.04	5.17	156.88	31.93
353	105.17	4.56	115.51	4.56
354	96.55	5.17	132.75	19.58
355	96.55	5.17	106.89	0
357	98.27	9.6	127.58	8.96
358	101.72	0	122.41	8.96
359	122.41	0	205.15	46.92
360	121.42	4.28	164.27	12.85
361	117.14	0	147.13	21.42
362	125.71	0	151.41	8.57
363	129.99	4.28	181.41	4.28
364	125.71	0	177.12	8.57
365	112.85	4.28	162.84	23.38
366	104.28	4.28	117.14	0
367	129.99	4.28	237.1	17.14
368	125.71	0	237.1	8.57
369	112.85	4.28	232.82	21.42

Coupled continuous assay using 1.5 µM Sirtuin, 50 µM substrate peptide and 100 µM NAD^+. Values and errors are derived from at least three independent measurements. All values were normalized to a control reaction without 1,4-DHP.

Table A 7: Sirt2 deacetylation of αTub substrate peptide in presence of 10 µM or 100 µM 1,4-DHP.

UBCS	10 µM 1,4-DHP		100 µM 1,4-DHP	
	Rel. Activity [%]	STDEV	Rel. Activity [%]	STDEV
No 1,4-DHP	0	0		
No substrate	100	0.73		
123	108.51	3.75	141.04	8.76
124	83.49	10.24	111.64	12.87
125	79.73	6.62	108.51	10.48
126	85.99	9.93	114.76	5.45
127	128.21	9.86	113.2	9.49
128	93.5	22.99	78.48	11.26
129	97.25	4.6	108.51	18.2
130	84.11	5.63	81.48	24.13
131	78.48	10.55	89.21	13.74
132	126.03	9.82	138.54	11.53
133	113.2	16.53	106.63	14.58
333	102.19	2.63	33.58	0.73
334	102.19	2.63	102.92	0
335	101.46	4.44	96.35	4.38
336	99.63	3.28	100.73	1.26
337	101.82	3.28	105.11	1.26
338	96.35	2.53	96.35	2.19
339	99.27	1.93	110.22	1.93
340	92.7	2.63	95.62	2.63
341	103.65	1.46	108.03	8.61
342	103.65	1.46	99.27	15.71
342	104.38	0.73	110.22	0.73
343	102.92	2.53	105.11	2.53
344	101.82	3.28	107.3	4.56
345	101.46	1.46	116.79	9.15
350	100	2.92	104.38	3.18
351	100.73	1.26	107.3	1.26
352	104.38	1.46	108.76	8.42
353	103.65	1.93	103.65	4.79
354	101.46	0.73	102.92	7.9
355	103.65	1.93	91.97	4.38
357	104.01	1.09	102.19	3.86
358	102.19	1.93	98.54	8.76
359	102.92	1.26	99.63	1.09
360	104.37	2.31	112.85	1.54
361	98.97	5.56	112.85	3.08
362	108.99	2.31	104.37	2.31
363	122.1	1.54	95.12	6.94
364	111.3	2.67	119.01	8.16
365	111.3	4.63	123.64	8.16
366	103.6	1.54	95.89	6.72
367	105.14	1.54	139.06	0
368	111.3	2.67	160.64	3.08
369	115.93	4.63	109.76	9.38

Coupled continuous assay using 1.5 µM Sirtuin, 50 µM substrate peptide and 100 µM NAD^+. Values and errors are derived from at least three independent measurements. All values were normalized to a control reaction without 1,4-DHP.

Table A 8: Sirt3 deacetylation of ACS2.3 substrate peptide in presence of 10 µM or 100 µM 1,4-DHP.

UBCS	10 µM 1,4-DHP		100 µM 1,4-DHP	
	Rel. Activity [%]	STDEV	Rel. Activity [%]	STDEV
No 1,4-DHP	0	1.48		
No substrate	100	1.61		
123	87.34	2.38	117.9	2.53
124	101.9	2.32	103.8	3.03
125	77.22	2.28	175.93	8.21
126	143.93	4.08	329.21	12.01
127	82.92	2.92	122.78	1.44
128	73.97	2.52	95.12	3.59
129	86.98	2.58	191.12	2.13
130	86.98	1.79	149.35	10.1
131	98.37	3.51	458.77	14.65
132	77.22	3.75	243.51	6.32
133	108.86	3.68	213.9	4.26
333	104.67	5.9	49.07	3.27
334	94.86	8.65	125.93	5.67
335	98.13	7.13	106.31	7.76
336	85.05	3.27	114.49	11.45
337	104.67	10.73	109.58	4.33
338	99.77	10.73	98.95	8.14
339	98.13	9.95	103.85	13.51
340	86.68	8.73	107.53	10.09
341	106.31	4.91	107.94	8.65
342	107.94	4.33	124.3	7.13
342	103.04	9.95	132.48	9.95
343	99.77	5.9	124.3	1.64
344	96.5	6.01	130.84	10.21
345	103.04	8.18	121.03	12.35
350	90.36	4.19	129.61	5.44
351	101.4	5.67	125.93	11.68
352	107.94	3.27	150.47	7.22
353	106.31	5.67	119.8	8.82
354	116.12	7.5	119.8	11.04
355	107.94	4.33	98.13	8.65
357	109.58	4.33	98.13	11.45
358	111.21	4.91	114.49	4.33
359	102.63	5.06	103.85	41.27
360	112.44	6.76	124.16	5.86
361	112.44	3.38	118.3	8.94
362	112.64	0.2	109.52	8.78
363	121.23	2.93	131.96	5.16
364	112.44	3.38	122.2	7.04
365	118.3	5.86	126.11	14.08
366	108.54	1.95	116.35	8.51
367	102.68	7.81	150.51	2.93
368	104.64	10.33	132.94	2.93
369	120.25	5.16	120.25	28.75

Coupled continuous assay using 1.5 µM Sirtuin, 50 µM substrate peptide and 100 µM NAD^+. Values and errors are derived from at least three independent measurements. All values were normalized to a control reaction without 1,4-DHP.

Table A 9:Sirt5 desuccinylation of succCPS1 peptide in presence of 10 µM or 100 µM 1,4-DHP.

UBCS	10 µM 1,4-DHP		100 µM 1,4-DHP	
	Rel. Activity [%]	STDEV	Rel. Activity [%]	STDEV
No 1,4-DHP	0	4.38		
No substrate	100	6.41		
123	108.62	13.94	139	35.78
124	76.52	21.87	89.13	18.09
125	69.65	2.29	68.5	10.32
126	83.98	1.72	124.67	43.74
127	65.06	6.88	101.74	8.27
128	75.38	3.44	97.16	6.07
129	106.33	7.94	106.33	26.04
130	75.38	3.44	65.06	13.76
131	115.17	13.15	169.94	11.36
132	83.98	14.96	123.52	10.32
133	121.8	31.81	243.88	45.71
333	100.54	11.35	97.1	14.45
334	104.83	14.86	166.62	21.69
335	104.83	14.86	233.56	15.77
336	124.14	17.03	256.09	32.98
337	104.83	7.43	279.9	36.77
338	100.54	4.29	223.26	21.31
339	153.1	17.73	261.88	21.69
340	138.3	18.92	230.34	29.44
341	100.54	15.47	127.36	22.53
342	104.83	7.43	130.57	24.08
342	113.41	18.7	256.73	30.3
343	104.83	12.87	318.52	33.47
344	156.32	27.61	320.46	23.13
345	138.3	24.96	121.99	11.35
350	137.01	26.54	204.6	24.3
351	108.05	12.18	177.78	35.12
352	140.23	21.27	304.36	43.18
353	216.4	23.89	333.97	33.17
354	104.83	12.87	288.27	42.17
355	117.7	19.66	249.65	46.82
357	91.95	7.43	220.69	30.19
358	120.92	29.44	236.78	21.91
359	230.99	16.49	233.56	26.28
360	111.19	8.86	168.14	20.1
361	104.49	12.08	143.02	15.08
362	131.29	3.35	161.44	12.08
363	144.69	14.6	171.49	14.6
364	127.94	5.8	148.04	20.92
365	114.54	13.4	161.44	14.6
366	117.89	10.05	164.79	17.73
367	124.59	3.35	201.64	13.4
368	117.89	5.8	211.69	3.35
369	181.54	6.7	168.14	25.29

Coupled continuous assay using 1.5 µM Sirtuin, 50 µM substrate peptide and 100 µM NAD^+. Values and errors are derived from at least three independent measurements. All values were normalized to a control reaction without 1,4-DHP.

6.2.4. 1,4-DHP effects against zSirt5

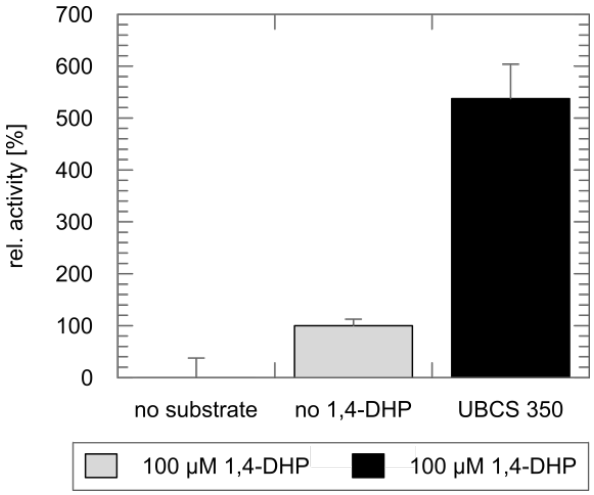

Figure A 4: zSirt5 activation by UBCS 350. *D. rerio* Sirt5 (zSirt5) is activated by 100 µM UBCS 350 in a similar manner as its human homologue (~ 5.5-fold activation). Coupled continuous assay using 1.5 µM zSirt5, 50 µM succCPS1, 100 µM NAD^+ ± 100 µM UBCS 350 and a final DMSO concentration of 5 %. (Error) bars derive from three independent experiments and resulted in rel. activities of 0.0 ± 37.5 % (no substrate), 100.0 ± 12.5 (no 1,4-DHP) and 537.5 ± 66.1 %.

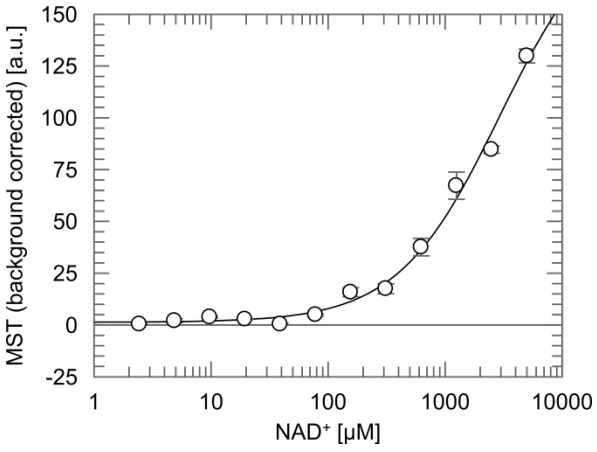

Figure A 5: Increasing NAD^+ concentrations result in a MST artifact. The K_D value for NAD^+ binding to Sirtuins ranges between 150 – 500 µM[82]. For FITC-Sirt3 this binding behavior cannot be reproduced in MST experiments as increasing NAD^+ concentrations result in further increasing MST values. Adversely, fixed NAD^+ concentrations can be used throughout MST experiments, e.g. to analyze its effect on the binding of further Sirtuin ligands.

Danksagung

An dieser Stelle möchte ich mich bei allen bedanken, die mich während meiner Doktorarbeit unterstützt haben.

Bei Prof. Dr. Clemens Steegborn bedanke ich mich für die Ermöglichung dieser Doktorarbeit. Ebenso möchte ich mich für die ständige Diskussionsbereitschaft, Hilfestellung und für die wissenschaftlichen Freiheiten während meiner Promotionsarbeit bedanken.

Der Studienstiftung des Deutschen Volkes danke ich für die finanzielle Unterstützung im Rahmen meines Promotionsstipendiums. Besonders möchte ich mich auch bei meinem Gutachter, Herrn Prof. Dr. Harald Kolmar, für das nette und interessante Auswahlgespräch bedanken.

Dr. Melanie Fischer (geb. Gertz), Dr. Frank Fischer, Dr. Michael Weyand und Dr. Matt Fuszard danke ich für die Einführung und Unterstützung in die Sirtuinwelt, Massenspektrometrie bzw. Strukturbiologie.

Mein besonderer Dank geht an meine Kollegen Martin Pannek und Dr. Sebastien Moniot für die technischen, wissenschaftlichen aber besonders auch für die außerfachlichen Diskussionen und ständige Hilfsbereitschaft.

Ebenso bedanke ich mich besonders für die ausgezeichnete technische Unterstützung durch Norbert Grillenbeck, Edith Guthmann, Lisa Meisel und Susanne Schäfer.

Meinen ehemaligen Kollegen Christian Seutter von Loetzen, Felix Husslik, Christian Feiler und Philipp Schmidpeter, den Mitgliedern der AG Steegborn, AG Blankenfeldt und AG Möglich sowie den Sekretärinnen Gabriele Kassler und Renate Crowe danke ich herzlich für die angenehme und entspannte Atmosphäre und Zusammenarbeit. Ebenso möchte ich mich bei Dr. Neha Garg und Dr. Winnie Zheng für die Analyse von zellulären Effekten der 1,4-Dihydropyridine und Sirtuin-PTMs bedanken.

Allen voran danke ich von ganzem Herzen dir, Christin, dass du mich in den letzten Jahren so wundervoll unterstützt hast. Ohne deine Hilfe wäre ich sicherlich nicht so weit gekommen. Danke, dass du mir immer den Rücken freigehalten hast und immer für mich da bist!

… there's nothing to be scared of. All it takes is a little self-confidence. You know, if you put your mind to it, you can accomplish anything.

Marty McFly

(Eidesstattliche) Versicherungen und Erklärungen

(§ 5 Nr. 4 PromO)

Hiermit erkläre ich, dass keine Tatsachen vorliegen, die mich nach den gesetzlichen Bestimmungen über die Führung akademischer Grade zur Führung eines Doktorgrades unwürdig erscheinen lassen.

(§ 8 S. 2 Nr. 5 PromO)

Hiermit erkläre ich mich damit einverstanden, dass die elektronische Fassung meiner Dissertation unter Wahrung meiner Urheberrechte und des Datenschutzes einer gesonderten Überprüfung hinsichtlich der eigenständigen Anfertigung der Dissertation unterzogen werden kann.

(§ 8 S. 2 Nr. 7 PromO)

Hiermit erkläre ich eidesstattlich, dass ich die Dissertation selbständig verfasst und keine anderen als die von mir angegebenen Quellen und Hilfsmittel benutzt habe.

(§ 8 S. 2 Nr. 8 PromO)

Ich habe die Dissertation nicht bereits zur Erlangung eines akademischen Grades anderweitig eingereicht und habe auch nicht bereits diese oder eine gleichartige Doktorprüfung endgültig nicht bestanden.

(§ 8 S. 2 Nr. 9 PromO)

Hiermit erkläre ich, dass ich keine Hilfe von gewerblichen Promotionsberatern bzw. -vermittlern in Anspruch genommen habe und auch künftig nicht nehmen werde.

…….

Ort, Datum, Unterschrift